UNIVERSITY OF CALIFORNIA
Los Angeles

Explicit Homotopies of Liouville Domains

A dissertation submitted in partial satisfaction
of the requirements for the degree
Doctor of Philosophy in Mathematics

by

Joseph John Breen

2022

ABSTRACT OF THE DISSERTATION

Explicit Homotopies of Liouville Domains

by

Joseph John Breen
Doctor of Philosophy in Mathematics
University of California, Los Angeles, 2022
Professor Ko Honda, Chair

This dissertation contains results that contribute to and use the theory of convex hypersurfaces in contact manifolds. First, we generalize a 3-dimensional convexity criterion result of Giroux [Gir91]. Specifically, we show that the criterion holds in contact manifolds of arbitrary dimension. As an application, we show that a particular closed hypersurface introduced by A. Mori [Mor11] is C^∞-close to a convex hypersurface. Second, inspired by the techniques of Honda and Huang in [HH19], we develop explicit local operations that may be applied to Liouville domains with the goal of simplifying the dynamics of the Liouville vector field. As an application, we show that Mitsumatsu's well-known Liouville-but-not-Weinstein domains are stably Weinstein, answering a question posed by Huang [Hua19].

The dissertation of Joseph John Breen is approved.

Gang Liu

Peter Petersen

Sucharit Sarkar

Ko Honda, Committee Chair

University of California, Los Angeles

2022

TABLE OF CONTENTS

LIST OF FIGURES

LIST OF TABLES

ACKNOWLEDGMENTS

It should go without saying, but I am deeply grateful for my advisor, Ko Honda. I have learned a lot of math from Ko, and his intuition has guided most of the work in this dissertation. Moreover, with six years of hindsight it is clear how important "personal fit" was for a student like me in choosing an advisor. Ko has been patient, supportive, and down to earth, and under him I was able to find a decent balance of productivity and (mental, physical, and emotional) health. I often wonder how much less enjoyable — or how abruptly shortened — my time in grad school could have been with a different advisor.

I also owe a great deal of thanks to Austin Christian, who I was lucky enough to have as a collaborator, mentor, and friend. Mathematically, I learned a wealth of symplectic and contact geometry from and with Austin, and many of the discoveries I made in this thesis would not have been possible without the many conversations we had over the years. I did my best to closely follow in his footsteps in navigating grad school and academia at large, and will likely continue to do so.

My parents, Kevin and Karen Breen, played an important role by being unequivocally proud and supportive of everything I do. This was especially important during difficult periods of the degree, when I was unsure I would make it to the end. I almost certainly don't tell them enough how grateful I am for their support, and I would not be where I am without them.

I have many friends at UCLA that have been an integral part of my experience. There are too many of you to name individually, so at the risk of leaving any one person out I'll only give a special acknowledgement to Ian Frankenburg, my closest friend. Ian has been a part of my exploration of math since high school in Ohio, and I will forever cherish the fact that we were able to reunite in grad school on the other side of the country. To all the other friends that have populated my life in Los Angeles, you know who you are.

Finally, I want to shout out many of the students I have had over the years that I have grown close to and have been lucky enough to teach and mentor. Again, there are too many

of you to name individually, but if you have left an impression on me — or vice versa — you know who you are. Teaching has been a crucial part of my time in grad school, bringing me endless joy and fulfillment, and I would not have survived the program without it.

Note. Chapter 3 is a rewrite of [Bre21]. I'd like to thank the anonymous referee for providing comments on this work, along with other helpful comments from Atsuhide Mori. Chapters 4, 5, and 6 are based on [BC21], which is joint work with Austin Christian. In particular, Austin had a heavy hand in writing Chapter 6, and also Section 1.2 from the introduction. I am grateful to him for allowing me to reproduce the work here. Finally, I was partially supported by NSF grant DMS-2003483.

VITA

2016	B.A. (Mathematics), Northwestern University, Evanston, Illinois.
2021	Beckenbach Fellowship, Department of Mathematics, University of California, Los Angeles

CHAPTER 1

Introduction

Symplectic geometry is a type of geometry that exists in even dimensions. *Contact geometry* is its natural odd-dimensional counterpart. Each informs the other, and it is difficult to study just one in isolation. This dissertation contains results that are primarily contact, and also results that are primarily symplectic, but there is an underlying thread that binds them together: The notion of *convexity*. In particular, we contribute to the development of convex hypersurface theory in contact geometry and leverage its techniques to study questions in symplectic geometry. Specifically, this dissertation is based on two projects, [Bre21] and [BC21], the second of which was collaborative work with A. Christian.

Organizational remarks. The present chapter introduces both projects, including the main results. Background material for all of the concepts discussed here and in the rest of the dissertation is contained in Chapter 2. Section 1.1 introduces the material from [Bre21] and Subsection 1.1.1 describes the organization of the material from [Bre21] in the context of the dissertation. Likewise, Section 1.2 was written in collaboration with A. Christian and introduces the material from [BC21], and Subsection 1.2.5 describes the organization of the material from [BC21] in the context of the dissertation.

1.1 Morse-Smale characteristic foliations

In [Gir91], Giroux demonstrated the power of convex surface theory in three dimensional contact manifolds. Since then, convexity has been an effective tool in this setting; see for example [Hon00a, Hon00b]. Recently, a systematic development of convex hypersurface theory in arbitrary dimensions began in works such as [HH18], [HH19], and [Sac]. The

goal of the present chapter is to study further one aspect of convexity in higher dimensions.

In particular, one of Giroux's results in [Gir91] is that a closed surface in a 3 dimensional contact manifold with Morse-Smale characteristic foliation is convex. We recall the relevant definition.

Definition. A vector field on an oriented manifold is **Morse-Smale** if the following conditions are satisfied:

(i) There are finitely many critical points and periodic orbits, each of which is hyperbolic (in the dynamical systems sense).

(ii) Every flow line limits to either a critical point or an orbit in both forward and backward time.

(iii) The unstable manifold of any critical point or orbit is transverse to the stable manifold of any critical point or orbit.

A singular foliation is **Morse-Smale** if it is directed by a Morse-Smale vector field.

In [HH19], Honda and Huang adapted Giroux's argument to show that a hypersurface in a contact manifold of arbitrary dimension with so called Morse$^+$ characteristic foliation is convex. The Morse$^+$ hypothesis, which requires the existence of a Morse function for which the foliation is gradient-like, precludes the existence of periodic orbits in the characteristic foliation. Here, we generalize further to include the case where the foliation has periodic orbits. The main result of this chapter is the following.

Theorem 1.1. *Let $\Sigma^{2n} \subseteq (M^{2n+1}, \xi = \ker \alpha)$ be a closed, oriented hypersurface with Morse-Smale characteristic foliation. Then Σ is convex.*

Remark. The $+$ in the Morse$^+$ hypothesis in [HH19] is the assumption that there are no trajectories from negative singularities to positive singularities. It will be evident from the proof of Theorem 1.1 that the analogue of this assumption in Definition 1.1 is condition (iii). Also worth nothing is that Honda and Huang prove that a hypersurface with Morse characteristic foliation can be smoothly perturbed to have Morse$^+$ characteristic foliation.

Remark. When $\dim M = 3$, Theorem 1.1 (i.e., Giroux's original result) is especially powerful because Morse-Smale vector fields on 2-manifolds are dense in the C^∞-topology (see [PPM98] and the references within). This implies that a C^∞-generic closed surface has Morse-Smale characteristic foliation, and thus is convex. Morse-Smale vector fields are not C^∞-dense in higher dimensions.

The proof of Theorem 1.1 relies on an understanding of the induced 1-form $\beta = \alpha\,|_\Sigma$ of a contact form α near periodic orbits. The terminology we will use in this paper is:

Definition. Let $\beta := \alpha\,|_\Sigma$. A periodic orbit γ in the characteristic foliation Σ_ξ is **Liouville** if $g\beta$ is a Liouville form in a neighborhood of γ for some smooth $g > 0$. We say γ is **positive Liouville** if $d(g\beta)^n > 0$ and **negative Liouville** if $d(g\beta)^n < 0$.

Remark. Here is a simple criterion for an orbit to be Liouville. Pick any volume form Ω in a neighborhood of γ and consider the vector field X satisfying $i_X\Omega = \beta\,(d\beta)^{n-1}$ which directs the characteristic foliation. If $\operatorname{div}_\Omega X \neq 0$, then γ is Liouville. Indeed,

$$\operatorname{div}_\Omega(X)\,\Omega = d\,(i_X\Omega) = d\left(\beta\,(d\beta)^{n-1}\right) = (d\beta)^n$$

so that $d\beta$ is symplectic if $\operatorname{div}_\Omega(X) \neq 0$. One may easily check that the sign of $\operatorname{div}_\Omega(X)$ is independent of the choice of Ω.

The proof that the Morse$^+$ condition implies convexity relies on the fact that β is a Liouville form in a neighborhood of a critical point of the characteristic foliation. Also important is the fact that the Morse index of a critical point of a Liouville vector field satisfies $\operatorname{ind}(p) \leq n$, where $2n$ is the dimension of the Liovuille manifold (see Proposition 11.9 of [CE12]). One of the main steps in proving Theorem 1.1 is to show that hyperbolic periodic orbits exhibit the same behavior.

Proposition 1.2. *Let $\Sigma^{2n} \subseteq (M^{2n+1}, \xi = \ker\alpha)$ be an oriented hypersurface. If γ is a hyperbolic periodic orbit in the characteristic foliation, it is Liouville. Furthermore, if γ is positive Liouville then $\operatorname{ind}(\gamma) \leq n$.*

With this and a few other ingredients, the proof of Theorem 1.1 is a straightforward adaptation of Giroux's argument in three dimensions; see also the proof of Proposition 2.2.3 in [HH19].

As an application of this convexity criterion, we provide some further analysis on a closed hypersurface Σ_0 introduced by Mori in [Mor11]. We will review the definition of Σ_0 in Section 3.2. In [Mor11] it was claimed that Σ_0 cannot be smoothly approximated by a convex hypersurface. Using Theorem 1.1, we will prove:

Corollary 1.3. *The closed hypersurface Σ_0 is C^∞-close to a convex hypersurface.*

Remark. We emphasize that our work only shows that the *closed* hypersurface Σ_0 can be smoothly approximated by a convex hypersurface. In [Mor11], Mori also introduces a hypersurface with contact type boundary and states a conjectural Thurston-Bennequin-like inequality for convex hypersurfaces; see also [Mor09]. Theorem 1.1 and the proof of Corollary 1.3 do not apply to the hypersurface with boundary, or disprove the conjectured inequality.

1.1.1 Organization

There is one chapter dedicated to Theorem 1.1 and its consequences, Chapter 3.

1.2 Mitsumatsu's Liouville domains

A basic desire in symplectic geometry is develop a notion of Morse theory which is compatible with the symplectic structure. Morse theory is an indispensable tool in smooth topology, and one naturally wants to extend its utility to the symplectic setting. Unfortunately, not all symplectic manifolds admit a natural Morse theoretic description. The precise class of manifolds which do are called *Weinstein manifolds*. In this dissertation we are primarily concerned with the compact case, in which case *Weinstein domains* are exactly the symplectic manifolds with a compatible Morse theory.

In order to give a precise definition of a Weinstein domain, we begin with exact symplec-

tic manifolds-with-boundary (W, ω). A *Liouville structure* on such a manifold is a choice of symplectic potential λ with the property that X_λ points transversely out of ∂W, where X_λ is the vector field on W defined by $\iota_{X_\lambda}\omega = \lambda$. We call X_λ the *Liouville vector field* associated to λ, and refer to the pair (W, λ) as a *Liouville domain*. Flowing along a Liouville vector field induces a conformal transformation of the symplectic structure, and thus these vector fields are the natural candidate for gradient-like vector fields in a symplectic Morse theory. In [Wei91], Weinstein defined such a theory for a restricted class of Liouville domains. We will call a Liouville structure a *Weinstein structure* if there exists a Morse function $\phi\colon W \to \mathbb{R}$ which is locally constant on ∂W and for which X_λ is gradient-like. That is, there is a constant $c > 0$ and some Riemannian metric on W for which

$$d\phi(X_\lambda) > c(\|X_\lambda\|^2 + \|d\phi\|^2).$$

Weinstein domains may be built up using *Weinstein handles*, and thus their study has a distinctly topological flavor.

Throughout, we will consider Liouville structures (and Weinstein structures) up to *Liouville homotopy*. For Liouville domains, a Liouville homotopy is simply a smooth family λ_t of Liouville forms. For Liouville *manifolds* — a noncompact analogue of Liouville domains — the notion of Liouville homotopy is a bit more subtle, as is the notion of Liouville structure itself.

With these two definitions in hand, the obvious question is then whether or not a given Liouville structure is in fact a Weinstein structure, at least up to Liouville homotopy. In general, the answer is no, and there is a well-known topological obstruction which a Liouville domain must avoid if it is to admit a Weinstein structure.

Proposition 1.4. *Let (W, λ) be a Weinstein domain of dimension $2n$, and let ϕ be a Morse function for which X_λ is gradient-like. Then ϕ admits no critical points of index greater than n.*

This means that a Weinstein domain has the homotopy type of a half-dimensional CW-complex, and thus any Liouville domain without this property cannot possibly be Weinstein. In particular, as is the case for compact complex manifolds with pseudo-convex

boundary, Weinstein domains of dimension at least 4 must have connected boundaries. The first examples of Liouville-but-not-Weinstein domains were given by McDuff in [McD91], who constructed a Liouville structure on $DT^*\Sigma_g \setminus N(\Sigma_g)$, the disc cotangent bundle of a surface of genus g, with a neighborhood of the zero-section removed, for any $g > 1$.

Further examples of Liouville-but-not-Weinstein domains have been constructed by Geiges [Gei94], [Gei95], Mitsumatsu [Mit95], Massot-Niederkrüger-Wendl [MNW13], and Huang [Hua19], with such examples now existing in all even dimensions. To the best of our knowledge, all existing constructions of Liouville-but-not-Weinstein domains rule out the existence of a Weinstein structure by appealing to the topology of the Liouville domain. According to the *Weinstein existence theorem* (c.f. [CE12, Theorem 13.1]), a Liouville domain which has the homotopy type of a half-dimensional CW-complex must admit *some* Weinstein structure, and thus we are left with the following question.

Question 1.5. Let (W, λ) be a Liouville domain which has the homotopy type of a half-dimensional CW-complex. Must λ admit a Liouville homotopy to a Weinstein structure?

Wrapped up in this question are very delicate dynamical considerations. In the absence of a Lyapunov function, there is very limited control over the dynamics of a Liouville vector field X_λ, and thus the problem of homotoping X_λ into a vector field with severely restricted dynamical properties — all while maintaining the vector field's status as Liouville — seems to be enormously difficult. Our overarching goal is to better understand the extent to which wild Liouville vector fields may be tamed, provided their underlying domains have sufficiently simple topology.

1.2.1 Stabilizations and skeleta

Because a Liouville domain has "sufficiently simple topology" whenever it has the homotopy type of a half-dimensional CW-complex, we can achieve our topological criterion by increasing the dimension of our domain. The *stabilization* of a Liouville domain (W, λ) is

given by the product

$$(W, \lambda) \times (r_0\,\mathbb{D}^2, \lambda_{\mathrm{stab}}) = (W \times r_0\,\mathbb{D}^2, \lambda + \lambda_{\mathrm{stab}}),$$

for some $r_0 > 0$, where λ_{stab} is the standard Liouville form on $r_0\,\mathbb{D}^2$, defined by

$$\lambda_{\mathrm{stab}} = \tfrac{1}{2}(p\,dq - q\,dp).$$

The Liouville vector field $X_{\lambda_{\mathrm{stab}}} = \frac{1}{2}p\,\partial_p + \frac{1}{2}q\,\partial_q$ expands radially from the origin in $r_0\,\mathbb{D}^2$, and the Liouville vector field of the stabilization is given by $X_\lambda + X_{\lambda_{\mathrm{stab}}}$. It follows that stabilization does not fundamentally change the dynamics of a Liouville domain.

To make this last statement more precise, we introduce the notion of the *skeleton* of a Liouville domain. This is the set defined by

$$\mathrm{Skel}(W, \lambda) := \bigcap_{t<0} \psi^t(W),$$

where $\psi^t \colon W \to W$ is the time-t flow of the Liouville vector field X_λ. The interesting dynamics of (W, λ) are encoded on $\mathrm{Skel}(W, \lambda)$, and it is clear that the skeleton of the stabilization is given by $\mathrm{Skel}(W, \lambda) \times \{(0, 0)\}$.

For any Liouville domain, one can stabilize sufficiently many times to overcome the topological obstruction presented by Proposition 1.4, and thus arrive at a weaker version of Question 1.5.

Question 1.6. Is every Liouville domain *stably Weinstein*? That is, does every Liouville structure admit a Liouville homotopy to a Weinstein structure, following sufficiently many stabilizations?

While allowing stabilizations weakens the hypothesis of Question 1.5, a clear answer to Question 1.6 would still shed a great deal of light on the difference between Liouville and Weinstein dynamics. A Liouville domain which is not stably Weinstein would necessarily feature dynamics far more complicated than any witnessed on a Weinstein domain.

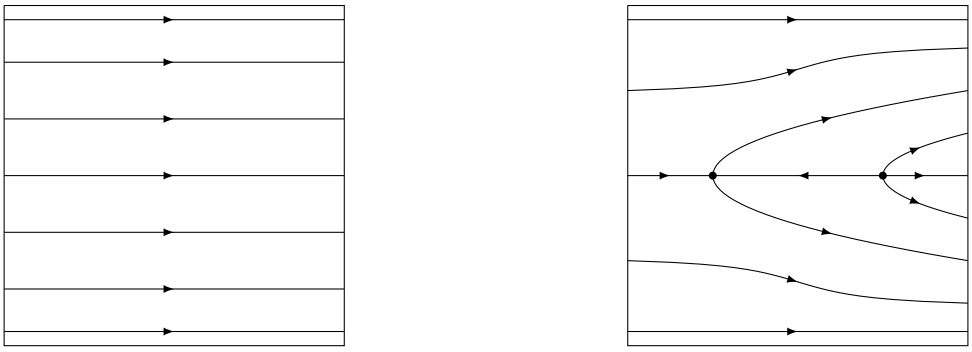

Figure 1.1: A box fold is installed in dimension 2 by identifying a region as on the left and replacing it (via a Liouville homotopy) with a region as on the right. Figure credit to A. Christian.

We point out that in the case of Liouville manifolds, an affirmative answer to Question 1.6 follows from work of Eliashberg-Gromov [EG91]. In fact, Eliashberg-Ogawa-Yoshiyasu showed in [EOY21] that if a Liouville manifold of dimension $2n$ has Morse type at most $n+1$, then a single stabilization suffices. However, the relevant Liouville homotopies are not known to be compactly supported, and thus Question 1.6 remains.

1.2.2 Hands-on homotopies

Our strategy for taming wild Liouville dynamics is to deal with the structures directly. Inspired by the techniques used by Honda and Huang in [HH19] to study hypersurfaces in contact manifolds, we construct explicit Liouville homotopies which can be installed as local operations. These local operations are meant to simplify the dynamics of our Liouville domain, with the goal of producing a Weinstein domain following their installation.

As a first example, consider the *two-dimensional box fold*, to be carefully defined in Sections 4.1 and 4.2. To install this operation on a two-dimensional Liouville domain (W, λ), we first identify a region $U \subset W$ of the form

$$(U, \lambda|_U) \cong ([0, s_0] \times [0, t_0], e^s\, dt).$$

On U, the Liouville vector field X_λ may be identified with ∂_s, meaning that flowlines of X_λ simply pass through U unperturbed. With the goal of interrupting chaotic behavior, the

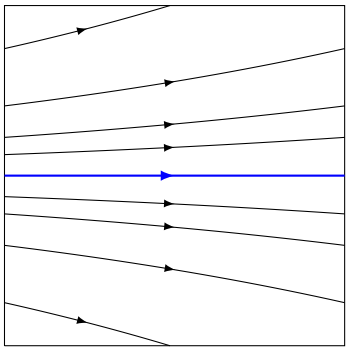

(a) This Liouville structure is not Weinstein, because the vector field is not gradient-like.

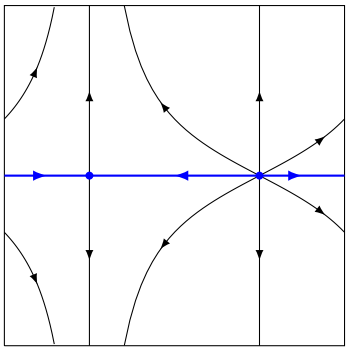

(b) The box fold introduces critical points which make the vector field gradient-like.

Figure 1.2: A Liouville structure on $S^1 \times [-1, 1]$, before and after the installation of a box fold. In both figures, the vertical edges are identified, and the skeleton is $S^1 \times \{0\}$. Figure credit to A. Christian.

box fold uses a Liouville homotopy to replace X_λ on U with a vector field which has two critical points — one of index 0 and another of index 1 — and is topologically equivalent to the vector field depicted in Figure 1.1. In other words, a box fold introduces a pair of cancelling critical points of index 0 and index 1.

The box fold will be far from sufficient as a general purpose operation on Liouville domains, but we can use it to demonstrate the spirit of our techniques. Consider a Liouville structure on $S^1 \times [-1, 1]$ whose Liouville vector field behaves as seen in Figure 1.2a. Namely, $S^1 \times \{0\}$ is a closed orbit of the Liouville vector field, repelling other orbits. The presence of a closed orbit precludes the existence of a Lyapunov function for our Liouville vector field, meaning that this structure is not Weinstein. After installing a box fold on a region which intersects the skeleton $S^1 \times \{0\}$, we obtain a Liouville domain of the type depicted in Figure 1.2b. By interrupting the backward flow of our Liouville vector field[1] we are able to produce a Weinstein domain.

While the box fold has the helpful feature of interrupting flowlines, it comes at the cost of a drastic holonomy for uninterrupted flowlines. That is, after the box fold is installed, there will be flowlines which pass through the region U with very different t-values along $\{s = 0\} \times [0, t_0]$ and $\{s = s_0\} \times [0, t_0]$. This local perturbation can then have unpredictable effects

[1] In this toy case, the Liouville vector field is admittedly not so much chaotic as simply *not gradient-like*.

on the global dynamics of our Liouville domain, making our increased local understanding substantially less useful.

Consequently, we see that there are two desired features in any local operation: That it traps Liouville flowlines in backward time, and that its effect on untrapped flowlines is controllable. In the analysis we will see that these desires are often at odds with one another, and that our control over the holonomy of these operations is hampered by the requirement that they be Liouville homotopies. However, we present in this paper an important local operation which can be installed in a stabilized setting.

1.2.3 The blocking apparatus

Now we introduce the key local operation, which we call the *blocking apparatus*. As with the box fold, the blocking apparatus is installed on a region $U \subset (W, \lambda)$ in a Liouville domain of dimension $2n$. We require that this region have the form

$$(U, \lambda|_U) \cong ([0, s_0] \times [0, t_0] \times W_0 \times r_0 \mathbb{D}^2, e^s(dt + \lambda_0 + \lambda_{\text{stab}})),$$

where (W_0, λ_0) is some Weinstein domain of dimension $2n-4$, and $r_0 > 0$ is some positive constant. In words, $(U, \lambda|_U)$ is required to be a symplectization of a contactization of a stabilization of a Weinstein domain. On U, the Liouville vector field X_λ may be identified with ∂_s, flowing directly from

$$\partial_- U := \{s = 0\} \times [0, t_0] \times W_0 \times r_0 \mathbb{D}^2$$

to

$$\partial_+ U := \{s = s_0\} \times [0, t_0] \times W_0 \times r_0 \mathbb{D}^2.$$

That is, backward Liouville flow induces a trivial holonomy map $\partial_+ U \to \partial_- U$; following the installation of the blocking apparatus, there will be a partially-defined holonomy map $\partial_+ U \dashrightarrow \partial_- U$ which we must consider.

In order to precisely state the effect of the blocking apparatus, we introduce some notation.

Definition. For any Liouville domain (W, λ), we let ψ^s denote the time-s flow of the Liouville vector field X_λ and define $\|\cdot\|_{(W,\lambda)} \colon W \to [0,1]$ as follows:

$$\|x\|_{(W,\lambda)} := \begin{cases} 0, & x \in \mathrm{Skel}(W,\lambda) \\ e^{-s_x}, & x \notin \mathrm{Skel}(W,\lambda) \end{cases},$$

where $s_x > 0$ is the unique number such that $\psi^{s_x}(x) \in \partial W$.

Remark. We will often simply write $\|\cdot\|_W$ in place of $\|\cdot\|_{(W,\lambda)}$.

Definition. On the Weinstein domain $(r_0\,\mathbb{D}^2, \lambda_{\mathrm{stab}})$, for any $r_0 > 0$, we define $\|(p,q)\|_{\mathrm{stab}} = \sqrt{p^2+q^2}$.

Remark. Note that $\|\cdot\|_{\mathrm{stab}} \neq \|\cdot\|_{(r_0\,\mathbb{D}^2,\lambda_{\mathrm{stab}})}$.

Definition. For any Liouville domain (W, λ) and any parameter $0 < \epsilon < 1$, we define

$$I_\epsilon(W,\lambda) := \|\cdot\|_W^{-1}([0, 1-\epsilon]),$$

obtained from W by removing an open neighborhood of the boundary ∂W.

With this notation established, we can now state the key effects of installing a blocking apparatus.

Proposition 1.7. *Consider the Weinstein cobordism* $(U = [0,s_0] \times [0,t_0] \times W_0 \times r_0\,\mathbb{D}^2, e^s\,(dt + \lambda_0 + \lambda_{\mathrm{stab}}))$. *Fix* $0 < \delta \ll t_0$ *and* $0 < \epsilon \ll 1$ *arbitrarily small. Then if* $r_0 > 0$ *is sufficiently large, a blocking apparatus can be installed in* U *such that there is a neighborhood* U_{trap} *of*

$$[\delta, t_0 - \delta] \times I_\epsilon(W_0, \lambda_0) \times \{(0,0)\},$$

with any flowline passing through $\{s = s_0\} \times U_{\mathrm{trap}} \subseteq \partial_+ U$ *converging to a critical point in backward time. Moreover, the partially-defined holonomy map* $h \colon \partial_+ U \dashrightarrow \partial_- U$ *satisfies*

(*i*) *for some constant* $0 < K < 1$, *we have* $\|h(x)\|_{W_0} \leq Ke^{s_0} \|x\|_{W_0}$;

(*ii*) *for the same constant* K, *we have* $\|h(x)\|_{\text{stab}} \leq Ke^{\frac{s_0}{2}} \|x\|_{\text{stab}}$, *whenever* $\|x\|_{W_0} < e^{-s_0}$;

(*iii*) *any element of* $([0,\delta) \cup (t_0 - \delta, t_0]) \times I_{1-e^{-s_0}}(W_0, \lambda_0) \times \{(0,0)\}$ *in* $\partial_+ U$ *which is not trapped is mapped by* h *to an element of* $([0, 2\delta) \cup (t_0 - 2\delta, t_0]) \times W_0 \times \{(0,0)\}$.

This local operation is somewhat opaque on a first reading, but the important points are as follows:

- in backward time, a codimension 0 subset of the flowlines intersecting $\partial_+ U$ will converge to a critical point in U;
- for flowlines which are not trapped, the effect of our local operation is controlled in each of our components. In fact, the effect can be made arbitrarily small in the t-component near the stabilization origin.

The second remark assumes that $s_0 > 0$ is relatively small, so that the holonomy in the W_0- and $\mathbb{D}^2$-components are also relatively small.

As stated here, the major advantage a blocking apparatus holds over a box fold is the control over the t-holonomy in certain regions. As can be seen in Figure 1.1, flowlines which are not trapped in backward time are forced by the box fold to fill up the t-interval $[0, t_0]$, wreaking havoc on the global dynamics. The blocking apparatus avoids this by rebalancing the holonomy in the W_0- and $\mathbb{D}^2$-components.

1.2.4 Applications

As we have discussed, our local operations are constructed with the goal of making Liouville domains Weinstein; less precisely, these operations are meant to "simplify Liouville dynamics." As an example of how such a simplification might play out, in Chapter 6 we will show that Mitsumatsu's well-known Liouville domains are stably Weinstein.

Mitsumatsu's construction will be reviewed in detail in Chapter 6, but for now let us recall that Mitsumatsu associates to each Anosov map $A\colon T^2 \to T^2$ a four-dimensional

Liouville domain (W_A, λ) whose skeleton is the mapping torus of A — a smooth, three-dimensional manifold. It follows that W_A does not admit a Weinstein structure, and thus (W_A, λ) is a Liouville-but-not-Weinstein domain.

However, we might wonder (as did Huang in [Hua19, Question 0.8]), whether (W_A, λ) is *stably* Weinstein. For instance, $W_A \times r_0\,\mathbb{D}^2$ has the homotopy type of a 3-manifold; can we conclude that $\lambda + \lambda_{\text{stab}}$ is Liouville homotopic to a Weinstein structure? In Chapter 6 we will show, using Proposition 1.7, that the answer is yes.

As was pointed out by Huang, this is an interesting phenomenon, because $W_A \times r_0\,\mathbb{D}^2$ is diffeomorphic to the cotangent bundle of $\mathrm{Skel}(W_A, \lambda)$, but cannot be symplectomorphic to this cotangent bundle, since the stabilization component of $W_A \times r_0\,\mathbb{D}^2$ allows us to displace the skeleton.

Our expectation is that the technology introduced in this paper can be used to simplify Liouville dynamics in more general settings. For instance, consider a Liouville domain (W^{2n}, λ) that admits a *global transversal* $M^{2n-1} \subset W$. That is, M is a codimension 1 submanifold-with-boundary through which all flowlines of W pass. If the contact manifold (M, λ) admits a partial open book decomposition compatible with the form[2] λ, then a collection of *partial* blocking apparatuses can be installed on the stabilization of (W, λ) to interrupt the flow through $M \times \{(0,0)\}$. This ensures that the flowlines of our perturbed stabilization flow backwards to critical points, and with a bit more care we can argue that this new domain is also free of broken loops. This strategy is inspired by the example of Honda-Huang in [HH19, Section 7.3]; continuing the analogy with Honda-Huang, one would hope to create a "backwards barricade" for an arbitrary (W, λ) — a collection of local transversals analogous to (M, λ) above — and then install several interrupters. The difficulty we currently face in carrying out this strategy lies in obtaining partial open book decompositions compatible with the contact forms on our local transversals. Certainly the strategy should not work if W does not have the homotopy type of a CW-complex of dimension $n+1$, and the question of how this topological consideration might interact

[2]We point out that compatibility with λ is strictly more difficult to achieve than is compatibility with $\ker \lambda$.

with the existence of a backwards barricade is the subject of ongoing investigation.

1.2.5 Organization

In Chapter 4 we develop the theory of box folds. This includes an an analysis of piecewise-linear box folds in Section 4.1 and a description of their smoothing in Section 4.2. Chapter 5 expands on the theory of box folds and develops more complicated variants that are used in the proof of Proposition 1.7. In particular, Section 5.1 develops the theory of chimney folds, and Section 5.2 introduces the blocking apparatus and proves Proposition 1.7. In Section 5.4 we begin developing the theory of partial folds, based over cobordisms. Finally, Chapter 6 — which was written in heavy collaboration with A. Christian — uses Proposition 1.7 to prove that Mitsumatsu's domains are stably Weinstein.

CHAPTER 2

Background

This chapter briefly introduces the necessary background on symplectic and contact geometry. More details on all of the concepts covered here can be found in standard references like [MS98], [Gei08], and [CE12].

2.1 Symplectic geometry

In symplectic geometry, the main objects of interest are symplectic manifolds. Here we introduce the basic notions and facts we will use, and defer to [MS98] and [CE12] for more information.

Definition. A **symplectic manifold** (W, ω) is a smooth manifold with a choice of closed, nondegenerate 2-form $\omega \in \Omega^2(W)$. The form ω is called a **symplectic form**. The symplectic manifold is **exact** if $\omega = d\lambda$ for some 1-form λ.

It is an exercise in linear algebra to show that any symplectic manifold is necessarily even dimensional. It is a second exercise via Stokes' theorem to show that there are no closed exact symplectic manifolds; exactness forces $(W, d\lambda)$ to either be open or with boundary. In this dissertation we will primarily be concerned with exact symplectic manifolds-with-boundary, and so we introduce some additional language.

Definition. A **Liouville form** on a symplectic manifold (W, ω) is a 1-form λ such that $\omega = d\lambda$. The vector field X_λ such that $i_{X_\lambda}\omega = \lambda$ is the **Liouville vector field** of λ.

Remark. Note that such a vector field X_λ exists and is unique by nondegeneracy of ω.

Definition. A **Liouville domain** is a compact[1] symplectic manifold (W, ω, X) with boundary, together with a globally defined Liouville vector field X which points transversally out of the boundary.

Remark. The data of a Liouville domain can also be given by (W, λ), where λ is the primitive 1-form of the symplectic form.

As discussed in the introduction, we are generally interested in the difference between Liouville domains and an upgraded type of symplectic manifold called a Weinstein domain.

Definition. A **Weinstein domain** (W, ω, X, f) is a Liouville domain (W, ω, X) equipped with a Morse function $f : W \to \mathbb{R}$ such that f is locally constant on ∂W and such that X is *gradient-like* for f, i.e.,

$$X(f) \geq \delta(|X|^2 + |df|^2)$$

for some choice of Riemannian metric on W and some $\delta > 0$.

Observe that if X is gradient-like for f, then Cauchy-Schawrz gives.

$$\delta|X|^2 \leq \delta(|X|^2 + |df|^2) \leq |X(f)| \leq |df||X| \quad \Rightarrow \quad \delta|X| \leq |df|.$$

On the other hand,

$$\delta|df|^2 \leq \delta(|X|^2 + |df|^2) \leq |X(f)| \leq |df||X| \quad \Rightarrow \quad |df| \leq \frac{1}{\delta}|X|.$$

Thus,

$$\delta|X| \leq |df| \leq \frac{1}{\delta}|X|.$$

In particular, the zeroes of X occur exactly at critical points of f, and $X(f) > 0$ away from critical points. This justifies the terminology. Furthermore, note that if ∇f is the gradient

[1] One can also define (open) Liouville manifolds and also Liouville cobordisms, but for now we will focus on Liouville domains.

vector field of $f : M \to \mathbb{R}$ for some choice of Riemannian metric, then

$$(\nabla f)(f) = df(\nabla f) = |\nabla f|^2 = \frac{1}{2}(|\nabla f|^2 + |df|^2)$$

so that gradient vector fields are indeed gradient-like.

Example 2.1. Here is the simplest example of a Weinstein domain. Consider the closed unit disc $W = \{x^2 + y^2 \leq 1\} \subseteq \mathbb{R}^2$ together with the standard symplectic form $\omega = dx \wedge dy$. Let $\lambda = \frac{1}{2}(x\,dy - y\,dx)$. Then $d\lambda = \omega$, hence λ is a Liouville form. An easy computation verifies that the radial vector field $X_\lambda = \frac{1}{2}(x\,\partial_x + y\,\partial_y)$. Indeed,

$$i_{\frac{1}{2}(x\,\partial_x + y\,\partial_y)}(dx \wedge dy) = \frac{1}{2}x\,dy - \frac{1}{2}y\,dx = \lambda.$$

The Liouville vector field X_λ is outwardly transverse to $\partial W = S^1$, so W is a Liouville domain.

Let $f : W \to \mathbb{R}$ be given by $f(x, y) = \frac{1}{4}(x^2 + y^2)$. Then f is Morse and constant on ∂W. Choose the standard Riemannian metric on $\mathbb{R}^2$. Then $X_\lambda = \nabla f$, hence X_λ is gradient-like for f and thus W is a Weinstein domain.

This example extends in the obvious way to the closed unit ball in $\left(\mathbb{R}^{2n}, \sum_{j=1}^n dx_j \wedge dy_j\right)$.

Weinstein domains have serious topological constraints. The following proposition describes this, and is a crucial motivating fact for much of the work in this dissertation.

Proposition 2.2. *Let (W^{2n}, ω, X, f) be a Weinstein domain. The index of each critical point of f does not exceed n.*

Proof. First, Cartan's formula gives

$$\mathcal{L}_{X_\lambda}\omega = i_{X_\lambda}d\omega + di_{X_\lambda}\omega = d\lambda = \omega.$$

The equation $\mathcal{L}_{X_\lambda}\omega = \omega$ implies that the flow ϕ_t of X_λ satisfies $\phi_t^*\omega = e^t\omega$. In words, the symplectic form expands as one flows along X_λ.

Let p be a critical point of f. Let

$$\Lambda_p = \left\{ q \in W \ : \ \lim_{t \to \infty} \phi_t(q) = p \right\}$$

be the stable manifold of p. For any $q \in \Lambda_p$,

$$\omega_q = e^{-t} \phi_t^* \omega_q.$$

Since $\phi_t(q) \to p$ as $t \to \infty$, sending $t \to \infty$ in the above equation gives $\omega_q = 0 \cdot \omega_p = 0$. So ω vanishes on Λ_p, hence Λ_p is an isotropic submanifold of W. It is a standard fact from symplectic linear algebra that an isotropic subspace of a symplectic vector space has dimension at most half the dimension of the full vector space; thus, $\dim \Lambda_p \leq n$. Since X_λ is (upward) gradient-like for f, this implies that the index of f at p is $\leq n$. □

Corollary 2.3. *For $n \geq 2$, the boundary of a $2n$-dimensional Weinstein domain is connected.*

Proof. By the previous proposition, every $2n$-dimensional Weinstein domain admits a handle decomposition involving k-handles for $k \leq n$. Observe that a $2n$-manifold has disconnected boundary only if it contains a $(2n-1)$-handle, since the belt sphere $\partial \mathbb{D}^\ell$ of a handle $\mathbb{D}^k \times \mathbb{D}^\ell$ is disconnected if and only if $\ell = 1$. If $n \geq 2$, a Weinstein domain has no $(2n-1)$-handles, and hence has connected boundary. □

Another class of vector fields that will (implicitly) very important for us is that of Hamiltonian vector fields.

Definition. Let $H : (W, \omega) \to \mathbb{R}$ be a smooth function, referred to as a **Hamiltonian function**. The unique vector field X_H satisfying $i_{X_H} \omega = dH$ is called the **Hamiltonian vector field** of H.

2.2 Contact geometry

Symplectic structures exist only in even dimensions. The natural odd dimensional counterpart is a *contact structure*. This section introduces the basic terminology and concepts that will be used throughout the dissertation; more details can be found in [Gei08].

Definition. A **contact manifold** is a pair (M^{2n+1}, ξ) where M is a smooth manifold of odd dimension, and ξ is a maximally nonintegrable hyperplane distribution. The distribution ξ is called a **contact structure**. When ξ is coorientable, we can write $\xi = \ker \alpha$ for some 1-form $\alpha \in \Omega^1(M)$ called a **contact form**.

Remark. The nonintegrability condition on ξ implies that if $\xi = \ker \alpha$ then

$$\alpha \wedge (d\alpha)^n \neq 0$$

on M, and hence a choice of contact form induces an orientation of M. Note also that if α is a contact form for ξ, then $f\,\alpha$ is also a contact form for ξ for any smooth $f : M \to \mathbb{R}^+$.

Example 2.4. The **standard contact structure** on $\mathbb{R}^{2n+1}$ is given by

$$\xi_{\text{std}} := \ker \alpha_{\text{std}} := \ker \left(dz - \sum_{j=1}^{n} y_j \, dx_j \right).$$

Example 2.5. Another common contact structure we will use on $\mathbb{R}^{2n+1}$ is the **radial standard contact structure**, given by

$$\xi_{\text{rad}} := \ker \alpha_{\text{rad}} := \ker \left(dz + \frac{1}{2} \sum_{j=1}^{n} x_j \, dy_j - y_j \, dx_j \right).$$

These two contact structures are actually the "same" from the viewpoint of contact geometry, in a way that is made precise by the following definition.

Definition. A **contactomorphism** between contact manifolds is a diffeomorphism $\phi : (M_1, \xi_1) \to (M_2, \xi_2)$ such that $\phi_* \xi_1 = \xi_2$. On the level of contact forms, if $\xi_j = \ker \alpha_j$

then $\phi : (M_1, \xi_1) \to (M_2, \xi_2)$ is a contactomorphism if $\phi^* \alpha_2 = f \alpha_1$ for some smooth $f : M \to \mathbb{R}^+$. A contactomorphism satisfying $\phi^* \alpha_2 = \alpha_1$ is called a **strict contactomorphism**. Finally, two contact structures ξ_1 and ξ_2 on the same manifold M are **isotopic** if there is a contactomorphism $\phi : (M, \xi_1) \to (M, \xi_2)$ that is isotopic (through contactomorphisms) to the identity.

Generally we only care about contact structures up to contactomorphism, or even isotopy. The standard contact structures ξ_{std} and ξ_{rad} are contactomorphic, and more generally one can show that contact structures have no local invariants, just as in symplectic geometry.

Theorem 2.6 (Darboux's theorem)**.** *Let (M^{2n+1}, ξ) be a contact manifold, and let $p \in M$. There is an open neighborhood $p \in U$ and a contactomorphism $\phi : (U, \xi \mid_U) \to (\mathbb{R}^{2n+1}, \xi_{\text{std}})$ with $\phi(p) = 0$.*

A natural source of examples of contact manifolds, particularly in the context of this thesis, is as the boundary of a Liouville or Weinstein domain, or more generally as any hypersurface in an exact symplectic manifold transverse to a Liouville vector field. For example, suppose that (W, λ) is a Liouville domain with boundary ∂W. Let $\alpha := \lambda \mid_{\partial W}$. Note that

$$\lambda \wedge (d\lambda)^{n-1} = i_{X_\lambda} d\lambda \wedge (d\lambda)^{n-1} = \frac{1}{n} i_{X_\lambda} (d\lambda)^n.$$

Since $(d\lambda)^n$ is a volume form on W and $X \pitchfork \partial W$, $i_{X_\lambda}(d\lambda)^n$ restricts to a volume form on ∂W, hence α is contact.

More generally, there is a strong interplay between contact and exact symplectic structures that will be used extensively throughout this dissertation.

Definition. Let (M, α) be a contact manifold. The **symplectization of** (M, α) is the exact symplectic manifold

$$(\mathbb{R}_s \times M,\ \lambda := e^s \alpha)$$

Let (W, λ) be an exact symplectic manifold. The **contactization of** (W, β) is the contact manifold

$$(\mathbb{R}_z \times W,\ \alpha := dz + \lambda).$$

2.2.1 Convex hypersurface theory

There is a certain class of hypersurfaces in contact manifolds of central importance. These are the so called *convex* hypersurfaces, first investigated by Eliashberg, Gromov, and Giroux [EG91, Gir91]. We begin by discussing characteristic foliations of general hypersurfaces.

Definition. If Σ is a hypersurface in a contact manifold $(M, \xi = \ker \alpha)$, the **characteristic foliation** is the singular 1-dimensional foliation

$$\Sigma_\xi = (T\Sigma \cap \xi \mid_\Sigma)^\perp$$

where $\perp$ is the symplectic orthogonal complement taken with respect to the conformal symplectic structure on ξ. If $\beta := \alpha \mid_\Sigma$, then

$$\Sigma_\xi = \ker \left(d\beta \mid_{\ker \beta} \right).$$

If Σ is oriented, Σ_ξ inherits a natural orientation. In this case, a convenient way to compute the characteristic foliation on an orientable hypersurface $\Sigma^{2n} \subset M^{2n+1}$ is given by Lemma 2.5.20 in [Gei08].

Lemma 2.7. [*Gei08*] *Let $\beta = \alpha \mid_\Sigma$ and let Ω be a volume form on Σ. The characteristic foliation Σ_ξ is directed by the vector field X satisfying*

$$i_X \Omega = \beta \, (d\beta)^{n-1}. \tag{2.1}$$

In three dimensional contact manifolds, the characteristic foliation alone determines the contact germ near a hypersurface [Gir91]. In higher dimensions we have the following weaker fact.

Lemma 2.8. [*HH19*] *Let $(M, \xi_i = \ker \alpha_i)$ for $i = 0, 1$ be two contact structures on the same manifold. Let $\beta_i = \alpha_i \mid_\Sigma$ and suppose that $\beta_0 = g\beta_1$ for some $g > 0$. Then there is an isotopy $\phi_s : M \to M$ such that $\phi_s(\Sigma) = \Sigma$, $\phi_0 = id_M$, and $(\phi_1)_*(\xi_0) = \xi_1$ in a neighborhood of Σ.*

Any submanifold of Σ transverse to the characteristic foliation is a contact submanifold of M. Furthermore, flowing along the characteristic foliation induces a contactomorphism of the transversal.

Definition. A **contact vector field** V in a contact manifold $(M, \xi = \ker \alpha)$ is one whose flow $\phi_t : M \to M$ is a contactomorphism for all t.

There is a one-to-one correspondence between contact vector fields V and "contact Hamiltonian functions" $C^\infty(M)$, see Section 2.3 of [Gei08]. Given $H \in C^\infty(M)$, the corresponding contact vector field is determined uniquely by the conditions

$$\alpha(X_H) = H \qquad \text{and} \qquad i_{X_H} d\alpha = dH(R_\alpha)\,\alpha - dH. \tag{2.2}$$

A vector field V is contact if and only if $\mathcal{L}_V \alpha = g\alpha$ for some smooth $g : M \to \mathbb{R}$. The Reeb vector field R_α is an example of a contact vector field.

Definition. A hypersurface $\Sigma \subset (M, \xi)$ is **convex** if there is a contact vector field V everywhere transverse to Σ.

One can characterize convexity at the differential form level as follows.

Lemma 2.9. [*Gir91*] *An embedded oriented hypersurface Σ is convex if and only if there is an neighborhood $\Sigma \times \mathbb{R}$ of $\Sigma = \Sigma \times \{0\}$ in M such that $\xi = \ker(u\,dt + \beta)$, where t is the $\mathbb{R}$-coordinate, β is a (t-independent) 1-form on Σ, and u is a (t-independnet) function $u : \Sigma \to \mathbb{R}$.*

Note that any 1-form on $\mathbb{R} \times \Sigma$ can be written $u_t\,dt + \beta_t$ for some family of smooth functions $u_t : \Sigma \to \mathbb{R}$ and family of 1-forms β_t on Σ. Convexity requires a form which is t-invariant. A convex hypersurface is naturally divided into three regions in the following way. Write $\alpha = u\,dt + \beta$ near Σ. Then

$$R^+(\Sigma) = \{u > 0\} \quad \text{and} \quad R^-(\Sigma) = \{u < 0\}$$

are the positive and negative region, respectively, and $\Gamma = \{u = 0\}$ is a codimension 1 submanifold of Σ called the dividing set. The dividing set (which depends on the choice of contact vector field) is well-defined up to isotopy of dividing sets.

Remark. In a convex hypersurface, $R^+(\Sigma)$ and $R^-(\Sigma)$ inherit a Liouville structure from $\beta = \alpha\,|_{R^{\pm}(\Sigma)}$. If X denotes the Liouville vector field (for either $R^+(\Sigma)$ or $R^-(\Sigma)$), then the characteristic foliation on $R^+(\Sigma)$ is directed by X and the characteristic foliation on $R^-(\Sigma)$ is directed by $-X$.

CHAPTER 3

Morse-Smale characteristic foliations

In this chapter we study convexity of hypersurfaces in contact manifolds by way of their characteristic foliations as outlined in Section 1.1. In particular, in Section 3.1 we prove Theorem 1.1, the generalization of Giroux's convexity criterion [Gir91]. Specifically, we prove Proposition 1.2, which classifies the local symplectic behavior of periodic orbits, and use this to prove Theorem 1.1. In Section 3.2 we analyze the closed hypersurfaces due to Mori [Mor11] and use Theorem 1.1 to prove their (perturbed) convexity.

3.1 Proof of Theorem 1.1

We begin by proving Proposition 1.2, which allows us to definitively place an orbit in either the positive or negative region. First, the dynamical systems notion of hyperbolicity will be central in Chapter 3. We refer to [PPM98] for more details.

Definition. Let γ be a periodic orbit of a vector field X, and let L be a transversal to X which intersects γ once. The **Poincare first return map** is the map $P : V \subset L \to L$ defined by following the trajectories of X from some open subset V of L to their first point of return to L. The orbit γ is **hyperbolic** if the eigenvalues μ of TP satisfy $0 < |\mu| \neq 1$.

Proof of Proposition 1.2. The general strategy of the proof is to show that the divergence of a vector field directing the characteristic foliation near the hyperbolic periodic orbit γ is nonzero. This proves that γ is Liouville.

Step 1: Analyzing the differential of the Poincare first-return map.

Let L be a transversal to the periodic orbit and $V \subset L$ an open subset diffeomorphic

to $\mathbb{R}^{2n-1}$ containing $\{0\} = \gamma \cap L$ such that the Poincare first-return map $P : V \to L$ is defined. Let $\lambda = \alpha \mid_L$ be the induced contact form on L. Because P is defined by following the trajectories of the flowlines of Σ_ξ, P is a contactomorphism. Thus, $P^*\lambda = f\lambda$ for some $f > 0$.

Next, we compute a matrix representative for $T_0P : T_0V \to T_0L$. Let $R = R_\lambda(0)$, the Reeb vector field for λ at 0, and let $\{R, v_1, \ldots, v_{2n-2}\}$ be a basis for T_0V such that $\{v_1, \ldots, v_{2n-2}\}$ is a symplectic basis for $\ker \lambda$ with respect to the symplectic structure induced by $d\lambda$. Write $T_0P(R) = C\,R + v$ for some constant C and some $v \in \ker \lambda$. Since P is a contactomorphism, $\ker \lambda$ is invariant under P. Thus, with respect to the above basis we have

$$[T_0P] = \begin{pmatrix} C & 0 \\ * & M \end{pmatrix}$$

where 0 is a $1 \times (2n-2)$ matrix of zeroes and $*$ is a $(2n-2) \times 1$ matrix determined by $T_0P(v)$. Since

$$C = \lambda(C\,R + v) = \lambda(T_0P(R)) = P^*\lambda(R) = f(0)$$

it follows that one of the eigenvalues of T_0P is $C = f(0)$. The assumption that γ is hyperbolic is precisely the assumption that the eigenvalues of $T_0P : T_0V \to T_0L$ satisfy $|\mu| \neq 1$ (and $\mu \neq 0$). Thus, $C > 1$ or $0 < C < 1$.

Next, since $P^*d\lambda = df\,\lambda + f\,d\lambda$,

$$P^*d\lambda \mid_{\ker \lambda} = f(0)\,d\lambda \mid_{\ker \lambda}.$$

This implies that $M^T J_0 M = C\,J_0$, where J_0 is the skew-symmetric matrix corresponding to the symplectic structure on $\ker \lambda$. Let $M' = C^{-\frac{1}{2}}M$. Then

$$(M')^T J_0 (M') = C^{-1} M^T J_0 M = J_0$$

so that M' is a symplectic matrix. Thus, to summarize Step 1:

$$[T_0 P] = \begin{pmatrix} C & 0 \\ * & \sqrt{C}\, M' \end{pmatrix} \tag{3.1}$$

where either $0 < C < 1$ or $C > 1$, and M' is a symplectic matrix.

Step 2: Determining the divergence of the characteristic foliation.

Let X be a vector field directing the characteristic foliation near γ. Let θ be a coordinate on γ. By considering a volume form $\Omega = d\theta\, \Omega'$ where Ω is a (possibly θ-dependent) volume form in the transverse direction, we may assume that $X = \partial_\theta + Y$ where Y is a vector field in the transverse direction which has a hyperbolic zero at 0. By considering the divergence, to show that γ is Liouville it suffices to show that $\operatorname{div}(Y)(= \operatorname{div}(X))$ is nonzero along γ.

Reparametrizing if necessary, we may further assume that $P(x) = \phi_t(x)$, where ϕ_1 is the flow of Y. By the Hartman-Grobman theorem (see Section 2.4 of [PPM98]), in a small neighborhood of 0 it is sufficient to consider the flow of the linearization of Y, which we denote by Ax. Here $x \in \mathbb{R}^{2n-1}$ and A is a square matrix.

Note that $(\operatorname{div} Y)(0) = \operatorname{tr} A(0)$. Because $P(x) = \phi_1(x)$, by standard linear dynamical systems theory it follows that $[T_0 P] = e^{A(0)}$. Since $\det(e^A) = e^{\operatorname{tr} A}$,

$$(\operatorname{div} Y)(0) = \operatorname{tr} A(0) = \log \det [T_0 P].$$

Since the determinant of any symplectic matrix is 1, (3.1) implies $\det[T_0 P] = C \cdot \sqrt{C}^{2n-2} = C^n$. Thus,

$$(\operatorname{div} Y)(0) = n \log C.$$

Since $C > 1$ or $0 < C < 1$, this shows that $\operatorname{div} X \neq 0$ in a sufficiently small neighborhood of γ.

This proves that a hyperbolic orbit is Liovuille. In particular, if $f(0) > 1$ then γ is positive Liouville and if $f(0) < 1$ then γ is negative Liouville.

Step 3: Computing the index of a positive orbit.

Suppose that γ is a positive hyperbolic orbit. Consider $[T_0P]$ as in (3.1). Since γ is positive, $C > 1$. Let E^- denote the subspace of generalized eigenvectors with eigenvalues of modulus < 1. We claim that $\dim E^- \leq n-1$. The final claim in the proposition then follows, as the dimension of the stable manifold is $\leq (n-1)+1 = n$ after accounting for the orbit direction.

It is a standard fact (see, for example, [MS98]) that if μ' is an eigenvalue of a symplectic matrix M', then $(\mu')^{-1}$ is also an eigenvalue with the same multiplicity. This implies that if μ is an eigenvalue of $M = \sqrt{C}\,M'$, then $C\mu^{-1}$ is also an eigenvalue of M with equal multiplicity. In particular, if $|\mu| < 1$ then $|C\mu^{-1}| > 1$. Thus, there are at most $n-1$ eigenvalues of M with modulus less than 1, which proves the claim.

□

Now we can adapt the arguments in [Gir91] and [HH19] to prove that a Morse-Smale characteristic foliation is sufficient for convexity in arbitrary dimensions.

Proof of Theorem 1.1. Suppose that Σ_ξ is Morse-Smale. To show that Σ is convex (up to a contact isotopy of M which fixes Σ), it suffices by Lemma 2.8 to construct a vertically invariant contact form α_1 on a neighborhood of Σ such that $\beta_1 = g\beta$ for some $g > 0$. Here $\beta_1 = \alpha_1 \,|_\Sigma$ and $\beta = \alpha\,|_\Sigma$. Throughout the proof we will loosely use g to denote a sufficient positive function.

Classify each singular point p of Σ_ξ as either positive or negative in the natural way, i.e., based on the orientations of ξ_p and $T_p\Sigma$. Classify each periodic orbit as either positive or negative according to Proposition 1.2.

We claim that there is no flow line from a negative critical point or orbit to a positive critical point or orbit. Indeed, as mentioned in the introduction, the Morse index of a positive critical point p satisfies $\mathrm{ind}(p) \leq n$. By Proposition 1.2, the Morse index of any positive orbit also satisfies $\mathrm{ind}(\gamma) \leq n$. The transversality assumption in Definition 1.1 implies that the stable manifold of any positive critical point or orbit and the unstable

manifold of any negative critical point or orbit either do not intersect, or the dimension of the intersection is 0. In either case, there can be no flow line (necessarily one-dimensional) from a negative point or orbit to a positive point or orbit.

Next, we will construct open sets U^+ and U^- in Σ containing all positive and negative points and orbits, respectively, and then use the resulting decomposition of Σ to define α_1. In particular, U^+ and U^- will be "prototypes" for $R^+(\Sigma)$ and $R^-(\Sigma)$.

Step 1: Constructing U^+.

For any set $S \subset \Sigma$, let $\mathrm{Op}(S)$ denote a sufficiently small open neighborhood of S in Σ.

Let $\{x_1, x_2, \cdots, x_M\}$ be the list of positive orbits and points (i.e., x_i can be a critical point or an orbit). Let U_k be the union of $\mathrm{Op}(\{x_1, x_2, \cdots, x_k\})$ with sufficiently small tubular neighborhoods of the stable manifolds of $x_1, \ldots, x_{k-1}$. Because there is no trajectory from a negative point or orbit, we may assume that the list $\{x_1, \ldots, x_M\}$ is ordered so that a tubular neighborhood of the stable manifold of x_{k+1} intersects ∂U_k in a contact submanifold. Here the contact assumption comes from choosing U_k so that ∂U_k is transverse to the characteristic foliation. Finally, let $U^+ = U_M$.

Step 2: Defining β_1 on U^+.

We will define β_1 on U^+ by inducting on k. Note that $U_1 = \mathrm{Op}(x_1)$ and by assumption, $\beta_1 := g\beta$ is positive Liouville on U_1 for some $g > 0$. Now suppose that β_1 has been constructed on U_k. By assumption, $g\beta$ is Liouville on $\mathrm{Op}(x_{k+1})$. Using the flow of the characteristic foliation and the above remark about the stable manifold of x_{k+1}, we may identify

$$U_{k+1} \setminus (U_k \cup \mathrm{Op}(x_{k+1}))$$

with $[0,1] \times L$ where L is a contact submanifold. Here, $\{0\} \times L \subseteq \partial U_k$ and $\{1\} \times L \subseteq \partial \mathrm{Op}(x_{k+1})$. Because L is a contact submanifold of M, $\lambda = \beta\,|_L$ is a contact form on L. Since the flow of the characteristic foliation is a contactomorphism of L, we have $\beta = h\,\lambda$ on

$[0,1]_s \times L$ for some smooth $h > 0$. Note that

$$d\beta = \frac{\partial h}{\partial s}\, ds\, \lambda + d_L h\, \lambda + h\, d\lambda$$

and so

$$(d\beta)^n = nh^{n-1}\, \frac{\partial h}{\partial s}\, ds\, \lambda\, (d\lambda)^{n-1}. \tag{3.2}$$

Thus, β is Liouville if $\frac{\partial h}{\partial s} > 0$. After scaling β by a sufficiently large constant on $\mathrm{Op}(x_{k+1})$, the function h can be multiplied by a positive function $\frac{h_1}{h}$ so that $\frac{\partial h_1}{\partial s} > 0$ on $[0,1]_s \times L$. With β_1 defined on U_{k+1} in this way, β_1 is positive Liouville on U_{k+1}.

Inductively, this defines β_1 on U^+ so that $\beta_1 = g\beta$ is a positive Liouville form.

Step 3: Constructing U^- and defining β_1 on U^-.

Define an open neighborhood U^- together with a negative Liouville form $\beta_1 = g\beta$ in the analogous way using negative singular points and negative periodic orbits together with the unstable manifolds of each.

Step 4: Defining β_1 near the dividing set.

By the above steps, U^+ and U^- are disjoint open sets in Σ containing all singular points and orbits. Furthermore, there are no flowlines running from U^- to U^+. Thus, using the flow of Σ_ξ we may identify $\Sigma \setminus (U^+ \cup U^-)$ with $[-1,1]_s \times \Gamma$ for some submanifold Γ, where $\{-1\} \times \Gamma = \partial U^+$, $\{1\} \times \Gamma = \partial U^-$, and Σ_ξ is directed by ∂_s. Let λ be the induced contact form on Γ. On $[-1,1] \times \Gamma$, $\beta = h\,\lambda$. We then have $\frac{\partial h}{\partial s} > 0$ near $\{-1\} \times \Gamma$ and $\frac{\partial h}{\partial s} < 0$ near $\{1\} \times \Gamma$ (see the remark after (3.2)). Multiply h by a function $\frac{h_1}{h}$ so that $\frac{\partial h}{\partial s} > 0$ for $-1 \leq s < 0$, $\frac{\partial h_1}{\partial s} = 0$ for $s = 0$, and $\frac{\partial h_1}{\partial s} < 0$ for $0 < s \leq 1$. Let $\beta_1 = h\,\lambda$.

Step 5: Defining the vertically invariant contact form α_1 on $\mathbb{R} \times \Sigma$.

Decompose $\mathbb{R}_t \times \Sigma$ as

$$\left(\mathbb{R} \times U^+\right) \cup \left(\mathbb{R} \times U^-\right) \cup \left(\mathbb{R} \times [-1,1] \times \Gamma\right).$$

Let $\alpha_1 = dt + \beta_1$ on $\mathbb{R} \times U^+$ and let $\alpha_1 = -dt + \beta_1$ on $\mathbb{R} \times U^-$. Since β_1 is positive (negative) Liouville on U^+ (U^-), α_1 defines a contact form on these regions. Furthermore, by construction, $\alpha_1 \mid_{U^\pm} = g\beta$ for some $g > 0$.

To define α_1 on $\mathbb{R} \times [-1,1] \times \Gamma$, let $u : [-1,1] \to \mathbb{R}$ be a smooth function such that $u'(s) < 0$ for $-1 < s < 1$, $u'(s) = 0$ for $|s| = 1$, $u(-1) = 1$, $u(0) = 0$, and $u(1) = -1$. Let $\alpha_1 = u\,dt + \beta_1$. Then α_1 is a smoothly defined 1-form on $\mathbb{R} \times \Sigma$, and

$$\alpha_1 \, (d\alpha_1)^n = n \left(u^n \, \frac{\partial h_1}{\partial s} - \frac{\partial u}{\partial s} \, h_1^n \right) dt \, ds \, \lambda \, (d\lambda)^{n-1}.$$

One may verify that with an appropriate choice of h_1 as defined in Step 4,

$$u^n \, \frac{\partial h_1}{\partial s} - \frac{\partial u}{\partial s} \, h_1^n > 0. \tag{3.3}$$

If n is even, then for $0 < s \leq 1$ we require

$$\left| \frac{\partial h_1}{\partial s} \right| < \left| \frac{\partial u}{\partial s} \right| \cdot \left| \frac{h_1}{u} \right|^n$$

which can be arranged by making h_1 sufficiently flat. Otherwise, the definitions of u and h_1 force (3.3) to hold. Thus, α_1 is a vertically invariant contact form defined near Σ such that $\alpha_1 \mid_\Sigma = g\beta$ for some positive function g. By the remark at the beginning of the proof, Σ is convex.

□

3.2 Applications

In this section we provide some further analysis on a non-convex hypersurface introduced by A. Mori. We begin with some generalities, and then in 3.2.1 we review the definition of the hypersurface, the argument for its non-convexity, and then prove that there is C^∞-small perturbation of the hypersurface to a convex hypersurface.

First, a lemma which computes the perturbation of the characteristic foliation in a

particular model.

Lemma 3.1. *Consider the contact manifold $\mathbb{R}_t \times S^1_\theta \times L^{2n-1}$ with contact form $\alpha = t\,d\theta + \lambda$, where λ is a contact form on L. Let $H : L \to \mathbb{R}$ be a smooth function, and let $\tilde{\Sigma} = \{t = H\}$. Let X_H be the contact vector field corresponding to the contact Hamiltonian H as in* (2.2)*. Then the characteristic foliation of $\tilde{\Sigma}$ is directed by $\partial_\theta - X_H$.*

Proof. Let $\Omega = d\theta\,\lambda\,(d\lambda)^{n-1}$. Since $\lambda\,(d\lambda)^{n-1}$ is a volume form on L and $\tilde{\Sigma}$ is a graph over $\{t = 0\}$, Ω is a volume form on $\tilde{\Sigma}$. Using (2.2), one may compute

$$\begin{aligned} i_{\partial_\theta - X_H}\Omega &= \lambda\,(d\lambda)^{n-1} + d\theta\, i_{X_H}\left(\lambda\,(d\lambda)^{n-1}\right) \\ &= \lambda\,(d\lambda)^{n-1} + H\,d\theta\,(d\lambda)^{n-1} + (n-1)\,d\theta\,\lambda\,dH\,(d\lambda)^{n-2}. \end{aligned}$$

On the other hand, let $\beta = \alpha\,|_{\tilde{\Sigma}}$. Then $\beta = H\,d\theta + \lambda$ and $d\beta = dH\,d\theta + d\lambda$ so that

$$\beta\,(d\beta)^{n-1} = \lambda\,(d\lambda)^{n-1} + H\,d\theta\,(d\lambda)^{n-1} + (n-1)\,d\theta\,\lambda\,dH\,(d\lambda)^{n-2} = i_{\partial_\theta - X_H}\Omega.$$

By Lemma 2.7, $\partial_\theta - X_H$ directs the characteristic foliation. □

This lemma becomes useful in the context of Theorem 1.1 when X_H is a pseudo-gradient for a Morse function on L. In this case, $\tilde{\Sigma} \cong S^1 \times L$ has Morse-Smale characteristic foliation. Indeed, there are finitely many hyperbolic periodic orbits directed by ∂_θ corresponding to the zeroes of X_H.

The existence of a Morse function admitting a gradient-like contact vector field is the defining feature of a *convex contact structure*, first introduced by Eliashberg and Gromov in [EG91] and studied further by Giroux in [Gir91].

Theorem 3.2 (Giroux, see [CM18, Sac])**.** *Every contact manifold admits a contact vector field which is gradient-like for some Morse function.*

With this fact and Theorem 1.1, we have the following corollary.

Corollary 3.3. *Let $\Sigma^{2n} \subset (M^{2n+1}, \xi = \ker \alpha)$ be a hypersurface in a contact manifold diffeomorphic to $S^1 \times L^{2n-1}$ for some closed manifold L. Suppose that the characteristic foliation Σ_ξ consists of completely degenerate periodic orbits, so that the foliation is directed by ∂_θ for some choice of coordinate θ on S^1. Then there is an arbitrarily C^∞-small perturbation of Σ to a convex hypersurface.*

Proof. Because $\{\theta\} \times L \subset \Sigma$ is transverse to the characteristic foliation, $\alpha \mid_{\{\theta\}\times L}$ is contact. By Lemma 2.8, we may take a sufficiently small neighborhood of Σ to be contactomorphic to $\mathbb{R}_t \times S^1_\theta \times L^{2n-1}$ with contact form $\alpha = t\, d\theta + \lambda$, where λ is a contact form on L and $\Sigma = \{t = 0\}$. By Theorem 3.2, we may choose a contact vector field X_H on L which is gradient-like for some Morse function on K. By scaling the corresponding contact Hamiltonian H, we may assume that the C^∞ norm of H is as small as we like. Then $\tilde{\Sigma} = \{t = H\}$ will be C^∞-close to Σ, and by Lemma 3.1 the characteristic foliation of $\tilde{\Sigma}$ is directed by $\partial_\theta - X_H$. Since this vector field is Morse-Smale, by Theorem 1.1, Σ is convex. □

In particular, the proof of this corollary shows that any completely degenerate periodic orbit in a characteristic foliation can be locally perturbed to be hyperbolic.

3.2.1 Mori's hypersurface

In [Mor11], Mori introduced a particular non-convex hypersurface. We review the definition here. Consider

$$\mathbb{R}^{2n+1} = \mathbb{R}_z \times \mathbb{R}^2_{r,\theta} \times \mathbb{R}^2_{\rho_1,\phi_1} \times \cdots \times \mathbb{R}^2_{\rho_{n-1},\phi_{n-1}}$$

where (r, θ) and (ρ_i, ϕ_i) are polar coordinates in their respective planes. Let

$$\alpha = (2r^2 - 1)\, dz + r^2(r^2 - 1)\, d\theta + \sum_{i=1}^{n-1} \rho_i^2\, d\phi_i. \tag{3.4}$$

One can check that α is a contact form. Next, for $0 < \varepsilon << 1$, let

$$\Sigma_0 = \left\{ r^2 + \varepsilon^{-2} \left(z^2 + \sum_{i=1}^{n-1} \rho_i^2 \right) = 1 + \varepsilon \right\}.$$

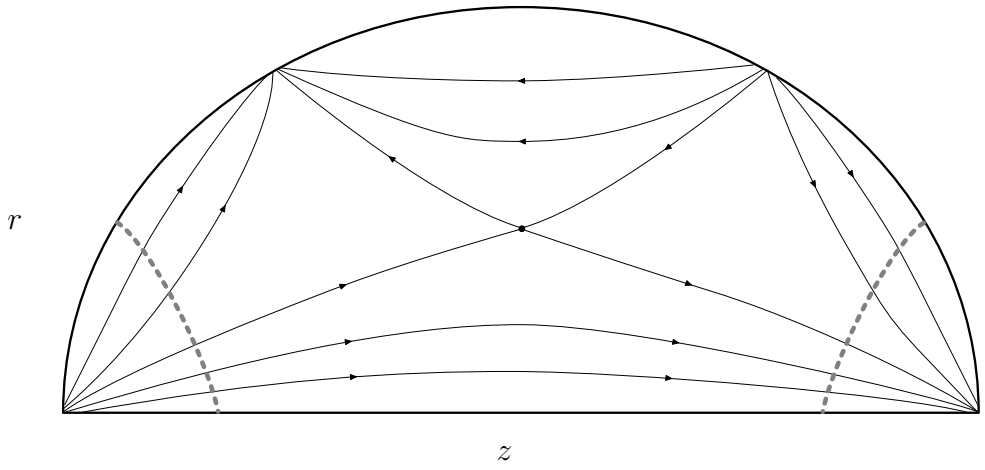

Figure 3.1: The pushforward of X to $\tilde{X}$ on the quarter ellipsoid $\tilde{\Sigma}$, followed by a further projection of $\tilde{X}$ to the (z, r)-plane.

Note that Σ_0 is diffeomorphic to S^{2n}.

Lemma 3.4. [*Mor11*] *The characteristic foliation on* $\Sigma_0 \subset (\mathbb{R}^{2n-1}, \ker \alpha)$ *is directed by the vector field*

$$\begin{aligned} X = \left[(r^2-1)^2 + (2r^2-1)(\varepsilon^{-2}z^2 - \varepsilon)\right]\, \partial_z \\ + \varepsilon^{-2} r(r^2-1) z\, \partial_r + (1 + 2\varepsilon - 2\varepsilon^{-2}z^2)\, \partial_\theta \\ + \varepsilon^{-2}(2r^2-1) z \sum_{i=1}^{n-1} \rho_i\, \partial_{\rho_i} + \varepsilon^{-2}(2r^4 - 2r^2 + 1) \sum_{i=1}^{n-1} \partial_{\phi_i}. \end{aligned} \tag{3.5}$$

We may visualize the characteristic foliation as follows [Mor11]. Observe that the vector field X from Lemma 3.4 does not depend on θ or ϕ_i. Thus, if we project $P : \Sigma_0 \to \tilde{\Sigma}_0$ to the quarter ellipsoid $\tilde{\Sigma}_0 = \{z^2 + r^2 + \rho^2 = 1 + \varepsilon\} \subseteq \{\, (z, r, \rho) \;:\; r, \rho \geq 0 \,\}$ where $\rho^2 = \rho_1^1 + \cdots + \rho_{n-1}^2$, the vector field X has a well-defined pushforward $\tilde{X}$ given by

$$\begin{aligned} \tilde{X} = \left[(r^2-1)^2 + (2r^2-1)(\varepsilon^{-2}z^2 - \varepsilon)\right]\, \partial_z \\ + \varepsilon^{-2} r(r^2-1) z\, \partial_r + \sqrt{n-1}\varepsilon^{-2}(2r^2-1) z\rho\, \partial_\rho. \end{aligned}$$

This pushforward is visualized in Figure 3.1. Observe that $\tilde{X}$ is Morse-Smale.

In [Mor11] it was proven that Σ_0 is not convex. For completeness, we provide the argument here with some more details.

Lemma 3.5. [*Mor11*] *The hypersurface Σ_0 is not convex.*

Proof. Let $p = (0, r^*, 1 + \varepsilon - (r^*)^2)$ denote the point on $\tilde{\Sigma}_0$ which is the hyperbolic zero of $\tilde{X}$. Observe that

$$P^{-1}(p) = \left\{ (\theta, \rho_1, \phi_1, \ldots, \rho_{n-1}, \phi_{n-1}) \ : \ \rho^2 = 1 + \varepsilon - (r^*)^2 \right\}$$

is diffeomorphic to $S^1_\theta \times S^{2n-3}$. The characteristic foliation along $P^{-1}(p)$ is directed by the vector field

$$(1 + 2\varepsilon)\, \partial_\theta + \varepsilon^{-2}(2(r^*)^4 - 2(r^*)^2 + 1) \sum_{i=1}^{n-1} \partial_{\phi_i}$$

By adjusting ε if necessary, we may assume that this vector field foliates $S^1 \times S^{2n-3}$ with periodic orbits, hence the characteristic foliation along $P^{-1}(p)$ consists of parallel leaves.

Suppose for the sake of contradiction that Σ_0 is convex. Then there is a dividing set Γ. Because $(\Sigma_0)_\xi$ is independent of θ and ϕ_i, we may isotope Γ so that $\Gamma = P^{-1}(C)$ for some multicurve $C \subset \tilde{\Sigma}_0$.

We claim that C does not contain p. Suppose it did: then Γ contains the linearly foliated $P^{-1}(p)$. By [Gir91], there is a function $u : \Sigma \to \mathbb{R}$ for which $X(u) < 0$ on $P^{-1}(p)$, which contradicts the fact that X has closed orbits on $P^{-1}(p)$. Thus, C avoids p. Finally, note that the singular points of X are

$$(z = \pm\varepsilon\sqrt{1 + \varepsilon}, r = 0, \theta, \rho_1 = 0, \phi_1, \ldots, \rho_{n-1} = 0, \phi_{n-1}).$$

For divergence reasons, these must lie in the negative and positive region, respectively. The remaining singular points of $\tilde{X}$ are

$$(z = \pm\varepsilon\sqrt{\varepsilon}, r = 1, \rho = 0)$$

which lift under P to periodic orbits that must lie in the positive and negative region,

respectively. Consequently, C must contain a component which is isotopic to one of the dashed gray curves in Figure 3.1.

The lift of either of these curves under P is diffeomorphic to S^{2n-1}. Moreover, there are necessarily other components of Γ. This contradicts a theorem of McDuff [McD91], as the positive region of Σ_0 is then a symplectic manifold with convex boundary of the type $S^{2n-1} \sqcup S'$ for some other $2n-1$-manifold S'. Thus, no such dividing set can exist and so Σ_0 is not convex.

□

Using ideas inspired by the the proof of Corollary 3.3, we prove Corollary 1.3.

Proof of Corollary 1.3. By Theorem 1.1, it suffices to perturb Σ_0 so that the resulting characteristic foliation is Morse-Smale. Lemma 3.4, the subsequent discussion, and the proof of Lemma 3.5 show that the characteristic foliation is close to being Morse-Smale. The obstruction is $P^{-1}(p) \cong S^1 \times S^{2n-3}$, which is foliated by parallel leaves. The pushforward $\tilde{X}$ (in the $\tilde{\Sigma}_0$ direction) is Morse-Smale, so it suffices to perturb the hypersurface near $P^{-1}(p)$ so that the resulting foliation, when restricted to $P^{-1}(p)$, is Morse-Smale.

Observe that for any fixed θ_0, the contact form α in (3.4) restricts to the standard contact structure on $L = \{\theta_0\} \times S^{2n-3} \subseteq P^{-1}(p)$. Let U be a small neighborhood of p in $\tilde{\Sigma}_0$. Then $U \times L$ is transverse to the characteristic foliation and hence is also contact. Using the flow of the characteristic foliation starting at $U \times L$, we isolate a "column" $[0,1]_s \times U \times L$ where the characteristic foliation is directed by ∂_s. Note that we may take the foliation on top of the L component to already be "straight", so this identification only straightens out the foliation above the U component. By Lemma 2.8, we may assume that a neighborhood of the column is given by

$$\mathbb{R}_t \times [0,1]_s \times U \times L \quad \text{with contact form} \quad t\,ds + \lambda$$

where λ is contact on $U \times L$, $\lambda\,|_L$ is the standard contact form on S^{2n-3}, and Σ_0 is identified with $\{t = 0\}$. Finally, note that $[0,1]_s \times \{p\} \times L \subset P^{-1}(p)$. Our perturbation will be

supported in this column.

Pick a C^∞-small contact Hamiltonian $H : L \to \mathbb{R}$ such that the corresponding contact vector field X_H is gradient-like for a Morse function. In particular, we may choose X_H to be gradient-like for a height function on the sphere ([Gir91], [Sac]) so that X_H has one source singularity and one sink singularity. Extend H to $U \times L$ via a bump function which is constant near p. Finally, extend H in the s direction so that it is supported in the column $[0,1]_s \times U \times L$. Let $\Sigma_1 = \{t = H\}$. Because $\tilde{X}$ is hyperbolic at p and thus structurally stable [PPM98], the location of the zero may shift slightly from p to some other point p_1, when perturbed as above, but the hyperbolic dynamics in the $\tilde{\Sigma}_0$ direction persist if the perturbation is small enough. As in Corollary 3.3, the degenerate dynamics of the characteristic foliation on $P^{-1}(p_1)$ will be perturbed by the gradient-like vector field X_H in the L direction. As a result, the characteristic foliation of Σ_1 is Morse-Smale, as desired.

□

CHAPTER 4

Box folds

We now shift our focus toward the study of Liouville domains, with the ultimate goal of showing that Mitsumatsu's Liouville domains are stably Weinstein. To begin, in this chapter we develop the theory of *box folds*, the basic local perturbation we use to construct Liouville homotopies. Given a Liouville domain, a box fold is a graphical perturbation in the contactization of the domain designed to introduce singularities to the Liouville vector field. In particular, a box fold is a smooth approximation of the indicator function $\mathbf{1}_B$ of some subset B of the Liouville domain. The original idea is due to [HH19].

On a high level, the effect of a graphical perturbation to a Liouville domain is straightforward. Namely, if (W, λ) is a Liouville domain with Liouville vector field X_λ and $F : W \to \mathbb{R}$ is a smooth function, there is an induced Liouville homotopy from (W, λ) to $(W, dF + \lambda)$. The Liouville vector field of the latter is $X_F + X_\lambda$, where X_F is the Hamiltonian vector field of F with respect to $d\lambda$. Thus, a graphical perturbation simply changes the Liouville vector field by a Hamiltonian vector field.

The local operation used to prove Proposition 1.7 builds on a careful understanding of the dynamics of the corresponding Hamiltonian vector field. We need to not only understand where critical points are introduced and the nature of their stable manifolds, but also the induced *holonomy* of nearby points. As such, the next two sections are dedicated to comprehensively studying all aspects of the dynamics of certain Hamiltonian vector fields X_F. We emphasize that this is sophisticated, but completely elementary.

The philosophy of our analysis, which is central to this chapter and the next, draws from the techniques developed in [HH19] regarding convex hypersurface theory. Given a Liouville domain (W, λ), we consider the contactization $(\mathbb{R}_z \times W, dz + \lambda)$. After identifying

some codimension 0 subset $B \subset W$, we then fix $z_0 > 0$ and consider the piecewise-smooth hypersurface

$$W_B := \text{graph}\,(z_0 \mathbf{1}_B) \cup ([0, z_0] \times \partial B)\,.$$

In words, W_B is the graph of the (scaled) indicator function of B together with a vertical wall connecting the components of the graph. This is not a graphical hypersurface over W, nor is it smooth, and thus it does not yield a genuine Liouville homotopy of (W, λ). However, we can consider a smooth function $F : W \to \mathbb{R}$ such that graph(F) approximates the above hypersurface with arbitrary precision. Loosely speaking, the qualitative dynamical behavior of the Liouville vector field $X_F + X_\lambda$ converges to that of the characteristic foliation of W_B as graph(F) converges to W_B. We remind the reader that we will abuse language slightly and will make no distinction between an oriented characteristic foliation and a vector field directing the foliation. Thus, we initiate our box fold analysis by studying the characteristic foliation of non-graphical piecewise-linear hypersurfaces as defined above. In the next section, we will discuss the complications arising from taking a smooth, graphical approximation.

The present chapter is organized as follows. In 4.1.1 we define the piecewise-linear box fold in a low dimensional model and study its characteristic foliation. In 4.1.2 we extend this piecewise-linear model to arbitrary dimensions. In 4.1.3 we discuss a variant of a box fold called a *box hole*. Finally, in 4.1.4 we introduce a piecewise-linear fold — technically not a box fold — called a *pre-chimney* fold. This is preparation for Section 5.1, where we define the notion of a (full) chimney fold.

4.1 Piecewise-linear box folds

4.1.1 Piecewise-linear box folds in dimension 2

We begin with the piecewise-linear box fold in a standard low dimensional model. In particular, consider

$$\left(\mathbb{R}^3_{z,s,t},\, \alpha = dz + e^s\, dt\right).$$

Here we view $\mathbb{R}^3$ as the contactization of $(\mathbb{R}^2, e^s\,dt)$. The surface $W = \{z = 0\}$ represents a region of a 2-dimensional Liouville domain that we wish to perturb. Observe that the Liouville vector field of $(W, e^s\,dt)$ is ∂_s, and that this directs the (unoriented) characteristic foliation of W. An important convention throughout the rest of the paper is the following: *we choose to orient all characteristic foliations with respect to the backward Liouville flow*. That is, the Liouville vector field of W is ∂_s, and the oriented characteristic foliation of W is directed by $-\partial_s$. We will refer to this choice of orientation throughout as the *backward time* or simply *backward* orientation. This choice of orientation is simply to clarify the arguments in this section, since our analysis focuses on the backward Liouville flow.

Definition. Fix $z_0, s_0, t_0 > 0$. A **(piecewise-linear, low-dimensional) box fold with parameters** z_0, s_0, t_0, denoted Π^{PL}, is the surface

$$\Pi^{PL} := \overline{\partial\left([0, z_0] \times [0, s_0] \times [0, t_0]\right) \setminus \{z = 0\}}.$$

We will refer to $[0, s_0]$ as the *s-support* or *symplectization length* of the fold, and $[0, t_0]$ as the *t-support* or *Reeb length* of the fold. Note that this instance of "Reeb" is not referring to ∂_z, which is the Reeb vector field of the contactization of W. We will also use the following shorthand notation to refer to the various sides of Π^{PL}:

$$\underline{z = z_0} := \Pi^{PL} \cap \{z = z_0\}$$

and likewise with the other sides $\underline{t = 0}$, $\underline{t = t_0}$, $\underline{s = 0}$, and $\underline{s = s_0}$.

We wish to study the dynamics of the oriented characteristic foliation of Π^{PL} according to the convention above. The foliation of each side of Π^{PL} is given by the following table, where we have used Lemma 2.7. Note that the orientation of each side is chosen to be consistent with the backward Liouville flow.

The most important feature of a box fold is that, in backward time, it traps some of the flowlines entering the fold through $\underline{z = 0} \cap \underline{s = s_0}$. The flowlines that are not trapped

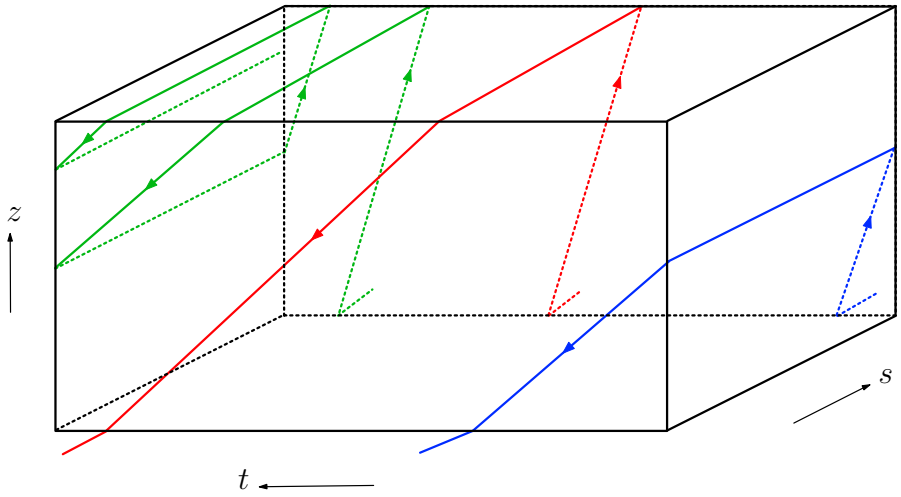

Figure 4.1: A box fold with $z_0 < t_0$ and the three qualitative types of flowlines entering the fold according to Lemma 4.1. The flowline in green is trapped in backward time, because it spirals around $\underline{t = t_0} \cap \underline{z = z_0}$ via the faces $\underline{s = s_0} \to \underline{z = z_0} \to \underline{s = 0} \to \underline{t = t_0} \to \underline{s = s_0}$. The flowline in red passes through the fold, and its holonomy is given by a shift in the t-direction. The flowline in blue also passes through the fold, but its holonomy is given by a scaling in the t-direction.

Side	Area form	Restriction of $dz + e^s\,dt$	Characteristic foliation
$\underline{z = z_0}$	$-e^s\,ds\,dt$	$e^s\,dt$	$-\partial_s$
$\underline{s = 0}$	$-dz\,dt$	$dz + dt$	$\partial_t - \partial_z$
$\underline{s = s_0}$	$-dt\,dz$	$dz + e^{s_0}\,dt$	$-\partial_t + e^{s_0}\partial_z$
$\underline{t = 0}$	$-ds\,dz$	dz	$-\partial_s$
$\underline{t = t_0}$	$-dz\,ds$	dz	∂_s

Table 4.1: The oriented characteristic foliation of a box fold in dimension 2.

reach $\underline{z = 0} \cap \underline{s = 0}$ and subsequently exit the fold after experiencing some holonomy in the t-direction; see Figure 4.1. We emphasize that for a flowline to exit the fold, it must reach $\underline{z = 0} \cap \underline{s = 0}$.

The following lemma summarizes all of the induced dynamical behavior of a piecewise-linear box fold in low dimensions.

Lemma 4.1. *Let* $h^{PL} : \{z = 0\} \times \{s = s_0\} \times [0, t_0] \dashrightarrow \{z = 0\} \times \{s = 0\} \times [0, t_0]$ *be the partially-defined holonomy map given by the oriented characteristic foliation of* Π^{PL}*. The domain of*

h^{PL} is

$$\left(0,\, e^{-s_0}\min(z_0,t_0)\right)_t \cup \left(e^{-s_0}\min(z_0,t_0),\, t_0-(1-e^{-s_0})\min(z_0,t_0)\right)_t$$

and

$$h^{PL}(t)=\begin{cases} e^{s_0}t & t\in(0,\, e^{-s_0}\min(z_0,t_0)) \\ t+(1-e^{-s_0})z_0 & t\in(e^{-s_0}\min(z_0,t_0),\, t_0-(1-e^{-s_0})\min(z_0,t_0)) \end{cases}.$$

In particular, if $z_0 \geq t_0$ then the domain of h^{PL} is $(0, e^{-s_0}t_0)$, and $h^{PL}(t) = e^{s_0}t$.

Remark. Before we prove Lemma 4.1, we include some discussion about its statement and role in the context of this dissertation.

(1) Most of the box folds in this paper will satisfy $z_0 \geq t_0$ (in fact, most will satisfy $z_0 \geq e^{s_0}t_0$), so for simplicity, the reader can focus on the "in particular" statement.

(2) We will often abuse notation and refer to the domain of h^{PL} as either $\{z=0\}\times\{s=s_0\}\times[0,t_0]$, $\{s=s_0\}\times[0,t_0]$, or sometimes simply $[0,t_0]$. The complement of the domain of h^{PL} in $[0,t_0]$ is the set of points whose Liouville flowlines do not pass through the fold. For example, if $z_0 \geq t_0$ then this region is $[e^{-s_0}t_0, t_0]$. We will refer to this as the *trapping region* of the box fold. Also, because Π^{PL} is not a smooth hypersurface, we are abusing the notion of "flowline." In the present section, this is unimportant, but it leads to some subtle and significant complications when we round corners and smooth out the hypersurface in Section 4.2. Another consequence is that, in the discussion of piecewise-linear folds, we will be sloppy about including and not including certain t-values like $0, t_0$, and $e^{-s_0}t_0$. For example, we may refer to a trapping region of Π^{PL} as $(e^{-s_0}t_0, t_0)$ or $[e^{-s_0}t_0, t_0]$, even though there are technically no flowlines passing through $\{s=s_0\}\times\cap\{t=t_0\}$ or $\{s=s_0\}\times\cap\{t=e^{-s_0}t_0\}$ due to edges and corners of the fold. Again, this is unimportant in the context of piecewise-linear folds.

(3) Both the statement of Lemma 4.1 and the proof presented below may obfuscate the simplicity and elementary nature of the idea. The picture that the reader should keep in mind is Figure 4.2. In particular, the proof may seem unnecessarily detailed,

because the qualitative behavior of the flowlines can be visualized easily and computed algebraically using Figure 4.2 as a reference. However — to state the obvious — the dynamics become more complicated in higher dimensions, and it becomes impossible to visualize the behavior in its entirety. Thus, we will need to rely on casework arguments by working with the characteristic foliation directly. In that sense, the primary purpose of the proof of Lemma 4.1 is to function as a warm-up for the more intricate arguments in higher dimensions.

Proof. Assume first that $z_0 \geq t_0$.

Suppose that a flowline enters the fold along $\underline{z = 0} \cap \underline{s = s_0}$ with initial t-coordinate $\bar{t} \in (0, e^{-s_0} t_0)$. The characteristic foliation of $\underline{s = 0}$ is directed by $-\partial_t + e^{s_0}\, \partial_z$. Because $\bar{t} < e^{-s_0} t_0$ and $z_0 > t_0$, the flowline reaches $\underline{t = 0}$ before $\underline{z = z_0}$. It reaches $\underline{t = 0}$ with z-coordinate $e^{s_0}\bar{t} < t_0 \leq z_0$. Along $\underline{t = 0}$ the flowline travels via $-\partial_s$ to $\underline{s = 0}$. Here the characteristic foliation is $\partial_t - \partial_z$. Since the z-coordinate $e^{s_0}\bar{t}$ is less than z_0, the flowline reaches $\underline{z = 0}$ before $\underline{t = t_0}$ and exits the fold with t-coordinate $e^{s_0}\bar{t}$. This proves that $h^{PL}(t) = e^{s_0} t$ for $t \in (0, e^{-s_0} t_0)$.

Next, suppose that a flowline enters along $\underline{z = 0} \cap \underline{s = s_0}$ with initial t-coordinate $\bar{t} \in (e^{-s_0} t_0, t_0)$. The characteristic foliation of $\underline{s = 0}$ is directed by $-\partial_t + e^{s_0}\, \partial_z$. The flowline reaches either $\underline{t = 0}$ or $\underline{z = z_0}$.

Case 1: the flowline reaches $\underline{t = 0}$.

The flowline reaches $\underline{t = 0}$ with z-coordinate $e^{s_0}\bar{t} > t_0$. It travels along $\underline{t = 0}$ via $-\partial_s$ to $\underline{s = 0}$. Here the foliation is directed by $\partial_t - \partial_z$. Because $e^{s_0}\bar{t} > t_0$, the flowline reaches $\underline{t = t_0}$ with z-coordinate $e^{s_0}\bar{t} - t_0 > 0$. Along $\underline{t = t_0}$ it follows ∂_s, returning to $\underline{s = s_0}$. Note that the z-coordinate has increased from the last time the flowline was on $\underline{s = s_0}$. Here the flowline follows $-\partial_t + e^{s_0}\, \partial_z$ and we reach either Case 1 (again) or Case 2. Everytime the flowline cycles through Case 1, the z-coordinate increases. Thus, eventually, the initial z-coordinate along $\underline{s = s_0}$ will be large enough for the flowline to enter Case 2.

Case 2: the flowline reaches $\underline{z = z_0}$.

Let $\tilde{t} > 0$ denote the t-coordinate at which the flowline reaches $\underline{z = z_0}$. The characteristic foliation here is directed by $-\partial_s$, and so the flowline then reaches $\underline{s = 0}$. Since $z_0 \geq t_0$ and $\tilde{t} > 0$, the flowline follows $\partial_t - \partial_z$ and reaches $\underline{t = t_0}$ with z-coordinate $z_0 - (t_0 - \tilde{t})$. Here the foliation is ∂_s, and thus the flowline travels to $\underline{s = s_0}$. The flowline then follows $-\partial_t + e^{s_0}\,\partial_z$, returning to $\underline{z = z_0}$, i.e., returning to Case 2, with t-coordinate $t_0 - e^{-s_0}(t_0 - \tilde{t}) > \tilde{t}$. Note that the t-coordinate has increased upon return to $\underline{z = z_0}$.

The above analysis shows that every flowline entering the fold with initial t-coordinate in $(e^{-s_0}t_0, t_0)$ cycles through Case 1 sufficiently many times (if necessary) to reach Case 2, which is then cycled through indefinitely; see Figure 4.2. The flowline spirals around $\underline{z = z_0} \cap \underline{t = t_0}$, never exiting the fold. This completes the proof of Lemma 4.1 when $z_0 \geq t_0$.

The casework for a fold with $z_0 < t_0$ is essentially identical, if not more tedious because of the presence of a third case. Again, we refer to Figure 4.2. □

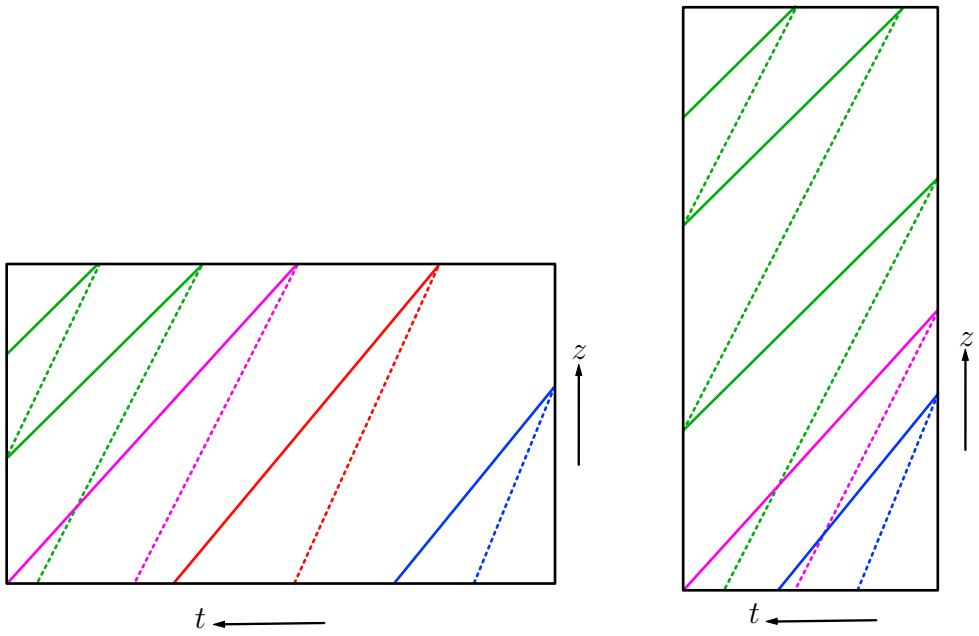

Figure 4.2: A head-on view of two different box folds, one with $z_0 < t_0$ (left) and $z_0 > t_0$ (right). This is a visual depiction of Lemma 4.1. All of the dashed lines on $\underline{s = s_0}$ have (t, z) slope $-e^{s_0}$ and all of the solid lines on $\underline{s = 0}$ have (t, z) slope -1. The pink flowlines represent the lower threshold of the trapping region. Observe on the right picture that increasing z_0 beyond t_0 (with s_0 fixed) does not increase the size of the trapping region.

Before moving on to piecewise-linear box folds in higher dimensions, we include a remark on the holonomy of a box fold under a shift in the symplectization direction. We have defined Π^{PL} as a fold with s-support $[0, s_0]$, but it will be necessary for us to install box folds with symplectization support in some other interval $[s_1, s_2]$, where $s_2 - s_1 = s_0$. The only change to the characteristic foliation is that the (t, z)-slope on $\underline{s = s_1}$ is $-e^{s_1}$, and on $\underline{s = s_2}$ it is $-e^{s_2}$. It should be clear from the proof of Lemma 4.1, and in particular Figure 4.2, that such a fold with $z_0 \geq e^{s_1} t_0$ has identical holonomy to a box fold installed with $z_0 \geq t_0$ and symplectization support in $[0, s_1]$. In other words, the holonomy of a box fold only depends on the symplectization *length*, and not the actual interval, provided we increase z_0 accordingly. This poses no problem for us. In the future, when we say "install a box fold with s-support $[s_1, s_2]$" it will be understood that the z-parameter is adjusted accordingly to mimic the model computations above.

4.1.2 Piecewise-linear box folds in high dimensions

The box fold defined above yields (or will eventually yield, after smoothing) a Liouville homotopy of a 2-dimensional Liouville domain. In general, we wish to install box folds on Liouville domains of arbitrary dimensions. To do this, we will consider folds based over the symplectization of a *contact handlebody*.

Definition. A **contact handlebody** is a contact manifold of the form

$$(H_0 := [0, t_0] \times W_0,\ dt + \lambda_0)$$

where (W_0, λ_0) is a Weinstein domain.

Remark. Presently, it is important that (W_0, λ_0) is a domain, as opposed to a cobordism with nonempty negative boundary. When we discuss pre-chimney folds in 4.1.4 we will weaken this, but for now our analysis crucially uses the assumption that (W_0, λ_0) has a skeleton and outward pointing Liouville vector field. We also point out that we should be including the data of a Lyapunov Morse function ϕ_0 when referring to a Weinstein domain (W_0, λ_0, ϕ_0).

However, the actual Morse function is unimportant, so we will typically omit it.

The low-dimensional box fold from 4.1.1 is based over the contact handlebody $([0, t_0], dt)$ where $W_0 = \{\text{pt}\}$. The standard example of a contact handlebody that the reader should keep in mind as it pertains to this paper is $([0, t_0] \times \mathbb{D}^2,\ dt + \frac{1}{2}r^2\, d\theta)$; here, the Liouville vector field of $(W_0 = \mathbb{D}^2,\ \lambda_0 = \frac{1}{2}r^2\, d\theta)$ is the radial vector field $\frac{1}{2}r\, \partial_r$.

Let $(H_0 = [0, t_0] \times W_0^{2n-2},\ dt + \lambda_0)$ be a contact handlebody and let

$$([0, s_0] \times H_0,\ e^s(dt + \lambda_0))$$

be its symplectization. This represents a region in our given $2n$-dimensional Liouville domain that we wish to perturb. Observe, again, that the Liouville vector field of this model is ∂_s. In practice, given an arbitrary Liouville domain we will identify such a region by finding a contact handlebody transverse to the Liouville vector field and considering its time-s_0 flow.

As before, we realize this region as the hypersurface $\{z = 0\}$ inside its contactization:

$$(\mathbb{R}_z \times [0, s_0] \times H_0,\ dz + e^s(dt + \lambda_0))\,.$$

Definition. Fix $z_0, s_0 > 0$, and $H_0 = [0, t_0] \times W_0$ as above. A **(piecewise-linear, high-dimensional) box fold with parameters** z_0, s_0, t_0, denoted Π^{PL}, is the hypersurface

$$\Pi^{PL} := \overline{\partial\left([0, z_0] \times [0, s_0] \times H_0\right) \setminus \{z = 0\}}.$$

We use the same language and notation as before. This time, there is an additional vertical side to consider:

$$\underline{\partial W_0} = [0, z_0] \times [0, s_0] \times [0, t_0] \times \partial W_0.$$

The following lemma computes the characteristic foliation of each side of Π^{PL}, oriented to be consistent with the backward Liouville flow.

Lemma 4.2. *Let X_{λ_0} denote the Liouville vector field of (W_0^{2n-2}, λ_0), let $\eta_0 := \lambda_0 \mid_{\partial W_0}$ be the induced contact form on the boundary of W_0, and let R_{η_0} denote the Reeb vector field on ∂W_0 of η_0. The backward oriented characteristic foliation of Π^{PL} is given by Table 4.2.*

Side	Characteristic foliation
$\underline{z = z_0}$	$-\partial_s$
$\underline{s = 0}$	$\partial_t - \partial_z$
$\underline{s = s_0}$	$-\partial_t + e^{s_0}\partial_z$
$\underline{t = 0}$	$-\partial_s + X_{\lambda_0}$
$\underline{t = t_0}$	$\partial_s - X_{\lambda_0}$
$\underline{\partial W_0}$	$\partial_t - R_{\eta_0}$

Table 4.2: The oriented characteristic foliation of a high dimensional box fold.

Remark. Observe that the foliation is identical to the low-dimensional fold on $\underline{z = z_0}$, $\underline{s = 0}$, and $\underline{s = s_0}$. On the sides $\underline{t = 0}$ and $\underline{t = t_0}$ there is an additional $\pm X_{\lambda_0}$ term, inducing motion in the W_0 direction. This motion, together with the new side $\underline{\partial W_0}$, is the key feature that distinguishes the behavior of the high-dimensional and low-dimensional folds. We also point out that the vector fields on the latter three sides project to the characteristic foliation of ∂H_0 in H_0.

Proof. We will consider the sides $\underline{t = 0}$, $\underline{t = t_0}$, and $\underline{\partial W_0}$ that feature new behavior; the other three sides are similar. As before, we use Lemma 2.7.

First, consider $\underline{t = 0}$. A correctly oriented volume form on this side is

$$\Omega = e^{(n-1)s}\, dz\, ds\, (d\lambda_0)^{n-1}.$$

Let $\beta := (dz + e^s\,(dt + \lambda_0)) \mid_{\underline{t=0}} = dz + e^s\,\lambda_0$. Then $d\beta = e^s\, ds\, \lambda_0 + e^s\, d\lambda_0$, and so

$$\begin{aligned}\beta\,(d\beta)^{n-1} &= [dz + e^s\,\lambda_0]\,\left[(n-1)e^{(n-1)s}\, ds\,\lambda_0\,(d\lambda_0)^{n-2} + e^{(n-1)s}\,(d\lambda_0)^{n-1}\right] \\ &= e^{(n-1)s}\,\left[(n-1)\, dz\, ds\,\lambda_0\,(d\lambda_0)^{n-2} + dz\,(d\lambda_0)^{n-1}\right].\end{aligned}$$

Note that

$$\begin{aligned}\iota_{-\partial_s+X_{\lambda_0}}\Omega &= e^{(n-1)s}\left[dz\,(d\lambda_0)^{n-1}+(n-1)\,dz\,ds\,\lambda_0\,(d\lambda_0)^{n-2}\right]\\ &= \beta\,(d\beta)^{n-1}.\end{aligned}$$

By Lemma 2.7, it follows that $-\partial_s + X_{\lambda_0}$ directs the characteristic foliation of $\underline{t=0}$. The computation for $\underline{t=t_0}$ is identical, using the volume form $\Omega = -e^{(n-1)s}\,dz\,ds\,(d\lambda_0)^{n-1}$.

Finally, consider $\underline{\partial W_0}$. A correctly oriented volume form on this side is

$$\Omega = (n-1)e^{(n-1)s}\,dz\,ds\,dt\,\eta_0\,(d\eta_0)^{n-2}.$$

Let $\beta := (dz + e^s\,(dt+\lambda_0))\,|_{\underline{\partial W_0}} = dz + e^s(dt+\eta_0)$. Then $d\beta = e^s\,ds\,(dt+\eta_0) + e^s\,d\eta_0$, and so

$$\begin{aligned}\beta\,(d\beta)^{n-1} &= [dz+e^s(dt+\eta_0)]\,\left[(n-1)e^{(n-1)s}\,ds\,(dt+\eta_0)\,(d\eta_0)^{n-2}\right]\\ &= (n-1)e^{(n-1)s}\,\left[dz\,ds\,dt\,(d\eta_0)^{n-2}+dz\,ds\,\eta_0\,(d\eta_0)^{n-2}\right].\end{aligned}$$

Note that

$$\begin{aligned}\iota_{\partial_t-R_{\eta_0}}\Omega &= (n-1)e^{(n-1)s}\,\left[dz\,ds\,\eta_0\,(d\eta_0)^{n-2}+dz\,ds\,dt\,(d\eta_0)^{n-2}\right]\\ &= \beta\,(d\beta)^{n-1}.\end{aligned}$$

By Lemma 2.7, $\partial_t - R_{\eta_0}$ directs the characteristic foliation of $\underline{\partial W_0}$. □

As with piecewise-linear box folds in dimension 2, we wish to analyze the dynamics of this characteristic foliation to identify flowlines that are trapped by the fold, and to understand the holonomy of flowlines that pass through. Throughout the analysis, the reader should keep two distinct "contact projections" of Π^{PL} in mind: the projection to $[0,z_0]\times[0,s_0]\times[0,t_0]$, and the projection to $H_0 = [0,t_0]\times W_0$. See, for example, Figure 4.3.

We initiate the analysis with a key lemma that generalizes some of the behavior in the low dimensional case. As with Lemma 4.1, the proof involves some careful and seemingly

complicated casework. The reader should reference Figure 4.3 and keep track of the movement visually in these two contact projections.

Lemma 4.3. *Let Π^{PL} be a high-dimensional box fold (with no assumption on z_0). If a flowline reaches $\underline{t = t_0}$, it is trapped in backward time by the fold.*

Proof. Suppose that a flowline reaches $\underline{t = t_0}$ with z-coordinate $\bar{z}$, s-coordinate $\bar{s}$, and W_0-coordinate $\bar{w}$. The characteristic foliation here is directed by $\partial_s - X_{\lambda_0}$. Since (W_0, λ_0) is a domain, the flowline will travel to $\underline{s = s_0}$, concurrently moving toward $\mathrm{Skel}(W_0, \lambda_0)$. In particular, if ψ^s denote the time-s flow of X_{λ_0} on W_0, then the flowline reaches $\underline{s = s_0}$ with W_0-coordinate $\psi^{-(s_0-\bar{s})}(\bar{w})$. Here the foliation is directed by $-\partial_t + e^{s_0}\,\partial_z$. The flowline then reaches either $\underline{t = 0}$ or $\underline{z = z_0}$.

Case 1: the flowline reaches $\underline{t = 0}$.

The flowline reaches $\underline{t = 0}$ with z-coordinate $\bar{z} + e^{s_0}t_0$. Here the foliation is directed by $-\partial_s + X_{\lambda_0}$. There are two subcases: the flowline reaches either $\underline{s = 0}$ or $\underline{\partial W_0}$.

Case 1A: the flowline reaches $\underline{s = 0}$.

In this case, the flowline reaches $\underline{s = 0}$ with W_0-coordinate $\psi^{s_0}(\psi^{-(s_0-\bar{s})}(\bar{w})) = \psi^{\bar{s}}(\bar{w})$. Note that Case 1A is characterized precisely by the fact that $\psi^{\bar{s}}(\bar{w}) \in W_0 \setminus \partial W_0$. Along $\underline{s = 0}$ the flowline follows $\partial_t - \partial_z$. Since the current z-coordinate is $\bar{z} + e^{s_0}t_0 > t_0$, the flowline reaches $\underline{t = t_0}$ before $\underline{z = 0}$, and it does so with z-coordinate $\bar{z} + (e^{s_0} - 1)t_0 > \bar{z}$.

Observe that we return to the hypothesis of the lemma (reaching $\underline{t = t_0}$) with an increased z-coordinate and a W_0-coordinate which is closer to ∂W_0, namely, $\psi^{\bar{s}}(\bar{w})$. The flowline enters either Case 1 or Case 2. If the flowline continues to re-enter Case 1A, the W_0-coordinate will eventually be close enough to ∂W_0 to ensure that the flowline reaches $\underline{\partial W_0}$ before $\underline{s = 0}$, entering Case 1B.

Case 1B: the flowline reaches $\underline{\partial W_0}$.

Here the foliation is directed by $\partial_t - R_{\eta_0}$. The flowline travels around ∂W_0 via $-R_{\eta_0}$ and ultimately reaches $\underline{t = t_0}$, returning to the hypothesis of the lemma. Note that the

z-coordinate has increased from $\bar{z}$ and the s-coordinate has increased from $\bar{s}$. The flowline either re-enters Case 1 or enters Case 2. If it continues to re-enter Case 1B, its s-coordinate will eventually increase to the point where it enters Case 1A.

The upshot of the Case 1A/1B analysis above is the following. If a flowline cycles through Case 1, it cannot cycle through Case 1A forever or Case 1B forever. The flowline will cycle through Case 1A sufficiently many times to reach Case 1B, where it cycles through Case 1B sufficiently many times to reach Case 1A, and so on. Both Case 1A and Case 1B contribute to a net increase in the z-coordinate. Thus, eventually the flowline will cycle through Case 1 sufficiently many times for the z-coordinate to be large enough to enter Case 2.

Case 2: the flowline reaches $\underline{z = z_0}$.

Let $\tilde{z}$ denote the z-coordinate from which the flowline left $\underline{t = t_0}$ before reaching $\underline{z = z_0}$. Let $\tilde{t}, \tilde{w}$ denote the t-coordinate and W_0-coordinate at which the flowline reaches $\underline{z = z_0}$. Note that $\tilde{t} = t_0 - e^{-s_0}(z_0 - \tilde{z})$. Here the foliation is directed by $-\partial_s$, and so the flowline reaches $\underline{s = 0}$. It then follows $\partial_t - \partial_z$ to $\underline{t = t_0}$, attaining a z-coordinate of

$$z_0 - (t_0 - \tilde{t}) = z_0 - e^{-s_0}(z_0 - \tilde{z}) > \tilde{z}.$$

The s-coordinate is now 0 and the W_0-coordinate is still $\tilde{w}$.

The foliation along $\underline{t = t_0}$ is directed by $\partial_s - X_{\lambda_0}$. Thus, since (W_0, λ_0) is a domain, the flowline reaches $\underline{s = s_0}$ with W_0-coordinate $\psi^{-s_0}(\tilde{w})$. The flowline travels along $-\partial_t + e^{s_0}\,\partial_z$ to $\underline{z = z_0}$ with W_0-coordinate $\psi^{-s_0}(\tilde{w})$, re-entering Case 2.

The above analysis shows that when a flowline reaches Case 2, it continues to re-enter Case 2 indefinitely. The flowline does not exit the fold and spirals around $\underline{t = t_0} \cap \underline{z = z_0}$ while limiting towards $\mathrm{Skel}(W_0, \lambda_0)$. See Figure 4.3.

□

Lemma 4.3 is our first exposure to the following approximate principle: when a flowline

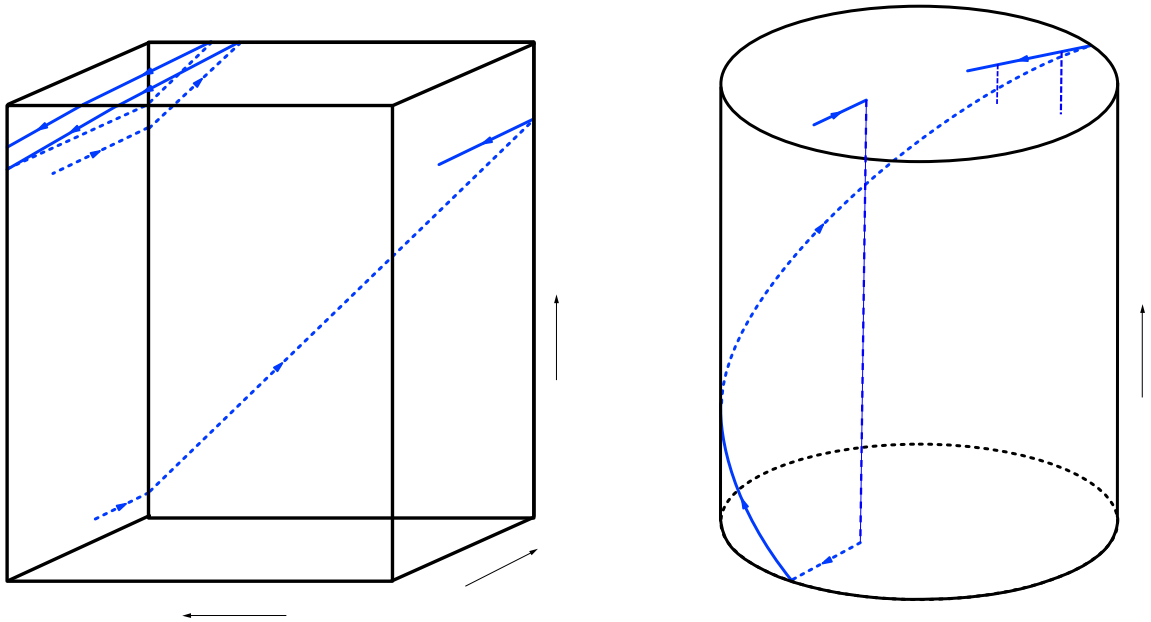

Figure 4.3: A visualization of Lemma 4.3. On the left is the (z, s, t) projection, and on the right is the contact handlebody $H_0 = [0, t_0] \times W_0$. The figure depicts a single sample flowline beginning on $\underline{t = t_0}$ at x_1. It travels along $\underline{t = t_0}$ and reaches $\underline{s = s_0}$ at x_2. Here the flowline is in Case 1, as it reaches $\underline{t = 0}$ at x_3 before reaching $\underline{z = z_0}$. Then the flowline is in Case 1B, because it travels along $\underline{t = 0}$ and reaches $\underline{\partial W_0}$ at x_4 before reaching $\underline{s = 0}$. Along $\underline{\partial W_0}$ the flowline swirls around ∂W_0 via $-R_{\eta_0}$ and reaches $\underline{t = t_0}$ at x_5. From here, the flowline enters Case 2. The flowline cycles through Case 2 indefinitely, ultimately swirling around $\underline{t = t_0} \cap \underline{z = z_0}$ on the left and limiting towards $\mathrm{Skel}(W_0, \lambda_0)$ on the right.

enters a high-dimensional box fold, its trajectory takes turns following the characteristic foliations in the (z, s, t) and H_0 projections. Of course, this is overly simplistic and not entirely correct, as the proof of Lemma 4.3 demonstrates, but it is a decently accurate visual principle to keep in mind when deciphering the dynamical casework above and in the future.

Using Lemma 4.3, we can effectively summarize the holonomy through a piecewise-linear, high-dimensional box fold. To do so, we introduce some notation that will persist throughout the rest of the dissertation. Given a Weinstein domain (W_0, λ_0), let ψ^s denote the time-s flow of the Liouville vector field X_{λ_0}. Define a distinguished collar neighborhood

of ∂W_0 as follows:

$$N^{s_0}(\partial W_0) := \bigcup_{s\in(-s_0,0]} \psi^s(\partial W_0).$$

In words, $N^{s_0}(\partial W_0)$ is the set of points in W_0 that reach the boundary after a time-s_0 flow of the Liouville vector field.

The following proposition is the generalization of Lemma 4.1 when $z_0 \geq e^{s_0}t_0$.

Proposition 4.4. *Let Π^{PL} be a high-dimensional box fold with $z_0 \geq e^{s_0}t_0$, and let $h^{PL} : \{z = 0\} \times \{s = s_0\} \times H_0 \dashrightarrow \{z = 0\} \times \{s = 0\} \times H_0$ be the partially-defined holonomy map given by the oriented characteristic foliation of Π^{PL}. Let $x \in H_0$ be the entry point of a flowline in H_0, and let $t(x)$ and $W_0(x)$ be the t-coordinate and W_0-coordinate of x, respectively.*

(*i*) *If either $t(x) \in (e^{-s_0}t_0, t_0)$ or $W_0(x) \in N^{s_0}(\partial W_0)$, then the flowline through x is trapped in backward time.*

(*ii*) *For all $(t, w) \in H_0$ in the domain of h^{PL},*

$$h^{PL}(t, w) = (e^{s_0}t, \psi^{s_0}(w)).$$

Proof. We begin by proving (i).

Suppose first that $W_0(x) \in N^{s_0}(\partial W_0)$. Since $z_0 \geq e^{s_0}t_0$, the flowline enters Π^{PL} along $\underline{s = s_0}$ and travels via $-\partial_t + e^{s_0}\,\partial_z$ to $\underline{t = 0}$. Here the foliation is directed by $-\partial_s + X_{\lambda_0}$. Because $W_0(x) \in N^{s_0}(\partial W_0)$, the flowline reaches $\underline{\partial W_0}$ before reaching $\underline{s = 0}$. Here it follows $\partial_t - R_{\eta_0}$ up to $\underline{t = t_0}$. By Lemma 4.3, the flowline is ultimately trapped.

Next, suppose that $t(x) \in (e^{-s_0}t_0, t_0)$. We may further suppose that $W_0(x) \notin N^{s_0}(\partial W_0)$. Again by the assumption that $z_0 \geq e^{s_0}t_0$, the flowline enters Π^{PL} and travels across $\underline{s = s_0}$ via $-\partial_t + e^{s_0}\,\partial_z$ to $\underline{t = 0}$, attaining a z-coordinate of $e^{s_0}t(x) > t_0$. Because $W_0(x) \notin N^{s_0}(\partial W_0)$, it then follows $-\partial_s + X_{\lambda_0}$ to $\underline{s = 0}$. Here it follows $\partial_t - \partial_z$. Since the z-coordinate upon entry to $\underline{s = 0}$ exceeds t_0, the flowline reaches $\underline{t = t_0}$ and is ultimately trapped by Lemma 4.3.

Now we prove (ii). By (i) we necessarily have $t(x) < e^{-s_0}t_0$ and $W_0(x) \notin N^{s_0}(\partial W_0)$. The flowline travels along $\underline{s = s_0}$ via $-\partial_t + e^{s_0}\,\partial_z$ to $\underline{t = 0}$ where it attains a z-coordinate of $e^{s_0}t(x) < t_0$. Here it follows $-\partial_s + X_{\lambda_0}$. Since $W_0(x) \notin N^{s_0}(\partial W_0)$, it reaches $\underline{s = 0}$ with

W_0-coordinate $\psi^{s_0}(W_0(x))$. Here it travels along $\partial_t - \partial_z$ to $\underline{z = 0}$, where it exits the fold with t-coordinate $e^{s_0}t(x)$ and W_0-coordinate $\psi^{s_0}(W_0(x))$. This proves (ii). □

Remark. We make the assumption $z_0 \geq e^{s_0}t_0$ in Proposition 4.4 mostly for convenience. In particular, this assumption ensures that every flowline entering the fold first reaches $\underline{t = 0}$. Furthermore, most of the folds we will use in Section 5.2 satisfy this assumption. A more general statement (similar to Lemma 4.1) can be obtained with more casework.

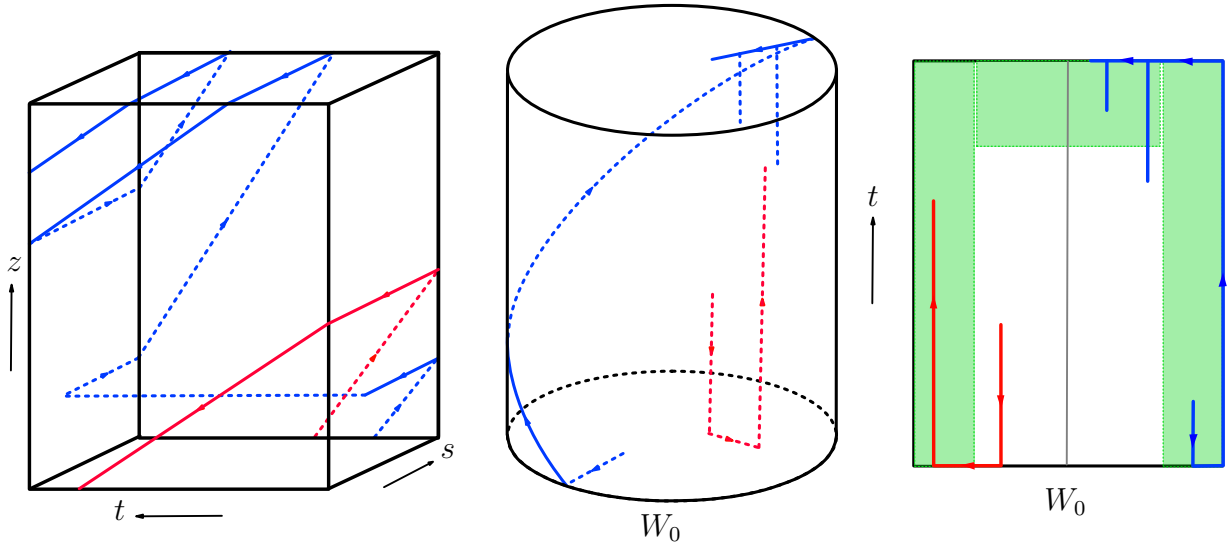

Figure 4.4: A visualization of Proposition 4.4. In particular, the depiction of two flowlines entering the fold in various projections: on the far left is the (z, s, t) projection, in the middle is the $H_0 = [0, t_0] \times W_0$ projection, and the far right is a further projection of the middle picture for the sake of clarity. The shaded green regions on the far right are the trapping regions described in (i), and the gray line indicates $\mathrm{Skel}(W_0, \lambda_0)$. The blue flowline enters the fold in $N^{s_0}(\partial W_0)$ and is ultimately trapped. The red flowline enters the fold and passes through with holonomy given by h^{PL}.

4.1.3 Box holes

Here we briefly discuss the notion of a *box hole*. The primary function of a box fold installation as defined in 4.1.1 is to trap a portion of the flowlines entering the fold near the top of the Reeb chord $[0, t_0]$. Namely, the trapping region of a low-dimensional box fold (with $z_0 \geq t_0$) is $(e^{-s_0}t_0, t_0)$. For the purpose of our strategy in Section 5.2, it will be

desirable to instead trap a portion of the flowlines entering a certain fold near the *bottom* of the Reeb chord. This is possible by simply mirroring the installation of a box fold with a box-shaped hole.

Definition. Fix $z_0, s_0, t_0 > 0$. A **(piecewise-linear, low-dimensional) box hole with parameters** z_0, s_0, t_0, denoted $\amalg^{PL}$, is the surface

$$\amalg^{PL} := \overline{\partial\left([-z_0, 0] \times [0, s_0] \times [0, t_0]\right) \setminus \{z = 0\}}.$$

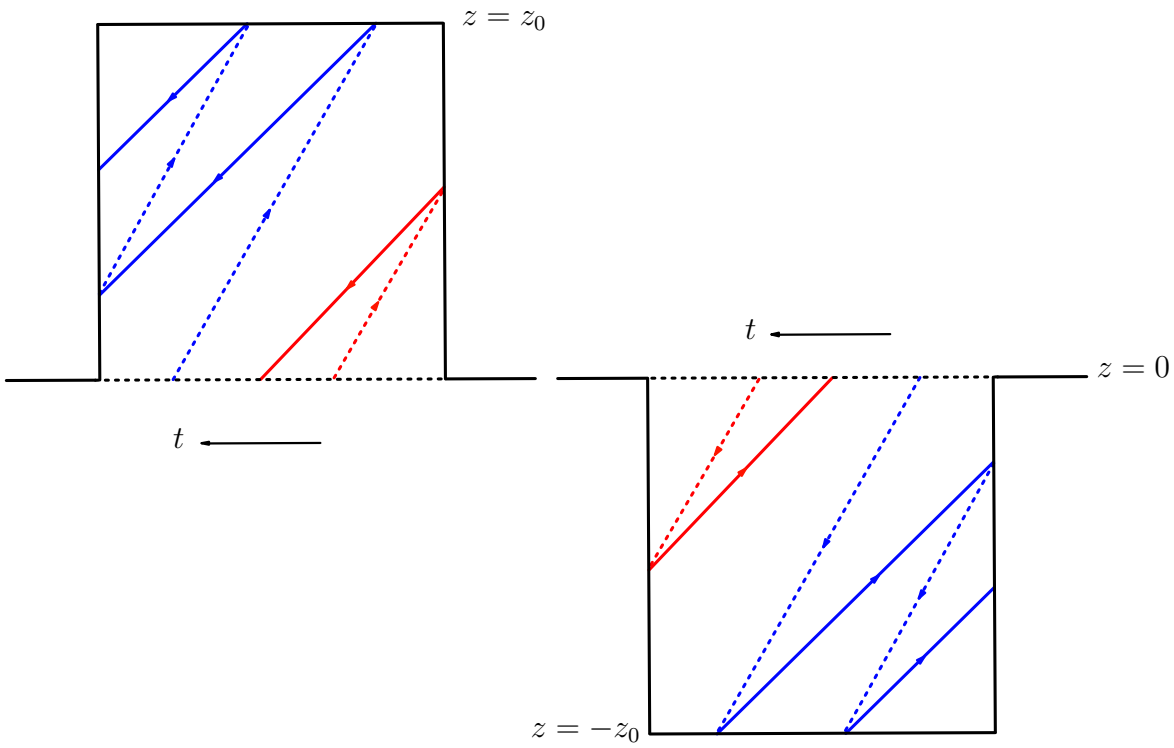

Figure 4.5: A depiction of a box fold on the left and a box hole on the right. The red flowlines pass through the folds, and the blue flowlines are trapped by the folds. Note that in a box hole, the flowlines entering near $t = 0$ are trapped, in contrast to a box fold.

By repeating the same analysis as in 4.1.1, we obtain the following description of the trapping region and holonomy of a low-dimensional box fold.

Lemma 4.5. *Let* $h^{PL} : \{z = 0\} \times \{s = s_0\} \times [0, t_0] \dashrightarrow \{z = 0\} \times \{s = s_0\} \times [0, t_0]$ *be the partially-defined holonomy map given by the oriented characteristic foliation of* $\amalg^{PL}$*. Assume that*

$z_0 \geq t_0$. *The domain of* h^{PL} *is* $((1-e^{-s_0})t_0, t_0)$ *and* $h^{PL}(t) = t_0 - e^{s_0}(t-t_0)$.

The extension to arbitrary dimensions is identical to 4.1.2. The box holes that we use in Section 5.2 will be relatively straightforward, so we will not dwell on the details here; the most important takeaway is simply that the Reeb holonomy mirrors that of a box fold.

4.1.4 Pre-chimney folds

Finally, we close with an analysis of a different kind of piecewise-linear fold, which we call a *pre-chimney fold*. We will not ever install a pre-chimney fold as described here, but the analysis will be helpful in understanding both the function and purpose of a chimney fold in Section 5.1, as well as in the study of partial folds in Section 5.4.

A box fold as we have defined it is based over (the symplectization of) a contact handlebody $([0,t_0] \times W_0,\, dt + \lambda_0)$. By definition, we require (W_0, λ_0) to be a Weinstein *domain*. One could relax this requirement and instead allow (W_0, λ_0) to be a Weinstein cobordism with nonempty negative boundary. According to the language of [HH19], in this case $([0,t_0] \times W_0, dt + \lambda_0)$ is a *generalized* contact handlebody and the corresponding box fold construction yields a *partial* box fold. In general, the dynamics of such a fold can differ significantly from a genuine box fold.

Here we wish to do something slightly different. Namely, we allow (W_0, λ_0) to be a cobordism between manifolds with boundary. For the purpose of this discussion as it relates to this paper, we will consider the two-dimensional trivial cobordism

$$(W_0 = [-r_0, 0]_r \times [0, \theta_0]_\theta,\, \lambda_0 = e^r\, d\theta).$$

In practice we will identify such a region as a small neighborhood near the boundary of a Weinstein domain.

With (W_0, λ_0) as above, let $H_0 = [0,t] \times W_0$ and consider the model

$$\left([0,s_0] \times H_0,\, e^s\,(dt + \lambda_0)\right).$$

As before, this represents some region of a Liouville domain that we wish to perturb, and we realize it as the hypersurface $\{z = 0\}$ inside its contactization:

$$([0, z_0] \times [0, s_0] \times H_0,\ dz + e^s\,(dt + \lambda_0))\,.$$

Definition. A (**piecewise-linear**) **pre-chimney fold**, denoted $pC\Pi^{PL}$, is the hypersurface

$$pC\Pi^{PL} := \overline{\partial\left([0, z_0] \times [0, s_0] \times H_0\right) \setminus \{z = 0\}}.$$

One can check easily enough using the techniques of this section (for example, the proof of Lemma 4.2) that the backward-oriented characteristic foliation of $pC\Pi^{PL}$ is given by the Table 4.3.

Side	Characteristic foliation
$\underline{z = z_0}$	$-\partial_s$
$\underline{s = 0}$	$\partial_t - \partial_z$
$\underline{s = s_0}$	$-\partial_t + e^{s_0}\,\partial_z$
$\underline{t = 0}$	$-\partial_s + \partial_r$
$\underline{t = t_0}$	$\partial_s - \partial_r$
$\underline{r = 0}$	$\partial_t - \partial_\theta$
$\underline{r = -r_0}$	$-\partial_t + e^{r_0}\,\partial_\theta$
$\underline{\theta = 0}$	$-\partial_r$
$\underline{\theta = \theta_0}$	∂_r

Table 4.3: The oriented characteristic foliation of a pre-chimney fold.

Observe that the vector fields on the latter six sides project to the characteristic foliation of ∂H_0 inside H_0, exactly as before. In particular, this table is consistent with the existing sides in the usual box fold case, where we have $X_{\lambda_0} = \partial_r$ and $R_{\eta_0} = \partial_\theta$.

Before we study the dynamics of $pC\Pi^{PL}$, we digress briefly to discuss some heuristics for context. One might initially expect that a pre-chimney fold as defined above does not trap any flowlines in backward time; after all, (W_0, λ_0) is a trivial cobordism and does not have a skeleton. With a partial box fold over a true generalized contact handlebody, this can indeed happen: if we were to fold over $([-r_0, 0] \times S^1,\ e^r\,d\theta)$ instead, the fold would not trap any flowlines in backward time. However, the difference between $([-r_0, 0] \times S^1,\ e^r\,d\theta)$

and $([-r_0, 0]_r \times [0, \theta_0]_\theta,\ e^r\, d\theta)$ is significant enough to change this behavior. As we will see, a pre-chimney fold *does* trap some flowlines in backward time, despite H_0 being based over a trivial cobordism. This will suggest the following principle: the mechanism by which a fold based over a region H_0 traps flowlines in backward time depends on the characteristic foliation of ∂H_0. In particular, if H_0 is any contact region such that ∂H_0 has a characteristic foliation with (positive) critical points, it will trap some flowlines in backward time. In a pre-chimney fold, ∂H_0 is diffeomorphic to S^2 (up to corner rounding) and has a singular characteristic foliation with an index 0 and index 2 critical point. In contrast, the generalized handlebody $([0, t_0] \times [-r_0, 0] \times S^1,\ dt + e^r\, d\theta)$ has a boundary with non-singular characteristic foliation (again, up to corner rounding).

The following lemma is similar to Lemma 4.3.

Lemma 4.6. *Let $pC\Pi^{PL}$ be a pre-chimney fold with $t_0 \geq \theta_0$. If a flowline reaches $\underline{t = t_0}$, it is trapped by the fold in backward time.*

Proof. Proving this lemma with backward time casework as in Lemma 4.3 is fairly tedious. Because of this, we will actually present a *forward* time argument — this is simpler, at the cost of slightly obfuscating the nature of the trapping mechanism of $pC\Pi^{PL}$. We emphasize that one can proceed as in Lemma 4.3, and we also refer to Figure 4.6.

To exit the fold, a flowline must reach $\underline{s = 0}$ with a z-coordinate no greater than t_0. In particular, it must necessarily reach $\underline{s = 0}$ from $\underline{t = 0}$ with a z-coordinate no greater than t_0. Consider such a flowline in *forward* time, beginning on $\underline{t = 0}$ with a z-coordinate no greater than t_0. We will argue that the flowline does *not* traverse $\underline{t = t_0}$, which will prove the lemma.

In forward time, the flowline follows $\partial_s - \partial_r$ to either $\underline{s = s_0}$ or $\underline{r = -r_0}$.

Case 1: the flowline reaches $\underline{s = s_0}$ in forward time.

Here it follows $\partial_t - e^{s_0}\, \partial_z$ and subsequently reaches $\underline{s = s_0} \cap \underline{z = 0}$, because the initial z-coordinate of the flowline was no larger than t_0. In this case, the flowline passes through the entire fold without traversing across $\underline{t = t_0}$.

Case 2: the flowline reaches $\underline{r = -r_0}$ in forward time.

Along $\underline{r = -r_0}$ the forward time foliation is directed by $\partial_t - e^{r_0}\,\partial_\theta$. Because $t_0 \geq \theta_0$, the flowline then reaches $\underline{\theta = 0}$, where it follows ∂_r to $\underline{r = 0}$. Here the forward time foliation is $-\partial_t + \partial_\theta$, so the flowline returns to $\underline{t = 0}$, and we re-enter either Case 1 or Case 2. Note that the s-coordinate has increased from its initial value at the beginning of the proof, and the z-coordinate has not changed. Note also that the flowline has not traversed across $\underline{t = t_0}$.

The point of the above casework is that, in forward time, a flowline beginning on $\underline{t = 0}$ with z-coordinate no larger than t_0 will cycle through Case 2 sufficiently many times until it reaches Case 1. Thus, any such flowline will pass through the fold without reaching $\underline{t = t_0}$, and therefore any flowline that does reach $\underline{t = t_0}$ is trapped in backward time.

□

It is possible to identify the trapping region of a pre-chimney fold precisely, but for the purpose of our arguments in Section 5.1 we will only need Lemma 4.6. For example, in a piecewise-linear pre-chimney fold with $t_0 \geq \theta_0$ and $z_0 \geq e^{s_0} t_0$, one can show that the trapping region of the fold is

$$\big((0, t_0)_t \times (-r_0, 0)_r \times (e^{-s_0}\theta_0, \theta_0)_\theta\big) \cup \big((e^{-s_0}t_0, t_0)_t \times (-r_0, 0)_r \times (0, \theta_0)_\theta\big) \subset H_0.$$

We also remind the reader of the following principle. There are two contact projections of $pC\Pi^{PL}$: the (z, s, t) projection and the H_0 projection. A flowline entering the fold essentially follows the characteristic foliations of both these projections, taking turns with each. A flowline that is trapped ultimately swirls around $\underline{z = z_0} \cap \underline{t = t_0}$ in the (z, s, t) projection and swirls around $\underline{t = t_0} \cap \underline{\theta = \theta_0}$ in the H_0 projection. See Figure 4.6.

4.2 Smooth box folds

To induce a genuine Liouville homotopy of a Liouville domain, we need to perform a smooth, graphical perturbation in the contactization. The piecewise-linear box folds de-

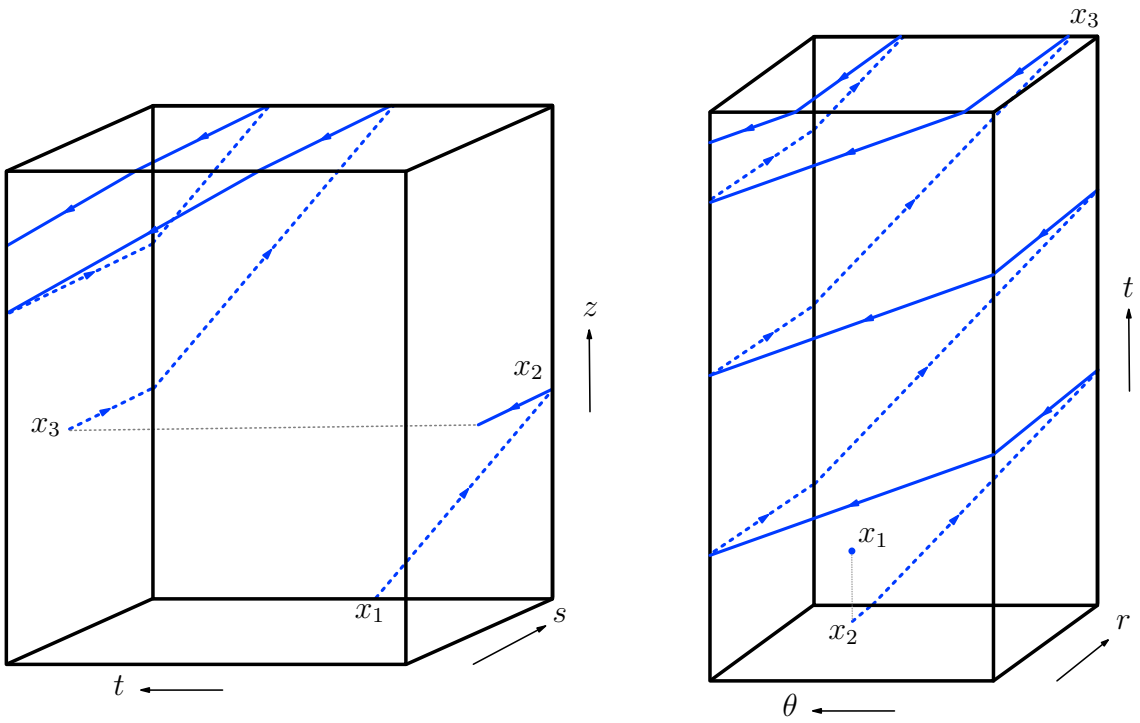

Figure 4.6: A sample flowline that is trapped by a pre-chimney fold. On the left is the (z, s, t) projection, and on the right is H_0 with coordinates (t, r, θ). The flowline enters the fold at x_1, travels to $x_2 \in \underline{t = 0} \cap \underline{s = s_0}$, and then follows the characteristic foliation of ∂H_0 all the way to $x_3 \in \underline{t = t_0} \cap \underline{r = 0}$. The flowline essentially follows the characteristic foliations of both contact projections, ultimately swirling around $\underline{t = t_0} \cap \underline{z = z_0}$ on the left and $\underline{t = t_0} \cap \underline{\theta = \theta_0}$ on the right.

fined in Section 4.1 are neither smooth nor graphical. In this section, we describe how to approximate Π^{PL} with such a perturbation, and discuss the resulting complications.

In general, the process of smoothing a piecewise-linear fold introduces new behavior to the holonomy which is not present otherwise. This new behavior is concentrated in arbitrarily small regions, but it has subtle and significant implications that need to be taken into consideration. Unfortunately, understanding the entire smooth holonomy of a box fold with precision is in general quite difficult. Thankfully, our strategy in Section 5.2 is robust enough for us to not need a precise understanding; for the most part, being able to identify regions where the complicated behavior begins and ends will be sufficient. Thus, broadly speaking, there are two main goals of this section:

(1) develop a formal but robust understanding of the dynamics of a smooth box fold, and

(2) develop a mostly informal understanding of the complications that are not described by (1).

The purpose of (2) is simply to motivate the strategy in Section 5.2, one that involves a more complicated fold, at the cost of being robust enough to mostly ignore the complications of (2).

This section is organized as follows. In 4.2.1, we perform a general Liouville vector field computation for a large class of smooth perturbations. In 4.2.2, we discuss smooth box folds in dimension 2, with goal (1) in mind. In 4.2.3, we do the same in arbitrary dimensions. Finally, in 4.2.4 we consider some complications with goal (2) in mind.

4.2.1 A general computation

We remind the reader of a comment from Section 4.1: from a sufficiently abstract point of view, the dynamical impact of a smooth box fold installation is immediate. Namely, if (W, λ) is a Liouville domain and $F : W \to \mathbb{R}$ is smooth, then a graphical perturbation in the contactization via F yields a Liouville homotopy to $(W, dF + \lambda)$, and the new Liouville vector field is $X_F + X_\lambda$. In fact, we can explicitly compute the vector field X_F in the setting of a box fold. We wish to consider smooth functions

$$F : [0, s_0] \times [0, t_0] \times W_0 \to \mathbb{R}$$

that decay quickly near the boundary of the region. The following lemma gives the Liouville vector field for a wide class of such perturbations.

Lemma 4.7. *Let $(H_0 = [0, t_0] \times W_0,\ dt + \lambda_0)$ be a contact handlebody, and let $([0, s_0] \times H_0,\ \lambda = e^s\,(dt + \lambda_0))$ be its symplectization. Let $F : [0, s_0] \times H_0 \to \mathbb{R}$ be smooth, and assume that $d_{W_0} F = 0$ away from a collar neighborhood of ∂W_0.*

(*i*) *On the region where $d_{W_0} F = 0$, the Liouville vector field of $dF + e^s\,(dt + \lambda_0)$ is*

$$\partial_s + e^{-s}\, X_F^{ds\,dt} - e^{-s} \frac{\partial F}{\partial t}\, X_{\lambda_0}.$$

Here, $X_F^{ds\,dt}$ is the Hamiltonian vector field of F with respect to the symplectic form $ds\,dt$.

(*ii*) *Identify the collar neighborhood of ∂W_0 as $([-\varepsilon, 0]_r \times \partial W_0,\ \lambda_0 = e^r\,\eta_0)$ where $\eta_0 := \lambda_0\,|_{\partial W_0}$. Suppose that $d_{\partial W_0} F = 0$. On this collar neighborhood, the Liouville vector field of $dF + e^s\,(dt + \lambda_0)$ is*

$$\partial_s + e^{-s}\, X_F^{ds\,dt} - e^{-s} \frac{\partial F}{\partial t}\, \partial_r - e^{-s} \frac{\partial F}{\partial r}\, \left(-\partial_t + e^{-r}\, R_{\eta_0}\right).$$

Proof. We will prove (i) explicitly, and leave (ii) to the reader. Since the Liouville vector field of $e^s\,(dt + \lambda_0)$ is ∂_s, it suffices to prove that the Hamiltonian vector field of $F : [0, s_0] \times H_0 \to \mathbb{R}$ with respect to $d\lambda = e^s\,ds\,(dt + \lambda_0) + e^s\,d\lambda_0$ is

$$e^{-s}\, X_F^{ds\,dt} - e^{-s} \frac{\partial F}{\partial t}\, X_{\lambda_0}.$$

Note that $d\lambda = e^s\,ds\,dt + e^s\,ds\,\lambda_0 + e^s\,d\lambda_0$, and so

$$\iota_{e^{-s}\, X_F^{ds\,dt}}(d\lambda) = dF + \frac{\partial F}{\partial t}\,\lambda_0.$$

Similarly,

$$\iota_{e^{-s}\frac{\partial F}{\partial t}\, X_{\lambda_0}}(d\lambda) = \frac{\partial F}{\partial t}\,\lambda_0$$

since $\lambda_0(X_{\lambda_0}) = 0$. Thus,

$$\iota_{e^{-s}\, X_F^{ds\,dt} - e^{-s}\frac{\partial F}{\partial t}\, X_{\lambda_0}}(d\lambda) = dF$$

as desired. This proves (i). The verification of (ii) is similar, using the fact that $\lambda = e^r\,\eta_0$ in the corresponding neighborhood.

□

Remark. In theory, one can deduce all of the dynamics of a smooth box fold — in particular,

the holonomy described in Section 4.1 — using these formulas. In practice, this is unwieldy, and the transparency and clarity provided by the piecewise-linear characteristic foliation approach is evident. With that being said, we will make use of this lemma. It is also a good exercise to qualitatively reconcile this lemma with the dynamics described in the previous section. For example, a typical folding function F will have $\frac{\partial F}{\partial t} > 0$ near $t = 0$ and $\frac{\partial F}{\partial t} < 0$ near $t = t_0$. Thus, according to (i), near $t = 0$ the Liouville vector field has a component in the *negative* X_{λ_0} direction, which means that there is movement in the *forward* X_{λ_0} direction in backward time. This agrees with the fact that the oriented characteristic foliation of $\underline{t = 0}$ in Section 4.1 is directed by $-\partial_s + X_{\lambda_0}$. The roles are reversed accordingly near $t = t_0$.

4.2.2 Smooth box folds in dimension 2

We begin by discussing smooth box folds in the low dimensional model. Broadly speaking, nothing very interesting occurs in this setting, because we are interested in the holonomy map $\{s = s_0\} \times H_0 \dashrightarrow \{s = 0\} \times H_0$, and in 2 dimensions, $H_0 = [0, t_0]$. The induced movement from smoothing is more significant in higher dimensions, when $H_0 = [0, t_0] \times W_0$.

Consider a piecewise-linear box fold Π^{PL} with parameters $z_0, s_0, t_0 > 0$ as defined in 4.1.1. For simplicity, assume that $z_0 > t_0$. By Lemma 4.1, any flowline passing through $(e^{-s_0}t_0, t_0)_t$ is trapped by the fold in backward time, and on $(0, e^{-s_0}t_0)_t$ the holonomy map is given by $h^{PL}(t) = e^{s_0}t_0$.

Fix a small smoothing parameter $\tau > 0$. Let $B = [0, s_0] \times [0, t_0]$ denote the base of the box fold, and let $B^\tau = [\tau, s_0 - \tau] \times [\tau, t_0 - \tau]$. Let $F^\tau_{\text{aux}} : \text{Op}(B) \to \mathbb{R}$ be a smooth function such that

(i) the support of F^τ_{aux} is B,

(ii) $0 \leq F^\tau_{\text{aux}} \leq z_0$ and $F^\tau_{\text{aux}} \equiv z_0$ on B^τ, and

(iii) if $\tau_1 < \tau_2 < \tau$, then we have an inequality of suprema:

$$\sup_{B \setminus B^{\tau_1}} F^\tau_{\text{aux}} \leq \sup_{B \setminus B^{\tau_2}} F^\tau_{\text{aux}}.$$

Here and in the future, $\mathrm{Op}(\cdot)$ denotes a small open neighborhood of the input. In words, F^τ_{aux} is simply an obvious and well-behaved smooth approximation of $z_0\,\mathbf{1}_B$, where there is no unnecessary wild behavior on $B \setminus B^\tau$. Clearly,

$$\mathrm{graph}(F^\tau_{\text{aux}}) \to \Pi^{PL}$$

as $\tau \to 0$.

One could conceivably define a smooth box fold as $\mathrm{graph}(F^\tau_{\text{aux}})$ in the contactization $(\mathbb{R}_z \times B,\ dz + e^s\,dt)$. However, because our goal is to produce a Weinstein domain, we want the new Liouville vector field to have nondegenerate singularities. Since Morse-Smale vector fields are C^∞-generic in two dimensions [PPM98], this is easy enough to achieve.

Definition. A function $F : B \to \mathbb{R}$ is **τ-admissible** if $\|F - F^\tau_{\text{aux}}\|_{C^\infty(B)} < \tau$ and $\mathrm{graph}(F)$ has Morse characteristic foliation in the contactization of B.

With such an admissible function, the induced Liouville vector field from Lemma 4.7 will have two nondegenerate critical points: an index 0 singularity corresponding to the piecewise-linear intersection $\underline{z = z_0} \cap \underline{t = t_0}$, and an index 1 singularity corresponding to the intersection $\underline{z = 0} \cap \underline{t = t_0}$; see Figure 4.7. Note the important difference between this and the C-folds of [HH19]: the non-graphical C-fold produces an index 2 singularity. With Morse Liouville vector fields in two dimensions, it is only possible to introduce singularities of index 0 or index 1.

Definition. Fix $z_0, s_0, t_0, \tau > 0$ and let $F^\tau : [0, s_0] \times [0, t_0] \to \mathbb{R}$ be τ-admissible. A **smooth box fold with parameters** z_0, s_0, t_0 **and smoothing parameter** τ, denoted Π^τ, is the surface $\mathrm{graph}(F^\tau)$.

Remark. We will often suppress the τ in the notation Π^τ. It will usually be clear from context when a box fold is smooth or piecewise-linear, if the distinction matters.

The following lemma is a fairly technical way of summarizing the principle that nothing interesting happens in 2 dimensions; we present it this way for the purpose of effectively adapting the statement to higher dimensions.

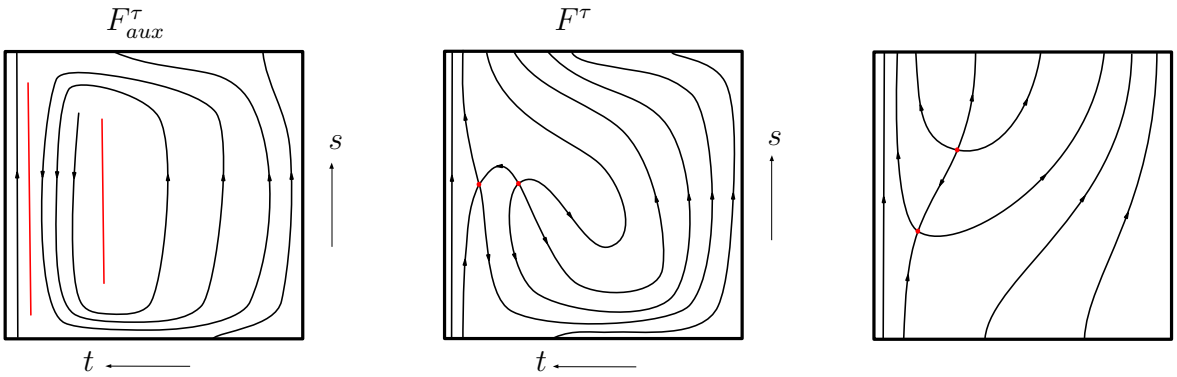

Figure 4.7: The effect of a smooth box fold installation in dimension 2. The figures are increasingly inaccurate from left to right. Before installation, the Liouville vector field is ∂_s. The leftmost figure depicts the (non-Morse) Liouville vector field after perturbing by F^τ_{aux}. The middle figure depicts the perturbation by the τ-admissible function F^τ, with some of the spiraling behavior unwound for visual convenience. The third picture is the middle picture, completely unwound for the sake of clarity on the topological nature of the vector field.

Lemma 4.8. *Suppose $z_0 > t_0$. Let $h^\tau : \{s_0\} \times [0, t_0] \dashrightarrow \{0\} \times [0, t_0]$ be the partially-defined holonomy map given by backward passage through Π^τ. There are closed intervals $H^\tau_{\text{trap}} \subset (e^{-s_0}t_0, t_0)$ and $H^\tau_{\text{pass}} \subset (0, e^{-s_0}t_0)$ such that:*

(*i*) *Any flowline entering H^τ_{trap} converges to a critical point in Π^τ in backward time; that is, H^τ_{trap} is not in the domain of h^τ.*

(*ii*) *As $\tau \to 0$,*

$$\left\| h^\tau - h^{PL} \right\|_{C^0(H^\tau_{\text{pass}})} \to 0.$$

(*iii*) *As $\tau \to 0$,*

$$|(e^{-s_0}t_0, t_0) \setminus H^\tau_{\text{trap}}| \to 0 \quad \textit{and} \quad |(0, e^{-s_0}t_0) \setminus H^\tau_{\text{pass}}| \to 0.$$

Here, $|\cdot|$ is the usual measure on $[0, t_0]$.

(*iv*) *If $t \in [0, t_0] \setminus (H^\tau_{\text{trap}} \cup H^\tau_{\text{pass}})$ is in the domain of h^τ, then $h^\tau(t) \in Op^\tau(\partial[0, t_0])$, where $|Op^\tau(\partial[0, t_0])| \to 0$ as $\tau \to 0$.*

In words, this lemma says the following: given a contact handlebody $[0, t_0]$, there are three fundamental regions: H^τ_{trap}, H^τ_{pass}, and $[0, t_0] \setminus (H^\tau_{\text{trap}} \cup H^\tau_{\text{pass}})$. Any flowline entering

the fold via H^τ_{trap} is trapped in backward time, and any flowline entering the fold via H^τ_{pass} passes through the fold with holonomy that is C^0-close to the piecewise-linear holonomy. Flowlines entering the third region — an open region with arbitrarily small measure given by the complement of the first two regions — exhibit comparatively unidentified behavior. Such a flowline could either be trapped or pass through the fold, but if it passes through the fold it exits near the boundary of the handlebody $[0, t_0]$. Of course, this last statement is uninteresting in this dimension — it will become significant with a handlebody of the form $[0, t_0] \times W_0$. Also note that we are not necessarily claiming that H^τ_{trap} is the *entire* trapping region of the fold; we simply need the existence of a such a region that satisfies the lemma.

Proof. Despite a seemingly technical statement, this lemma follows quickly from Lemma 4.1 and the fact that the characteristic foliation of Π^τ converges to that of Π^{PL} as $\tau \to 0$ away from the non-smooth corners of Π^{PL}. In particular, the trapping region of the smooth fold can be approximated with arbitrary precision, from which the existence of a closed interval H^τ_{trap} satisfying (i) and the first part of (iii) follows. Similarly, the piecewise-linear holonomy away from the trapping region can be approximated with arbitrary precision on a domain which is arbitrarily close to $(0, e^{-s_0}t_0)$; this gives (ii) and the second part of (iii). This leaves the remaining portion of $[0, t_0]$. Since $h^{PL}((0, e^{-s_0}t_0)) = (0, t_0)$, (iv) follows immediately. □

4.2.3 Smooth box folds in high dimensions

We define smooth box folds in arbitrary dimensions in the same fashion. To establish some convenient notation, define

$$H^{PL}_{\text{trap}} := [(0, t_0) \times N^{s_0}(\partial W_0)] \cup \left[(e^{-s_0}t_0, t_0) \times (W_0 \setminus N^{s_0}(\partial W_0))\right]$$
$$H^{PL}_{\text{pass}} := (0, e^{-s_0}t_0) \times (W_0 \setminus N^{s_0}(\partial W_0)).$$

The former is the trapping region of a piecewise-linear box fold with $z_0 > e^{s_0}t_0$ as described in (i) of Proposition 4.4, and H^{PL}_{pass} is the domain of h^{PL} from the same proposition. Here,

of course, (W_0, λ_0) is a Weinstein domain of any dimension.

Fix a small smoothing parameter $\tau > 0$. Let $B = [0, s_0] \times [0, t_0] \times W_0$ denote the base of the box fold and define

$$B^\tau := [\tau, s_0 - \tau] \times [\tau, t_0 - \tau] \times \overline{W_0 \setminus N^\tau(\partial W_0)}.$$

Let $F^\tau_{\text{aux}} : \text{Op}(B) \to \mathbb{R}$ be a smooth function such that

(i) the support of F^τ_{aux} is B,

(ii) $0 \leq F^\tau_{\text{aux}} \leq z_0$ and $F^\tau_{\text{aux}} \equiv z_0$ on B^τ, and

(iii) if $\tau_1 < \tau_2 < \tau$, then we have an inequality of suprema:

$$\sup_{B \setminus B^{\tau_1}} F^\tau_{\text{aux}} \leq \sup_{B \setminus^{\tau_2}} F^\tau_{\text{aux}}.$$

Definition. A function $F : B \to \mathbb{R}$ is **τ-admissible** if $\|F - F^\tau_{\text{aux}}\|_{C^\infty(B)} < \tau$ and $\text{graph}(F)$ has Morse characteristic foliation in the contactization of B.

Definition. Fix $z_0, s_0, t_0, \tau > 0$ and let $F^\tau : B \to \mathbb{R}$ be τ-admissible. A **smooth box fold with parameters** z_0, s_0, t_0 **and smoothing parameter** τ, denoted Π^τ, is the hypersurface $\text{graph}(F^\tau)$ in the contactization of B.

In this higher dimensional setting, we actually only need to perturb F^τ_{aux} in the (s, t) directions to obtain a τ-admissible function, since (W_0, λ_0) is a Weinstein domain. Thus, we can still appeal to C^∞-genericity in two dimensions. Indeed, by Lemma 4.7, the Liouville vector field of $dF + e^s(dt + \lambda_0)$ is, away from ∂W_0,

$$\partial_s + e^{-s} X_F^{ds\, dt} - e^{-s} \frac{\partial F}{\partial t} X_{\lambda_0} = \left(1 + e^{-s} \frac{\partial F}{\partial t}\right) \partial_s - e^{-s} \frac{\partial F}{\partial s} \partial_t - e^{-s} \frac{\partial F}{\partial t} X_{\lambda_0}.$$

The first two terms correspond to the Liouville vector field after installing a low-dimensional box fold as in 4.2.2. The third term is a nonzero multiple of X_{λ_0} near critical points of the first two terms, and hence is Morse in this direction.

Remark. It is important to have a discussion about the indices of the introduced critical points after a box fold installation. If $x \in W_0$ is a critical point of the vector field X_{λ_0} with index k, then a smooth box fold installation introduces two associated critical points to the Liouville vector field of B: one of index k, and one of index $k+1$. However, the discussion from 4.1.4 suggests a more general principle. Suppose that the supporting contact region H_0 has convex boundary, and suppose that the positive region $R_+(\partial H_0)$ of the convex boundary has a critical point of index k. Then the analogous box fold construction over H_0 produces corresponding critical points of index k and index $k+1$. When H_0 is a genuine contact handlebody, both the positive and negative region of ∂H_0 are naturally symplectomorphic to W_0, and the initial remark follows. When we define chimney folds in Section 5.1, we will fold over a region which is not a genuine contact handlebody, and there will be critical points in the positive region that are not present in the negative region. This will be important.

The following proposition is the high-dimensional generalization of Lemma 4.8, and the proof is identical.

Proposition 4.9. *Suppose $z_0 > t_0$. Let $h^\tau : \{s_0\} \times H_0 \dashrightarrow \{0\} \times H_0$ be the partially-defined holonomy map given by backward passage through Π^τ. There are closed regions $H^\tau_{\text{trap}} \subset H^{PL}_{\text{trap}}$ and $H^\tau_{\text{pass}} \subset H^{PL}_{\text{pass}}$ such that:*

(*i*) *Any flowline entering H^τ_{trap} converges to a critical point in Π^τ in backward time; that is, H^τ_{trap} is not in the domain of h^τ.*

(*ii*) *As $\tau \to 0$,*

$$\left\| h^\tau - h^{PL} \right\|_{C^0(H^\tau_{\text{pass}})} \to 0.$$

Here, the C^0-norm is defined by choosing some auxiliary metric on W_0.

(*iii*) *As $\tau \to 0$,*

$$|H^{PL}_{\text{trap}} \setminus H^\tau_{\text{trap}}| \to 0 \quad \textit{and} \quad |H^{PL}_{\text{pass}} \setminus H^\tau_{\text{pass}}| \to 0.$$

(*iv*) *If $x \in H_0 \setminus (H^\tau_{\text{trap}} \cup H^\tau_{\text{pass}})$ is in the domain of h^τ, then $h^\tau(x) \in Op^\tau(\partial H_0)$, where $|Op^\tau(\partial H_0)| \to 0$ as $\tau \to 0$.*

In the low-dimensional setting of Lemma 4.8, $\partial H_0 = \{0, t_0\}$ and so statement (iv) is fairly strong (and uninteresting). In the high-dimensional setting when $H = [0, t_0] \times W_0$, ∂H_0 is much larger and consequently the statement that $h^\tau(x) \in \mathrm{Op}^\tau(\partial H_0)$ is less insightful. Proposition 4.9 does not give any control over *where* the flowline exits near the boundary. This is significant, even though $H \setminus (H^\tau_{\mathrm{trap}} \cup H^\tau_{\mathrm{pass}})$ is an arbitrarily small subset of H_0. We will investigate this more in the next subsection.

Finally, we remark that smooth box holes are defined exactly as above, and the statement of Proposition 4.9 still holds (with the obvious reinterpretations in terms of the piecewise-linear box hole holonomy.)

4.2.4 Complications in the smooth holonomy

In Proposition 4.9, there is a region $H_0 \setminus (H^\tau_{\mathrm{trap}} \cup H^\tau_{\mathrm{pass}})$ for which the nature of the holonomy is currently unidentified, beyond exiting the fold near ∂H_0. This region has arbitrarily small measure in H_0 and acts as a membrane between ∂H_0, H^τ_{trap}, and H^τ_{pass}. The goal of this brief subsection is to convince the reader of the following principle: the holonomy of points entering $H_0 \setminus (H^\tau_{\mathrm{trap}} \cup H^\tau_{\mathrm{pass}})$ is influenced by the characteristic foliation of ∂H_0. The gravity of this influence is variable and hard to describe precisely. For our purposes, we only need a careful understanding of this principle in a one part of H_0.

A smooth box fold, by definition, is a smooth approximation of the hypersurface Π^{PL}. For now, we will focus on the complications arising from smoothing the edge $\underline{s = 0} \cap \underline{\partial W_0}$. Recall that the oriented characteristic foliation on $\underline{s = 0}$ is $\partial_t - \partial_z$, and on $\underline{\partial W_0}$ it is $\partial_t - R_{\eta_0}$. Also recall that the characteristic foliation on $\underline{t = 0}$ is $-\partial_s + X_{\lambda_0}$. Thus, in the piecewise-linear setting, any flowline travelling across $\underline{t = 0}$ eventually reaches either $\underline{s = 0}$ or $\underline{\partial W_0}$ (of course, ignoring the corner). If the flowline reaches $\underline{s = 0}$ with a small enough z-coordinate it will then exit the fold. If it instead reaches $\underline{\partial W_0}$, it will swirl around ∂W_0, eventually reaching $\underline{t = t_0}$, where it is ultimately trapped.

Once we round the corner $\underline{s = 0} \cap \underline{\partial W_0}$, there will be some flowlines along $\underline{t = 0}$ that reach the rounding region connecting the two sides. Along this rounded side, the characteristic

foliation will be directed by some interpolation of $\partial_t - \partial_z$ and $\partial_t - R_{\eta_0}$. There will be some flowlines that, upon reaching the rounded corner, will move in both the negative z-direction and in the $-R_{\eta_0}$ direction. Such a flowline could exit the fold somewhere near ∂H_0, having experienced significant movement in the $-R_{\eta_0}$ direction. This type of holonomy is not present in the piecewise-linear setting, nor is it described by (ii) of Proposition 4.9, and unfortunately it has irritatingly significant implications — for example, see the piecewise-linear proof of Proposition 1.7 in Section 5.2.

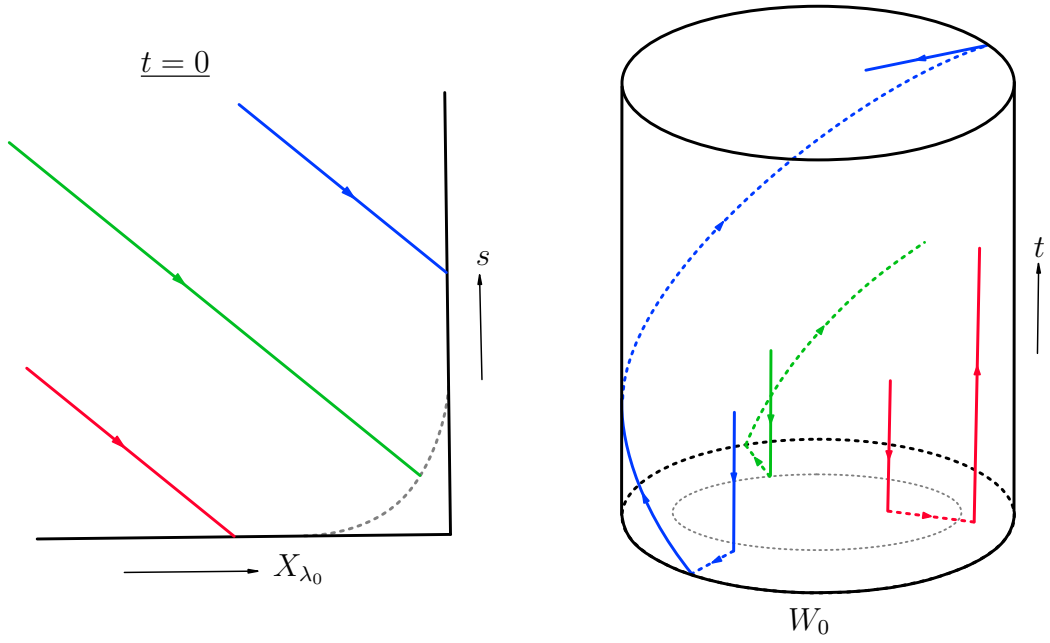

Figure 4.8: A heuristic depiction of complicated smooth holonomy arising from rounding the edge $\underline{s=0} \cap \partial W_0$. On the left is the projection of $\underline{t=0}$ to the s and X_{λ_0} directions; here the foliation is $-\partial_s + X_{\lambda_0}$. On the right is the projection to $H_0 = [0, t_0] \times W_0$. The flowline in blue reaches ∂W_0 before $\underline{s=0}$ and is ultimately trapped after reaching $\underline{t=t_0}$. The flowline in red reaches $\underline{s=0}$ first, and exits the fold after experiencing the holonomy described by h^{PL}. The flowline in green reaches the rounded corner in gray, and experiences some interpolation of $\partial_t - \partial_z$ and $\partial_t - R_{\eta_0}$. In particular, it experiences some motion in the $-R_{\eta_0}$ direction before exiting the fold.

For our purposes, we only need to carefully consider those flowlines entering the fold near $t = 0$. The following lemma is a technical summary of the following principle: if a point enters a smooth box fold near $t = 0$ and passes through the fold with a significant

increase in t-coordinate, then the holonomy was heavily influenced by the characteristic foliation of ∂H_0. That is, $h^\tau(x)$ is close to a finite time flow along the characteristic foliation of ∂H_0.

Lemma 4.10. *Let Π^τ be a smooth box fold, and let $\varepsilon(\tau) > 0$ be a quantity such that $\{0 \leq t < \varepsilon(\tau)\} \subset H_0 \setminus (H^\tau_{\text{trap}} \cup H^\tau_{\text{pass}})$. Suppose that $x \in H_0$ satisfies $t(x) \in [0, \varepsilon(\tau))$. Let $\psi^s_{\partial H_0} : \partial H_0 \to \partial H_0$ be the time-s flow of the characteristic foliation of ∂H_0. Let $\bar{t} := t(h^\tau(x))$ and suppose that $\bar{t} \gg \varepsilon(\tau)$. Then as $\tau \to 0$, there is some $\bar{s}$ such that*

$$\left\| h^\tau(x) - \psi^{\bar{s}}_{\partial H_0}(t = 0, W_0(x)) \right\| \to 0.$$

Here, the norm is defined by choosing some auxiliary metric on W_0.

Proof. This lemma is essentially a formalization of the discussion from above. Let $\bar{z}$ denote the maximum z-coordinate of the flowline through x as it passes through Π^τ. Since $t(x) < \varepsilon(\tau)$ and $\varepsilon(\tau) \to 0$ as $\tau \to 0$, the analysis of 4.1.2 implies that $\bar{z} = O(\tau)$. Since $\bar{t} \gg \varepsilon(\tau)$, the interpolation between the vector fields $\partial_t - \partial_z$ and $\partial_t - R_{\eta_0}$ near $\underline{s = 0} \cap \underline{\partial W_0}$ skews heavily in favor of the latter, with the disparity increasing as $\tau \to 0$. □

The usefulness of this fact will become clear in the proof of Proposition 1.7 in Section 5.2. We also emphasize that there is complicated behavior for nearly all flowlines entering $H_0 \setminus (H^\tau_{\text{trap}} \cup H^\tau_{\text{pass}})$, not just those entering near $t = 0$. For our strategy, it is unnecessary to dwell on this.

We do, however, wish to obtain an estimate on the strength of the induced movement in the Weinstein direction away from the skeleton. Recall that in a piecewise-linear fold, Proposition 4.4 describes the holonomy as

$$h^{PL}(t, w) = (e^{s_0} t, \psi^{s_0}(w))$$

where ψ^s is the time-s flow of X_{λ_0}, the Liouville vector field of the Weinstein base (W_0, λ_0). That is, every point experiencing holonomy simply flows for time s_0 in the X_{λ_0} direction.

In a smooth fold, this is approximately true for a large class of points according to (ii) of Proposition 4.9, but (iv) of the same proposition leaves open the possibility for erratic behavior near the boundary as described in the present subsection. However, the time-s_0 flow of X_{λ_0} still provides an "upper bound" for the holonomy in this direction, loosely speaking.

Lemma 4.11. *Let Π_0 be a smooth box fold installed over the contact handlebody $(H_0 = [0, t_0] \times W_0,\ dt + \lambda_0)$ with symplectization length s_0. Let $h : \{s_0\} \times H_0 \dashrightarrow \{0\} \times H_0$ be the partially-defined holonomy map given by backward passage through Π_0. Then*

$$\|h(x)\|_{W_0} \leq e^{s_0} \|x\|_{W_0}.$$

Proof. To obtain an estimate on $\|h(x)\|_{W_0}$ we need to estimate the net change in the X_{λ_0} direction in the statement of Lemma 4.7. According to that lemma, the coefficient in front of X_{λ_0} in the Liouville vector field is $-e^{-s}\frac{\partial F}{\partial t}$, where F is the folding function of Π_0. In particular, when $\frac{\partial F}{\partial t} > 0$ there is movement away from the skeleton in backward time, and when $\frac{\partial F}{\partial t} < 0$ there is movement toward the skeleton. Thus, to obtain an upper bound $\|h(x)\|_{W_0}$ of a point with holonomy, it suffices to assume $\frac{\partial F}{\partial t} \geq 0$ for the duration of the passage through the fold.

Lemma 4.7 also implies that the coefficient in front of ∂_s in the Liouville vector field is $1 + e^{-s}\frac{\partial F}{\partial t}$. Thus, the two relevant terms for determining the holonomy from $\{s = s_0\} \to \{s = 0\}$ are

$$\left(1 + e^{-s}\frac{\partial F}{\partial t}\right)\partial_s - e^{-s}\frac{\partial F}{\partial t}\, X_{\lambda_0}.$$

Since $1 + e^{-s}\frac{\partial F}{\partial t} > 0$, we may scale the vector field above to obtain

$$\partial_s - \frac{e^{-s}\frac{\partial F}{\partial t}}{1 + e^{-s}\frac{\partial F}{\partial t}}\, X_{\lambda_0}.$$

Note that

$$0 \leq \frac{e^{-s}\frac{\partial F}{\partial t}}{1 + e^{-s}\frac{\partial F}{\partial t}} \leq 1.$$

Thus, an upper bound for the movement away from the skeleton is given by the time-s_0 flow of the vector field X_{λ_0}. The lemma then follows from the fact that

$$\|\psi^{s_0}(x)\|_{W_0} = e^{-s_x+s_0} = e^{s_0}\,\|x\|_{W_0}\,.$$

□

CHAPTER 5

Box fold variants

JUST COPY AND PASTED FROM MITSU

5.1 Chimney folds

A box fold is based over the symplectization of a contact handlebody, which, by definition, is a Reeb-thickened Weinstein domain. The exact behavior of a box fold as described in Section 4.1 relies on the fact that a contact handlebody has Reeb chords of constant length, as well as the fact that the Weinstein direction is a domain. However, we have already seen in 4.1.4 that a fold installed over something other than a genuine contact handlebody can still trap flowlines in backward time; that is, it is possible to introduce critical points to the Liouville vector field of a Liouville domain by folding over regions that are more complicated than ordinary contact handlebodies.

A *chimney fold* — the main tool used in Section 5.2 to prove Proposition 1.7 — is such a fold. From one perspective, a chimney fold is simply a box fold based over a *subset* of a contact handlebody, rather than the entire contact handelbody. By carefully carving out the supporting region, we can influence which flowlines are trapped and also direct the holonomy in an advantageous way. We will define a chimney fold by identifying the supporting region in a way that is tailored to the proof of Proposition 1.7, but the analysis in this section should be viewed as a first step toward developing a more sophisticated understanding of local manipulations of Liouville vector fields.

Our motivation for the design of a chimney fold comes from the need to deal with complications in the smooth holonomy of a box fold as described in 4.2.4. Indeed, it is

possible to prove a piecewise-linear version of Proposition 1.7 with a single, ordinary box fold. For convenience and motivation, we give this proof in 5.2.2 and describe why it breaks down in the smooth setting. In fact, if the reader would like this motivation before tackling the details of chimney folds, 5.2.2 can be read independently of the present section.

5.1.1 Piecewise-linear chimney folds

As with box folds, we proceed by defining chimney folds in piecewise-linear form. For most of the section, we will restrict ourselves to chimney folds defined on 4-dimensional Liouville domains, where all of the interesting behavior occurs. In 5.1.3 we will extend chimney folds to arbitrary dimensions, which is a straightforward process and does not introduce any significant complications.

Fix $z_0, s_0, t_0 > 0$ and assume that $z_0 = e^{s_0} t_0$. We emphasize the importance of this last assumption for our setup. Let (W_0^2, λ_0) be a Weinstein domain of dimension 2. For our purpose, we will also assume that ∂W_0 is connected, so that $\partial W_0 \cong S^1$. Identify the collar neighborhood $N^{s_0}(\partial W_0)$ as in Sections 4.1 and 4.2 and recall that $N^{s_0}(\partial W_0)$ is naturally symplectomorphic to $((-s_0, 0]_r \times \partial W_0, e^r \eta_0)$. We begin by identifying a subset $C \subset N^{s_0}(\partial W_0)$ as follows. Let $\gamma_C \subset \partial W_0$ be any connected arc, and define

$$C := [-s_0 + \varepsilon_{\text{aux}}, 0]_r \times \gamma_C.$$

Here ε_{aux} is a small, unimportant auxiliary parameter.

As before, we can consider the contact handlebody $([0, t_0] \times W_0,\ dt + \lambda_0)$. Instead of folding over this entire handlebody, we will identify a subset $H_0^C \subset [0, t_0] \times W_0$ that supports the fold. Fix $0 < t_- \ll t_0$ and define

$$H_0^C := ([0, t_-] \times W_0) \cup ([0, t_0] \times C).$$

In words, H_0^C acts as a contact handlebody of sorts with Reeb chords of non-constant length: over $W_0 \setminus C$ Reeb chords have length t_-, and over C they have length t_0. From

another perspective, H is an ordinary contact handlebody $[0, t_-] \times W_0$ together with an appended contact region that resembles the supporting region of a pre-chimney fold (a Reeb-thickened trivial cobordism C).

Remark. We will refer to the region $[0, t_0] \times C$ as the *chimney* of H_0^C, and to $[0, t_-] \times (W_0 \setminus C)$ as the *stove*.

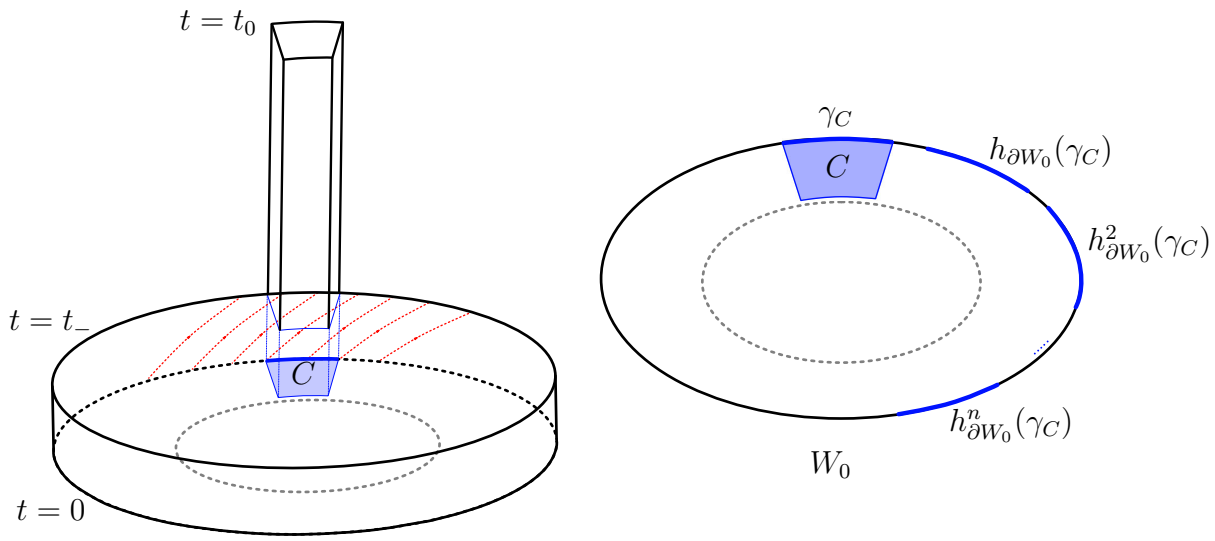

Figure 5.1: A depiction of the supporting region H_0^C in a chimney fold. On the left figure, the characteristic foliation $\partial_t - R_{\eta_0}$ of ∂W_0 is depicted by the dashed red lines; the main assumption about iterates of γ_C under $h_{\partial W_0}$ is depicted in the W_0 projection on the right. On both figures that dashed gray curve represents $N^{s_0}(\partial W_0)$.

Ultimately, a chimney fold will be given by a smooth approximation of a scaled indicator function of $[0, s_0]_s \times H_0^C$, exactly as with an ordinary box fold. However, to achieve the desired behavior we impose an important assumption.

To state this assumption, we need to introduce some notation. Let $h_{\partial W_0} : \{t = 0\} \times \partial W_0 \to \{t = t_-\} \times \partial W_0$ be the holonomy map given by the backward characteristic foliation of $[0, t_-] \times \partial W_0$ in the stove $([0, t_-] \times W_0,\ dt + \lambda_0)$. Recall that this characteristic foliation is directed by $\partial_t - R_{\eta_0}$. As always, we will abuse notation slightly and write $h_{\partial W_0} : \partial W_0 \to \partial W_0$.

Example 5.1. Suppose that $(W_0 = r_0\mathbb{D}^2, \lambda_0 = \frac{1}{2}r^2\, d\theta)$. The backward oriented characteristic

foliation of $[0, t_-] \times \partial W_0$ is directed by $\partial_t - \frac{2}{r_0^2}\partial_\theta$ and so

$$h_{\partial W_0}(\theta) = \theta - \frac{2}{r_0^2} t_-.$$

The key assumption needed to define a chimney fold is the following.

Main assumption. Let n be the smallest integer so that $nt_- > t_0$. Then $\gamma_C \cap h^j_{\partial W_0}(\gamma_C) = \emptyset$ for all $1 \leq j \leq n$.

This assumption ensures two main features of the boundary holonomy $h_{\partial W_0}$:

(1) the map $h_{\partial W_0}$ displaces γ_C, and

(2) the image of γ_C does not circle around the boundary back to itself after up to n iterates under $h_{\partial W_0}$.

See Figure 5.1. In practice, we will choose $t_- \ll t_0$ to be very small. Thus, (1) will come from a combination of γ_C being small and R_{η_0} being large near γ_C, and (2) will come from ensuring that ∂W_0 is long enough. It will become clear as we analyze the dynamics of a chimney fold why this assumption is necessary. We also remark that, more generally, this assumption can be stated by requiring n to satisfy $ne^{s_0}t_- > z_0$. Since we are assuming $z_0 = e^{s_0}t_0$, this simplifies to $nt_- > t_0$. The cost of increasing z_0 further is an increase in the value of n.

To define a chimney fold, we consider the contactization of the symplectization of H_0^C:

$$\left(\mathbb{R}_z \times [0, s_0] \times H_0^C,\, dz + e^s\,(dt + \lambda_0)\right)$$

Definition. Fix $z_0, s_0, t_0 > 0$ with $z_0 = e^{s_0}t_0$, and suppose that H_0^C is defined as above with the main assumption satisfied. A **piecewise-linear chimney fold with parameters** z_0, s_0, t_0, t_-, denoted $C\Pi^{PL}$, is the hypersurface

$$C\Pi^{PL} := \overline{\partial([0, z_0] \times [0, s_0] \times H_0^C) \setminus \{z = 0\}}.$$

As with piecewise-linear box folds, we adopt the following notation to refer to the various sides of $C\Pi^{PL}$:

$$\begin{aligned}
\underline{z = z_0} &:= \{z = z_0\} \times [0, s_0] \times H_0^C \\
\underline{s = 0} &:= [0, z_0] \times \{s = 0\} \times H_0^C \\
\underline{s = s_0} &:= [0, z_0] \times \{s = s_0\} \times H_0^C \\
\underline{t = 0} &:= [0, z_0] \times [0, s_0] \times \{t = 0\} \times W_0 \\
\underline{t = t_-} &:= [0, z_0] \times [0, s_0] \times \{t = t_-\} \times (W_0 \setminus C) \\
\underline{t = t_0} &:= [0, z_0] \times [0, s_0] \times \{t = t_0\} \times C \\
\underline{\partial W_0} &:= [0, z_0] \times [0, s_0] \times [0, t_-] \times \partial W_0 \\
\underline{\partial C} &:= [0, z_0] \times [0, s_0] \times [t_-, t_0] \times \partial C.
\end{aligned}$$

Observe the subtleties in the definition of sides such as $\underline{t = t_-}$ and $\underline{\partial W_0}$ in comparison to the ordinary box fold setting. This accounts for the various pieces of ∂H_0^C. As in Section 4.1, we compute the oriented characteristic foliation of each side in Table 5.1.

Side	Characteristic foliation
$\underline{z = z_0}$	$-\partial_s$
$\underline{s = 0}$	$\partial_t - \partial_z$
$\underline{s = s_0}$	$-\partial_t + e^{s_0}\partial_z$
$\underline{t = 0}$	$-\partial_s + X_{\lambda_0}$
$\underline{t = t_-}$	$\partial_s - X_{\lambda_0}$
$\underline{t = t_0}$	$\partial_s - X_{\lambda_0}$
$\underline{\partial W_0}$	$\partial_t - R_{\eta_0}$
$\underline{\partial C}$	$X_{\partial C}$

Table 5.1: The oriented characteristic foliation of a chimney fold.

Here, $X_{\partial C}$ is simply a placeholder for the backward oriented characteristic foliation of $\underline{\partial C}$. For example, we could write $X_{\partial W_0} = \partial_t - R_{\eta_0}$. The explicit description of $X_{\partial C}$ is given by the table in 4.1.4 that gives the characteristic foliation of a pre-chimney fold. Speaking loosely, most flowlines of $X_{\partial C}$ swirl around $\underline{\partial C}$ and up in the t-direction toward $\underline{t = t_0}$.

Our next goal is to prove the following proposition, which is the key feature of a chimney

fold.

Proposition 5.2. *Suppose that $x \in \{z = 0\} \times \{s = s_0\} \times (0, t_0) \times int(C)$. Then the flowline through x of the characteristic foliation of $C\Pi^{PL}$ is trapped in backward time.*

Informally, this proposition says that a chimney fold traps *everything* entering the chimney portion of H_0^C. The utility of the chimney fold in comparison to a pre-chimney fold is evident: with a chimney fold, one can trap everything in the chimney, at the cost of also folding over a large but t-thin stove $[0, t_-] \times (W_0 \setminus C)$. With a simple pre-chimney fold, it is obviously impossible to trap everything in the chimney region. The role and impact of the stove, together with the main assumption, will become clear in the proof of Proposition 5.2.

For convenience, we begin with a lemma. The proof will elucidate how a chimney fold exhibits the behavior of both an ordinary box fold and a pre-chimney fold in different regions.

Lemma 5.3. *If a flowline reaches $\underline{z = z_0}$ in a chimney fold, it is trapped in backward time.*

Proof. The characteristic foliation of $\underline{z = z_0}$ is directed by $-\partial_s$, so upon reaching $\underline{z = z_0}$ the flowline will travel to $\underline{s = 0}$. There are two cases to consider: the flowline reaches either $\underline{s = 0} \cap C$ or $\underline{s = 0} \cap (W_0 \setminus C)$.

Case 1: the flowline reaches $\underline{s = 0} \cap C$.

Along $\underline{s = 0}$ the foliation is directed by $\partial_t - \partial_z$. Over C, the length of the Reeb chords is t_0. Since $z_0 = e^{s_0} t_0 > t_0$, the flowline will reach $\underline{t = t_0}$. Because a chimney fold behaves like a pre-chimney fold near $\underline{t = t_0}$, and because the flowline came from $\underline{z = z_0}$, we may apply Lemma 4.6 to conclude that the flowline is ultimately trapped.

Case 2: the flowline reaches $\underline{s = 0} \cap (W_0 \setminus C)$.

This case essentially follows from Lemma 4.3, with one minor subtlety. For convenience, we give the argument here. Over $W_0 \setminus C$, the length of the Reeb chords is $t_- < z_0$. Thus, the flowline follows $\partial_t - \partial_z$ to $\underline{t = t_-}$. Here the foliation is directed by $\partial_s - X_{\lambda_0}$. Because C

is defined by the backward flow of some arc in ∂W_0, and because the flowline is currently in $W_0 \setminus C$, it follows $\partial_s - X_{\lambda_0}$ to $\underline{s = s_0}$ (as opposed to potentially reaching $\underline{\partial C}$). The W_0-coordinate has moved closer to $\mathrm{Skel}(W_0, \lambda_0)$, and the flowline is still in $W_0 \setminus C$.

Along $\underline{s = s_0}$ the flowline follows $-\partial_t + e^{s_0}\,\partial_z$. Because the flowline originally reached $\underline{t = t_-}$ from $\underline{z = z_0}$, the flowline will then reach $\underline{z = z_0}$. We return to Case 2. Note that the t-coordinate has increased, and the W_0-coordinate has moved closer to the skeleton. The flowline cycles through Case 2 indefinitely and never exits the fold.

□

Proof of Proposition 5.2. Let $x \in \{z = 0\} \times \{s = s_0\} \times (0, t_0) \times \mathrm{int}(C)$ denote the entry point of the flowline. The foliation is directed by $-\partial_t + e^{s_0}\,\partial_z$ along $\underline{s = s_0}$. Since $t(x) < t_0$ and $z_0 = e^{s_0} t_0$, the flowline reaches $\underline{t = 0}$ with z-coordinate $e^{s_0} t(x)$. Here it follows $-\partial_s + X_{\lambda_0}$. Since the flowline began in $C \subset N^{s_0}(\partial W_0)$, it then reaches $\underline{\partial W_0}$ before $\underline{s = 0}$.

Here it follows $\partial_t - R_{\eta_0}$. By the main assumption — in particular, the fact that $\gamma_C \cap h_{\partial W_0}(\gamma_C) = \emptyset$ — the flowline then reaches $\underline{t = t_-}$ (as opposed to $\underline{\partial C}$).

Along $\underline{t = t_-}$ the flowline follows $\partial_s - X_{\lambda_0}$. Since the flowline is currently in $W_0 \setminus C$, it will reach $\underline{s = s_0}$ (as opposed to $\underline{\partial C}$), as in the proof of Lemma 5.3. Along $\underline{s = s_0}$, the flowline follows $-\partial_t + e^{s_0}\,\partial_z$. If the flowline reaches $\underline{z = z_0}$, it is ultimately trapped by Lemma 5.3. Otherwise, it reaches $\underline{t = 0}$ with z-coordinate $e^{s_0} t(x) + e^{s_0} t_-$.

At this point, we essentially return to the beginning of the proof: the flowline has reached $\underline{t = 0}$, but now with an increased z-coordinate of $e^{s_0} t(x) + e^{s_0} t_-$. After j cycles through this process, the flowline will either reach $\underline{z = z_0}$, or it will reach $\underline{t = 0}$ with z-coordinate

$$e^{s_0} t(x) + j e^{s_0} t_-.$$

Furthermore, with each cycle through this process, the flowline travels along ∂W_0 via $h_{\partial W_0}$. Recall the main assumption: with n the smallest integer satisfying $n t_- > t_0$, we have $\gamma_C \cap h^j_{\partial W_0}(\gamma_C) = \emptyset$ for $1 \leq j \leq n$. This assumption ensures that the above process terminates only by reaching $\underline{z = z_0}$, rather that eventually reaching $\underline{\partial C}$. Indeed, after n

cycles through this process, the z-coordinate of the flowline would otherwise be

$$e^{s_0}t(x) + ne^{s_0}t_- > ne^{s_0}t_- > e^{s_0}t_0 = z_0.$$

See Figure 5.2 for a visualization of this argument.

□

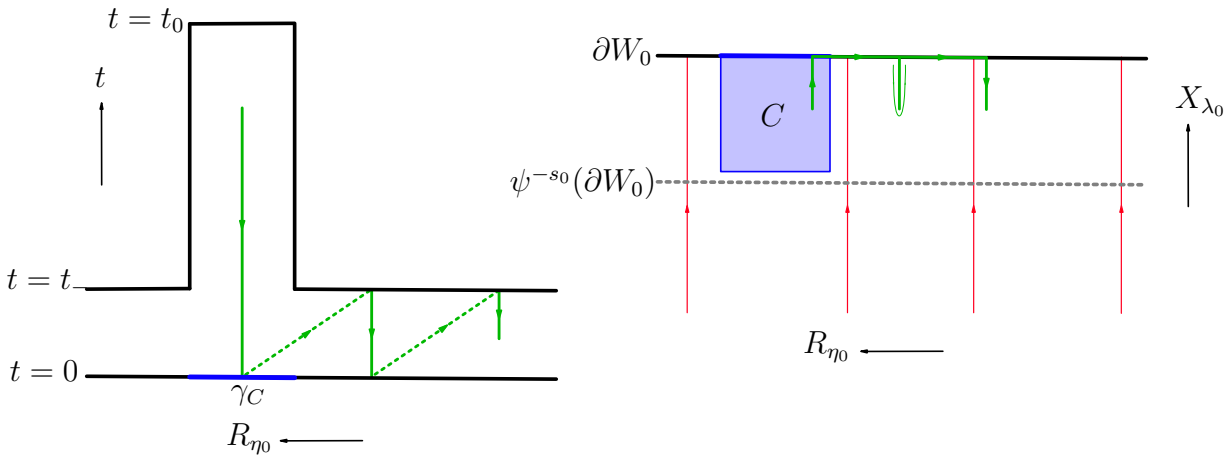

Figure 5.2: A flowline entering $C\Pi^{PL}$ in the chimney that eventually gets trapped according to Proposition 5.2. It initially travels down to $\underline{t = 0}$, then cycles through a process involving $h_{\partial W_0}$ a number of times before reaching $\underline{z = z_0}$.

Before moving on, we include some further discussion on what goes wrong without the main assumption as a way to clarify this aspect of the behavior of a chimney fold. In particular, we identify the regions of H_0^C that "expand" under the holonomy to fill in the chimney, which is entirely trapped by Proposition 5.2. This discussion is not necessary for the analysis in Section 5.2; it is simply meant to help the reader understand the role and function of a chimney fold.

Recall that in an ordinary (piecewise-linear) box fold, any flowline that reaches $\underline{\partial W_0}$ is ultimately trapped. Indeed, the foliation along this side is directed by $\partial_t - R_{\eta_0}$, so the flowline reaches $\underline{t = t_0}$ and is trapped by Lemma 4.3. In contrast, it is *not* the case that any

flowline reaching $\underline{\partial W_0}$ in a chimney fold is trapped. Any flowline that reaches $\underline{\partial W_0}$ via C is trapped — this is essentially the proof of Proposition 5.2 — but it possible to reach $\underline{\partial W_0}$ outside of C and eventually exit the fold.

For example, let

$$h^{-1}_{\partial W_0}(C) := [-s_0 + \varepsilon_{\text{aux}}, 0]_r \times h^{-1}_{\partial W_0}(\gamma_C)$$

and consider a flowline that enters the fold in H_0^C via $(0, e^{-s_0}t_-) \times h^{-1}_{\partial W_0}(C)$. Suppose that the initial r-coordinate of the flowline is $-\bar{s}$ for some $0 < \bar{s} < s_0 - \varepsilon_{\text{aux}}$. As the flowline enters the fold, it travels across $\underline{s = s_0}$ via $-\partial_t + e^{s_0}\,\partial_z$, reaching $\underline{t = 0}$ first. Here it follows $-\partial_s + X_{\lambda_0}$. Since $\bar{s} < s_0 - \varepsilon_{\text{aux}}$, the flowline will reach $\underline{\partial W_0}$. Note that the new s-coordinate is $s_0 - \bar{s}$. By definition of $h^{-1}_{\partial W_0}(C)$, the flowline follows $\partial_t - R_{\eta_0}$ and will eventually reach $\underline{\partial C}$, as opposed to $\underline{t = t_-}$; see Figure 5.3.

The flowline then follows the characteristic foliation of $\underline{\partial C}$, and a portion of such flowlines will reach $\underline{t = t_-}$ rather than spiral up toward $\underline{t = t_0}$. Note that traversing the characteristic foliation of $\underline{\partial C}$ does not change the s-coordinate. Thus, a flowline that reaches $\underline{t = t_-}$ via $\underline{\partial C}$ will do so with s-coordinate $s_0 - \bar{s}$. On $\underline{t = t_-}$ the flowline follows $\partial_s - X_{\lambda_0}$ to $\underline{s = s_0}$, again due to the definition of C. The r-coordinate (i.e., the X_{λ_0}-coordinate) of the flowline is now $-s_0 + \varepsilon_{\text{aux}} - \bar{s}$. Here the flowline follows $-\partial_t + e^{s_0}\,\partial_z$ to $\underline{t = 0}$ where it then follows $-\partial_s + X_{\lambda_0}$. Because the r-coordinate upon reaching $\underline{t = 0}$ is $-s_0 + \varepsilon_{\text{aux}} - \bar{s}$, the flowline reaches $\underline{s = 0}$ first, and it will do so with r-coordinate $-\bar{s} + \varepsilon_{\text{aux}}$. In particular, for most values of $\bar{s}$, the W_0-coordinate of the flowline will now be in C. Along $\underline{s = 0}$ the flowline follows $\partial_t - \partial_z$. Since the length of the Reeb direction over C is t_0, which is larger than than the current z-coordinate of the flowline, the flowline will travel up the chimney some distance and exit the fold.

This clarifies how the chimney is "filled in." Roughly speaking, points that enter in the chimney get funneled down and pass through the iterates $h^j_{\partial W_0}(C)$ in the stove for $1 \leq j \leq n$ before ultimately getting trapped. While this is happening, points entering through a collection of preimages $h^{-j}_{\partial W_0}(C)$ in the stove pass through the various iterates and eventually travel up the chimney and then exit the fold. As the z-coordinate of a flowline

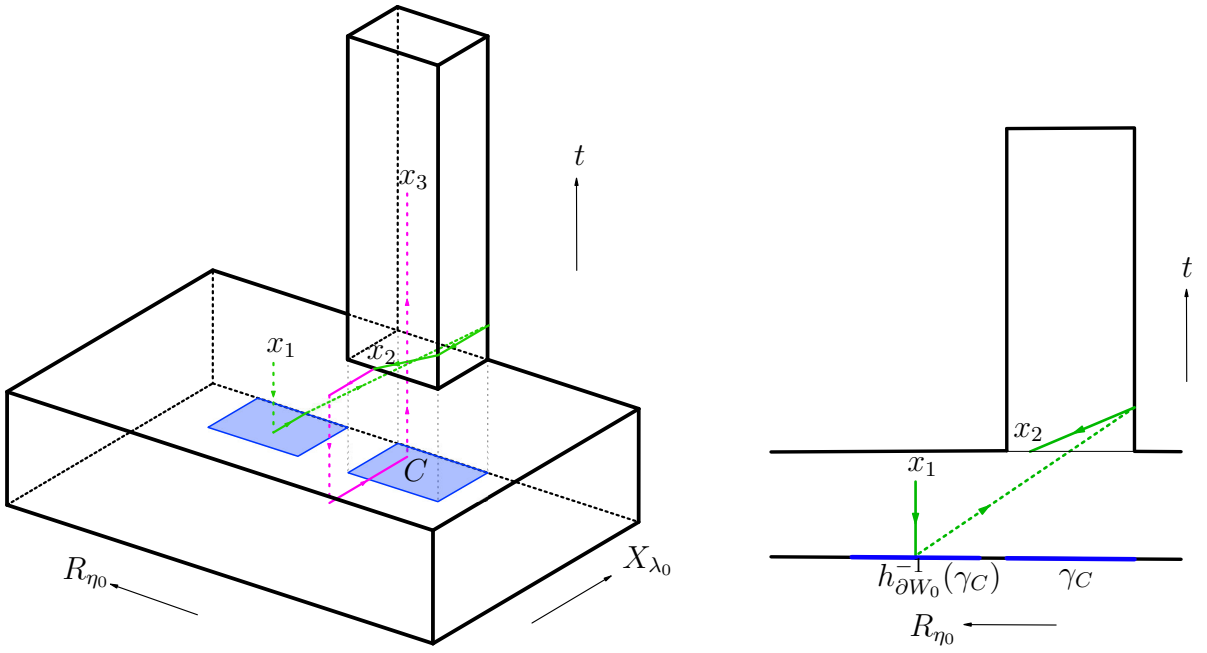

Figure 5.3: A depiction of a flowline that enters the fold in the stove above $h_{\partial W_0}^{-1}(C)$ and ultimately exits the fold after traveling up the chimney some distance. Two different phases of the flowline are color coded in green and pink for visual clarity, with the rightmost projection containing only the green phase. The flowline enters the fold at x_1 and exits the fold at x_3.

increases with each application of $h_{\partial W_0}$, it follows that points entering $h_{\partial W_0}^{-(j+1)}(C)$ with holonomy fill in a portion of the chimney above points entering $h_{\partial W_0}^{-j}(C)$ with holonomy. Thus, the role of the t-thin stove is two-fold: it provides enough room to funnel points entering the chimney away to be trapped, and it also provides a repository of points that will ultimately fill in the trapping region in the chimney. The main assumption in defining a chimney fold simply gaurantees that these two features function independently of each other.

Once again, we emphasize that this discussion is not important for the proof of Proposition 1.7; its purpose is simply to bolster intuition about the dynamics of a chimney fold. We do not need to carefully study the holonomy of points entering H_0^C away from the chimney region.

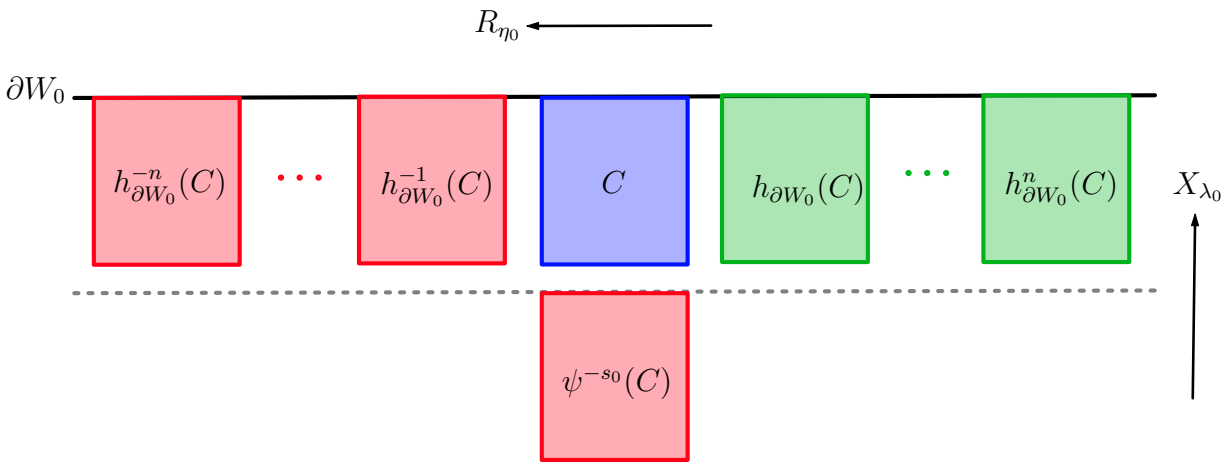

Figure 5.4: Various iterates of C under $h_{\partial W_0}$. Points entering the fold above C are funneled down and pass through the forward iterates, depicted in green. Some points entering the fold in the stove above the red regions ultimately fill in the chimney and exit the fold. The region $\psi^{-s_0}(C)$ fills in the lowest portion of the chimney; the first backward iterate $h^{-1}_{\partial W_0}(C)$ fills in the next lowest portion of the chimney, and the highest order backward iterate fills in the top part of the chimney.

5.1.2 Smooth chimney folds

Now we briefly discuss smooth chimney folds. As we have mentioned, we are fortunate to have a relatively robust strategy and thus it is unnecessary to study the smooth holonomy in detail: it will suffice to identify a smooth trapping region in the chimney.

Let $\tau > 0$ be a small smoothing parameter, and define $B^\tau := [\tau, s_0 - \tau] \times H_0^\tau$ where H_0^τ is an inner approximation of H_0^C defined as follows:

$$H_0^\tau := \left([\tau, t_- - \tau] \times \overline{W_0 \setminus N^\tau(\partial W_0)}\right) \cup \left([\tau, t_0 - \tau] \times [-s_0 + \varepsilon_{\text{aux}} + \tau, -\tau]_r \times \gamma_C^\tau\right).$$

Here, γ_C^τ is an inner approximation of γ_C such that $\gamma_C^\tau \to \gamma_C$ as $\tau \to 0$. In words, H_0^τ is simply a contracted version of H_0^C such that $H_0^\tau \to H_0^C$ as $\tau \to 0$. As before, we let F^τ_{aux} be an appropriate smooth function with support in B and $F^\tau_{\text{aux}} \equiv z_0$ on B^τ, and we further define τ-admissibility.

Definition. A function $F : B \to \mathbb{R}$ is **τ-admissible** if $\|F - F^\tau_{\text{aux}}\|_{C^\infty(B)} < \tau$ and graph(F)

has Morse characteristic foliation in the contactization of B.

Definition. Fix $z_0, s_0, t_0, t_-, \tau > 0$ with $t_- \ll t_0$ and $z_0 = e^{s_0} t_0$, and let $F^\tau : B \to \mathbb{R}$ be τ-admissible. A **smooth chimney fold with parameters** z_0, s_0, t_0, t_- **and smoothing parameter** τ, denoted $C\Pi^\tau$, is the hypersurface graph(F^τ) in the contactization of B.

We remind the reader that this definition implicitly includes the main assumption about $h_{\partial W_0}$. The next proposition identifies part of the trapping region of a smooth chimney fold in similar fashion to Proposition 4.9. The statement is immediate from Proposition 5.2.

Proposition 5.4. *Let $C\Pi^\tau$ be a smooth chimney fold. There is a closed set $int^\tau(C) \subset int(C)$ and a function $\varepsilon(\tau) > 0$ such that:*

(*i*) *Any flowline entering $[\varepsilon(\tau), t_0 - \varepsilon(\tau)] \times int^\tau(C)$ converges to a critical point in $C\Pi^\tau$ in backward time.*

(*ii*) *As $\tau \to 0$, $\varepsilon(\tau) \to 0$ and $|int(C) \setminus int^\tau(C)| \to 0$.*

We remark that the region $[\varepsilon(\tau), t_0 - \varepsilon(\tau)] \times \text{int}^\tau(C)$ described in (i) does not identify the *entire* trapping region of the chimney fold. There are certainly other flowlines that are trapped. For our purpose, it is only necessary to identify part of the trapping region in the chimney.

The one nontrivial aspect of the smooth holonomy of a chimney fold we need for our strategy in Section 5.2 is the following lemma. In words, it says that if a flowline exits the fold anywhere in or on the central chimney portion (above the stove, and below the top of the chimney), the initial W_0-coordinate of the flowline was not in $\text{int}^\tau(C)$.

Lemma 5.5. *Let $h^\tau : \{s = s_0\} \times H_0^C \dashrightarrow \{s = 0\} \times H_0^C$ be the partially-defined holonomy map given by the oriented characteristic foliation of $C\Pi^\tau$. If $t(h^\tau(x)) \in (2t_-, t_0 - t_-)$ then $W_0(x) \in W_0 \setminus int^\tau(C)$.*

Remark. The exact threshold that defines the central part of the chimney in this lemma (namely, the extra factor of t_- in the interval $(t_- + t_-, t_0 - t_-)$ is not so important for our application. We also stress that this lemma is primarily meant to rule out the possibility that

a flowline enters the fold inside $\text{int}^\tau(C)$ near $t = 0$ (below the trapping region) and exits the fold somewhere near the boundary of the central part of the chimney. The importance of this exclusion will become clear in Section 5.2.

Proof. To prove the lemma it suffices to show that if $W(x) \in \text{int}^\tau(C)$, then $t(h^\tau(x)) \notin (2t_-, t_0 - t_-)$. By Proposition 5.4, $[\varepsilon(\tau), t_0 - \varepsilon(\tau)] \times \text{int}^\tau(C)$ is not in the domain of h^τ (these points are trapped), so we only need to consider points with $t(x) > t_0 - \varepsilon(\tau)$ or $t(x) < \varepsilon(\tau)$.

This is where the discussion in 4.2.4 enters the play. In order for such points to exit the fold after experiencing significant movement in the t-direction, they must be heavily influenced by the characteristic foliation of ∂H_0^C. For points x entering the fold near $t = 0$, the main assumption — specifically, the fact that $\gamma_C \cap h_{\partial W_0}(\gamma_C) = \emptyset$ — ensures that any flowline through x will, at worst, follow the characteristic foliation of $\underline{\partial W_0}$ up to $\underline{t = t_-}$, missing the central part of the chimney; see Figure 5.1. In particular, $t(h^\tau(x)) < 2t_-$. For points near $t = t_0$, a flowline of the characteristic foliation of ∂H_0^C beginning on $\underline{t = t_0}$ descends no further than $t = t_0 - t_-$, again by the fact that $\gamma_C \cap h_{\partial W_0}(\gamma_C) = \emptyset$. See also the analysis of the pre-chimney fold characteristic foliation in 4.1.4. Thus, provided τ is small enough, we have $t(h^\tau(x)) > t_0 - t_-$ as desired. □

We close this subsection with a remark about the subset $C \subset W_0$. We defined C by choosing an arc $\gamma_C \subset \partial W_0$ and setting $C := [-s_0 + \varepsilon_{\text{aux}}, 0]_r \times \gamma_C$. It should be clear from the analysis presented above that we are in fact free to let C be any (simply connected, codimension 0) subset of $[-s_0 + \varepsilon_{\text{aux}}, 0]_r \times \gamma_C$. The qualitative behavior of the fold does not change in any significant way, besides altering the shape of the chimney portion of the fold.

5.1.3 High-dimensional chimney folds

The chimney folds we have discussed so far are based over

$$[0, s_0] \times H_0^C \subset [0, s_0] \times [0, t_0] \times \tilde{W_0}^2.$$

Here, at the risk of confusing the reader, we now refer to the preferred 2-dimensional Weinstein domain in the definition of a chimney fold as $(\tilde{W}_0^2, \tilde{\lambda}_0)$, rather than (W_0^2, λ_0). This is with an eye towards Proposition 1.7, where $(\tilde{W}_0^2, \tilde{\lambda}_0) = (r_0\,\mathbb{D}^2, \lambda_{\text{stab}})$. In particular, we would like to define a chimney fold based in a region of the form

$$[0, s_0] \times H_0^C \times W_0 \subset \times [0, t_0] \times \tilde{W_0}^2 \times W_0$$

where (W_0, λ_0) is a Weinstein domain of arbitrary dimension, distinct from $(\tilde{W_0}^2, \tilde{\lambda}_0)$. This new W_0 direction will correspond to the W_0 in the statement of Proposition 1.7. In short, we will extend the definition of a chimney fold to this setting by constructing a chimney fold as before in $[0, s_0] \times [0, t_0] \times \tilde{W}_0^2$ and simply decaying near the boundary of the new Weinstein direction W_0.

Definition. Fix $z_0, s_0, t_0, t_- > 0$ with $z_0 = e^{s_0} t_0$, and define $H_0^C \subset [0, t_0] \times \tilde{W}_0^2$ as before. A **(high-dimensional) piecewise-linear chimney fold with parameters** z_0, s_0, t_0, t_-0, denoted $C\Pi^{PL}$, is the hypersurface

$$C\Pi^{PL} := \overline{\partial([0, z_0] \times [0, s_0] \times H_0^C \times W_0) \setminus \{z = 0\}}.$$

The following proposition is the high-dimensional generalization of Proposition 5.2. Informally, it says that nothing interesting happens to the trapping behavior of a chimney fold in this high-dimensional extension: every flowline entering the chimney and anywhere in W_0 is trapped.

Proposition 5.6. *Suppose that $x \in \{z = 0\} \times \{s = s_0\} \times (0, t_0) \times \text{int}(C) \times \text{int}(W_0)$. Then the flowline through x of the characteristic foliation of $C\Pi^{PL}$ is trapped in backward time.*

Proof. The proof is essentially identical to the proof of Proposition 5.2. Initially, the foliation along $\underline{s = s_0}$ is directed by $-\partial_t + e^{s_0}\,\partial_z$, so the flowline will reach $\underline{t = 0}$. Here the foliation is $-\partial_s + X_{\tilde{\lambda}_0} + X_{\lambda_0}$. The flowline will either reach $\underline{\partial \tilde{W_0}^2}$ or $\underline{\partial W_0}$. In the former case, the same analysis in the proof of Proposition 5.2 shows that the flowline is trapped; the only

additional behavior is some inconsequential back and forth movement in the W_0-direction before ultimately limiting towards $\mathrm{Skel}(W_0, \lambda_0)$.

In the latter case — when the flowline reaches $\underline{\partial W_0}$ — it then follows $\partial_t - R_{\eta_0}$, where R_{η_0} is the Reeb vector field of $\eta_0 := \lambda_0 \,|_{\partial W_0}$. Note that this R_{η_0} is not the R_{η_0} of the previous subsection, which is now $R_{\tilde{\eta}_0}$. Since the $\tilde{W}_0$-coordinate of the flowline is in C, where Reeb chords have length t_0, the flowline follows $\partial_t - R_{\eta_0}$ and ultimately reaches $\underline{t = t_0}$. By Lemma 4.3 and Lemma 4.6, the flowline is trapped. □

The smoothing of chimney folds in arbitrary dimensions works exactly as in Section 4.2 and in 5.1.2. The following proposition is the high-dimensional generalization of Proposition 5.4, and the statement is immediate from Proposition 5.6. There is one complication regarding smoothing near $\underline{\partial W_0}$ which we will discuss after the statement of the proposition.

Proposition 5.7. *Let $C\Pi^\tau$ be a smooth, high-dimensional chimney fold. There is a closed set $int^\tau(C) \subset int(C)$ and a function $\varepsilon(\tau) > 0$ such that:*

(*i*) *Any flowline entering*

$$[\varepsilon(\tau), t_0 - \varepsilon(\tau)] \times int^\tau(C) \times \left(W_0 \setminus N^{\varepsilon(\tau)}(W_0)\right)$$

converges to a critical point in $C\Pi^\tau$ in backward time.

(*ii*) *As $\tau \to 0$, $\varepsilon(\tau) \to 0$ and $|int(C) \setminus int^\tau(C)| \to 0$.*

Finally, we point out that the smooth decay of the fold near $\underline{\partial W_0}$ introduces a complication in the smooth holonomy which explains the qualifier $\|x\|_{W_0} < e^{-s_0}$ in part (ii) of the statement of Proposition 1.7. According to the discussion in 4.2.4, after smoothing, a flowline can have a significant interaction with $\underline{\partial W_0}$, yet still exit the fold. This can produce some unintended t-holonomy. In particular, the main concern is is a flowline entering the chimney fold near the very bottom of the chimney, along the t-axis, yet very close to the boundary of ∂W_0. If such a flowline is not trapped, it could experience significant t-holonomy after being influenced by the characteristic foliation of $\underline{\partial W_0}$. In the low-dimensional chimney projection, the flowline would move a minor amount away

from the stabilization origin and then straight up the chimney. The significance of this complciation will be explained in Section 5.2. However, if $\|x\|_{W_0} < e^{-s_0}$, then the flowline passing through x does not interact with $\underline{\partial W_0}$ in this way.

5.2 The blocking apparatus and proof of Proposition 1.7

In this section we prove Proposition 1.7, the local operation that drives the strategy of Section 6. Recall that Proposition 1.7 describes the installation of a *blocking apparatus* in a trivial Weinstein cobordism of the form

$$\left(U = [0, s_0] \times [0, t_0] \times W_0 \times r_0\mathbb{D}^2,\, e^s\left(dt + \lambda_0 + \lambda_{\text{stab}}\right)\right).$$

According to the statement of the proposition, a blocking apparatus should trap a neighborhood of $[\delta, t_0 - \delta] \times I_\epsilon(W_0, \lambda_0) \times \{(0,0)\}$ in $\partial_+ U = \{s = s_0\}$ in backward time, and the holonomy $h_U : \partial_+ U \dashrightarrow \partial_- U$ of flowlines that pass through needs to satisfy the following three conditions:

(i) for some constant $0 < K < 1$, we have $\|h(x)\|_{W_0} \leq Ke^{s_0}\|x\|_{W_0}$;

(ii) for the same constant K, we have $\|h(x)\|_{\text{stab}} \leq Ke^{\frac{s_0}{2}}\|x\|_{\text{stab}}$, whenever $\|x\|_{W_0} < e^{-s_0}$;

(iii) any element of $([0, \delta) \cup (t_0 - \delta, t_0]) \times I_{1-e^{-s_0}}(W_0, \lambda_0) \times \{(0,0)\}$ in $\partial_+ U$ which is not trapped is mapped by h to an element of $([0, 2\delta) \cup (t_0 - 2\delta, t_0]) \times W_0 \times \{(0,0)\}$.

Note that $I_{1-e^{-s_0}}(W_0, \lambda_0) = W_0 \setminus N^{s_0}(\partial W_0)$. The point here is that when we apply Proposition 1.7 in Section 6, the skeleton of the ambient stabilized Liouville domain intersects U somewhere in

$$[0, s_0] \times [0, t_0] \times (W_0 \setminus N^{s_0}(\partial W_0)) \times \{(0,0)\}.$$

Thus, roughly, a blocking apparatus traps a local neighborhood of the skeleton of the stabilized domain such that the induced holonomy is controllable.

This section is organized as follows. In 5.2.1, we state a low-dimensional version of Proposition 1.7, which most of the section will be dedicated to proving. In 5.2.2, as a

means of motivation for the definition of a blocking apparatus, we prove a piecewise-linear version of the low-dimensional version of Proposition 1.7 and explain why the proof fails in the smooth setting. In 5.2.3 we define the low-dimensional blocking apparatus and in 5.2.4 we prove the low-dimensional version of Proposition 1.7. Finally, in 5.2.5 we define the high-dimensional blocking apparatus and prove that the low-dimensional version of Proposition 1.7 implies the full statement.

5.2.1 A reduction

We will spend most of this section proving the following proposition, a low-dimensional version of Proposition 1.7. Then in 5.2.5 we will show that Proposition 5.8 implies Proposition 1.7.

Proposition 5.8 (Low-dimensional blocking apparatus)**.** *Consider the Weinstein cobordism* $(U = [0, s_0] \times [0, t_0] \times r_0\,\mathbb{D}^2, e^s\,(dt + \lambda_{\mathrm{stab}}))$*. Fix* $0 < \delta \ll t_0$ *arbitrarily small. Then if* $r_0 > 0$ *is sufficiently large, a blocking apparatus can be installed in* U *such that there is a neighborhood* U_{trap} *of*

$$[\delta, t_0 - \delta] \times \{(0, 0)\},$$

with any flowline passing through $\{s = s_0\} \times U_{\mathrm{trap}} \subseteq \partial_+ U$ *converging to a critical point in backward time. Moreover, the partially-defined holonomy map* $h\colon \partial_+ U \dashrightarrow \partial_- U$ *satisfies*

(*i*) *for some constant* $0 < K < 1$*, we have* $\|h(x)\|_{\mathrm{stab}} \leq K e^{\frac{s_0}{2}}\,\|x\|_{\mathrm{stab}}$*;*

(*ii*) *any element of* $([0, \delta) \cup (t_0 - \delta, t_0]) \times \{(0, 0)\}$ *in* $\partial_+ U$ *which is not trapped is mapped by* h *to an element of* $([0, 2\delta) \cup (t_0 - 2\delta, t_0]) \times \{(0, 0)\}$*.*

5.2.2 The piecewise-linear case

In this subsection we provide a straightforward proof of the piecewise-linear version of Proposition 5.8 to motivate the more complicated strategy of 5.2.4, and we describe why it breaks down in the smooth setting. This proof also serves as a warm-up to the argument in 5.2.4, which shares many of the same ideas.

One of the key ideas is the following. To install a box fold, one needs to first identify a contact handlebody. There is an obvious choice of handlebody given by $([0,t_0]\times r_0\mathbb{D}^2,\, dt+\lambda_{\mathrm{stab}})$, but we are actually interested in folding over other contact handlebodies that are subsets of $[0,t_0]\times r_0\mathbb{D}^2$. Given any surface $W_1\subset[0,t_0]\times r_0\mathbb{D}^2$ transverse to the Reeb vector field ∂_t, we can build a handlebody inside $[0,t_0]\times r_0\mathbb{D}^2$ by flowing W_1 along ∂_t for some amount of time. The point here is that with different choices of W_1, the movement induced by the fold in the Weinstein direction can be manipulated in advantageous ways.

Proof of the piecewise-linear Proposition 5.8. Fix $s_1<s_0$ and $\delta_1<\delta$. Ultimately, we will install an ordinary piecewise-linear box fold with symplectization support $[0,s_1]\subset[0,s_0]$ such that the Weinstein domain base W_1 of the supporting contact handlebody H_1 is given by

$$W_1=\{t=\delta_1-c_1p\}\cap\{-p_1\le p\le p_1\}\cap\{-q_-\le q\le q_+\}$$

for some choice of $c_1,p_1,q_-,q_+>0$; see Figure 5.5. The contact form $dt+\lambda_{\mathrm{stab}}$ restricts to a Liouville structure on W_1, and one can check that the vector field

$$X_1:=\frac{1}{2}p\,\partial_p+\left(\frac{1}{2}q+c_1\right)\partial_q$$

is the resulting Liouville vector field.

We choose all of the necessary parameters needed to define the fold, and we include some informal explanation of each.

(1) Choose $c_1>0$.

This determines the strength of the tilt of the Weinstein base W_1, which determines the location of the isolated, index 0 critical point of X_1. In particular, the critical point is located at $(p=0,q=-2c_1)$.

(2) Choose $p_1>0$ so that $c_1p_1<\delta_1$.

This determines the p-width of W_1 and further ensures that the base has t-variation less than δ_1. This is necessary for the handlebody to be a subset of $[0,t_0]\times r_0\mathbb{D}^2$.

(3) Choose $q_->2c_1$.

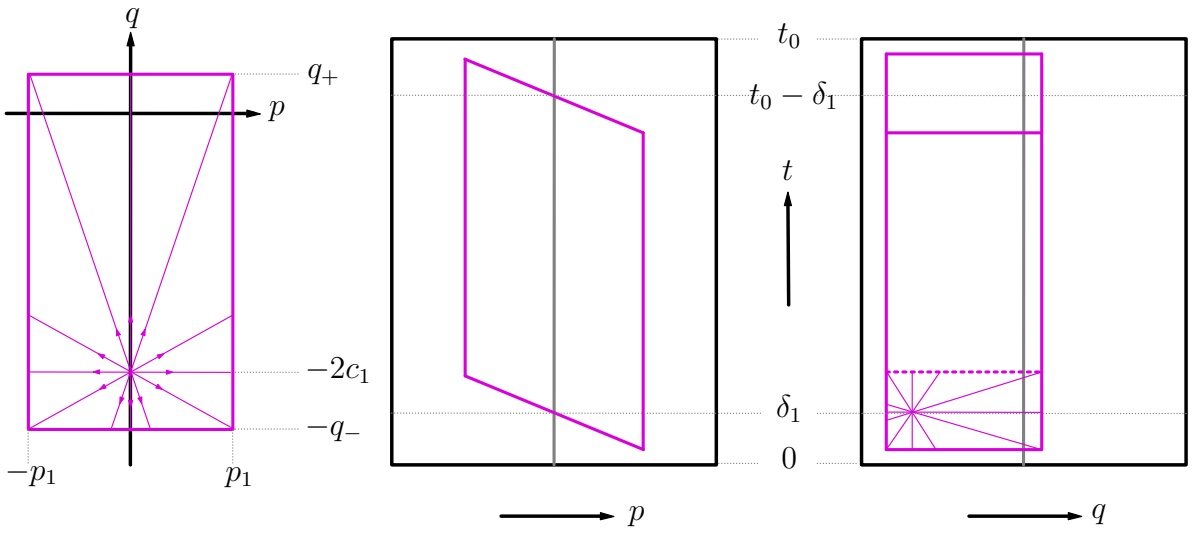

Figure 5.5: The contact handlebody H_1, visualized in various projections in $[0, t_0] \times r_0\mathbb{D}^2$. On the left is the Weinstein base W_1 with flowlines of the induced Liouville vector field X_1.

This determines the negative q boundary of W_1, and the inequality ensures that X_1 will be outward pointing to ∂W_1.

(4) Set $q_+ = 2c_1 \frac{1-e^{-\frac{s_1}{2}}}{1+e^{-\frac{s_1}{2}}}$.

This determines the positive q boundary of W_1, and ensures that the trapping region of the box fold is placed correctly, in a way which is compatible with the desired radial estimate in (i). In particular, if ψ^s denotes the time-s flow of $\left(\frac{1}{2}q + c_1\right)\partial_q$ on $\mathbb{R}$, this ensures that

$$\psi^{-s_1}(q_+) = -q_+.$$

Indeed, an elementary calculation shows that

$$\psi^{s_1}(-q_+) = e^{\frac{s_1}{2}}(-q_+ + 2c_1) - 2c_1.$$

Thus, $\psi^{s_1}(-q_+) = q_+$ is equivalent to

$$e^{\frac{s_1}{2}}(-q_+ + 2c_1) - 2c_1 = q_+$$

which simplifies to $q_+ = 2c_1 \frac{1-e^{-\frac{s_1}{2}}}{1+e^{-\frac{s_1}{2}}}$.

(5) Choose $r_0 > \sqrt{p_1^2 + q_-^2}$.

This is simply to ensure that $r_0\mathbb{D}^2$ is large enough to support a fold with the above parameters.

With these choices, let $W_1 := \{t = \delta_1 - c_1 p\} \cap \{-p_1 \leq p \leq p_1\} \cap \{-q_- \leq q \leq q_+\}$. We use (p, q) coordinates on W_1. The contact form $dt + \lambda_{\text{stab}}$ restricts to

$$\frac{1}{2} p\, dq - \left(\frac{1}{2} q + c_1\right) dp$$

on W_1, and hence W_1 is a Weinstein domain (up to corner rounding) with Liouville vector field X_1. Define a contact handlebody H_1 by flowing W_1 along the Reeb vector field ∂_t for time $t_0 - 2\delta_1$. Finally, let Π_1^{PL} be a piecewise-linear box fold installed over $[0, s_1] \times H_1$ with z-parameter $z_1 > e^{s_1} t_1$. Observe that the induced holonomy $\{s_0\} \to \{s_1\}$ is trivial.

First, we prove that any flowline entering a neighborhood of $[\delta, t_0 - \delta] \times \{(0, 0)\}$ in $\partial_+ R$ is trapped in backward time. Since $\delta_1 < \delta$, it follows that

$$[\delta, t_0 - \delta] \times \{(0, 0)\} \subset H_1.$$

Next, let $\psi_{X_1}^s$ denote the time-s flow of X_1. By Proposition 4.4, any flowline passing through a point $x \in \{s_1\} \times H_1$ with $(p(x), q(x)) \in N^{s_1}(\partial W_1)$ converges to a critical point in backward time in Π_1^{PL}. By choice (4),

$$\psi_{X_1}^{-s_1}(\{q = q_+\}) \subset \{q = -q_+\}.$$

In particular, $\{(0, 0)\} \in N^{s_1}(\partial W_1)$. Thus, any flowline passing through a point $x \in \{s_1\} \times [\delta_0, t_0 - \delta_0] \times \{(0, 0)\}$ converges to a critical point in R in backward time without passing through $\partial_- R$. This proves the first part of the proposition.

The claim in (ii) is immediate from the definition of Π_1^{PL}, as the holonomy for such points is trivial, if defined. Thus, it remains to prove (i). Note that if a flowline passes

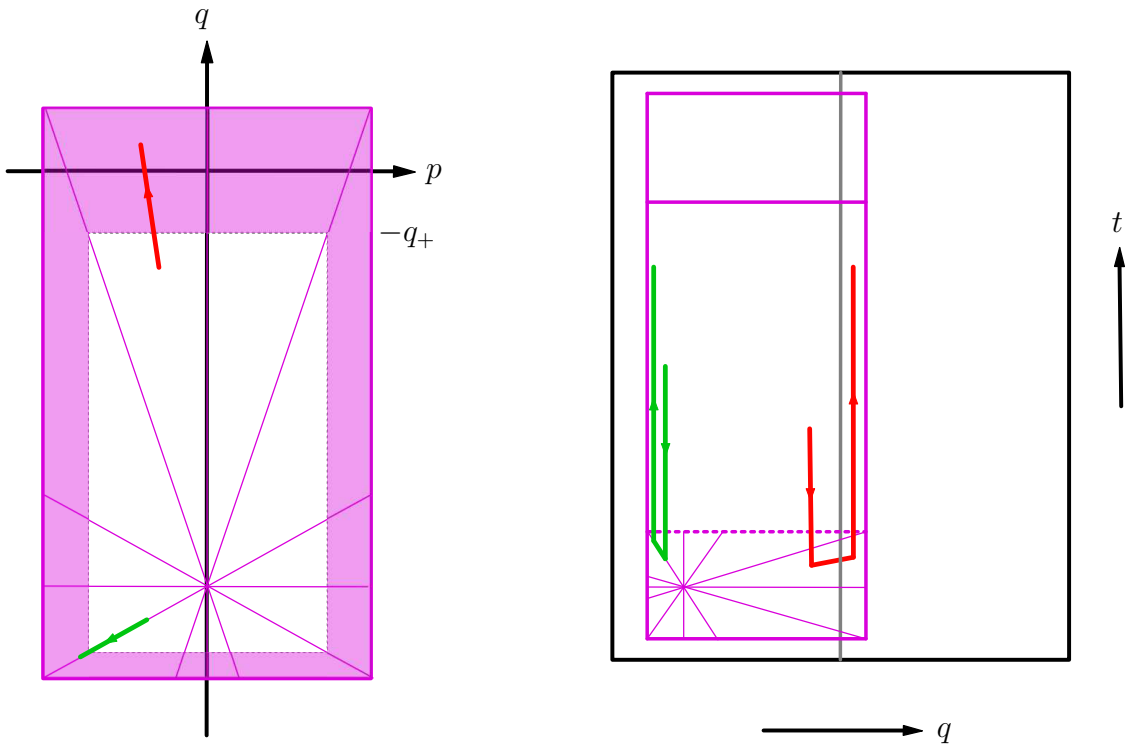

Figure 5.6: Visualizing the trapping region of Π_1^{PL}. On the left, the dashed gray line is the preimage of ∂W_1 under the time s_1 flow of X_1, and the shaded pink region is $N^{s_1}(\partial W_1)$. On both figures are sample points that enter the fold and pass through without being trapped. The green point corresponds to Case 1 and the red point corresponds to Case 2. In the statement of the proposition, (i) essentially says that the holonomy on the left figure induced by Π_1^{PL} is radially dominated by the time s_0 flow of $\frac{1}{2}p\,\partial_p + \frac{1}{2}q\,\partial_q$.

through $\{s_0\}$ away from H_1, the holonomy is trivial. That is, if

$$x \in \{s_0\} \times \left(\left([0,t_0] \times r_0\mathbb{D}^2\right) \setminus H_1\right)$$

then $\|h(x)\|_{\text{stab}} = \|x\|_{\text{stab}}$ and (i) holds trivially. Thus, it suffices to consider a point $x \in \{s_0\} \times H_1$. By the above remark, if $(p(x), q(x)) \in N^{s_1}(\partial W_1)$ then x is not in the domain of h, so it suffices to consider $x \in \{s_0\} \times H_1$ with $(p(x), q(x)) \in W_1 \setminus N^{s_1}(\partial W_1)$. In particular, it suffices to consider points with $q(x) < -q_+$. By Proposition 4.4 and the fact that the Reeb vector field is ∂_t,

$$\|h(x)\|_{\text{stab}} = \|\psi_{X_1}^{s_1}(x)\|_{\text{stab}}$$

where, on the right side of the equality, we are abusing notation and writing x in place of $(p(x), q(x))$. In words, this simply says that the change in stabilization coordinate of the flowline as it exits R is given by the time-s_1 flow of X_1. Note that

$$\psi_{X_1}^{s_1}(p,q) = \left(e^{\frac{s_1}{2}}p, e^{\frac{s_1}{2}}(q+2c_1) - 2c_1\right).$$

We claim that, on $[-p_1, p_1] \times [-q_-, q_+]$, we have $\|\psi_{X_1}^{s_1}(p,q)\|_{\text{stab}} < e^{\frac{s_1}{2}}\|(p,q)\|_{\text{stab}}$. We consider two cases.

Case 1: $e^{\frac{s_1}{2}}(q+2c_1) - 2c_1 \leq 0$.

Note the trivial inequality

$$e^{\frac{s_1}{2}}q < e^{\frac{s_1}{2}}(q+2c_1) - 2c_1 \leq 0.$$

This is immediate from the observation that $2c_1(e^{\frac{s_1}{2}} - 1) > 0$. Thus,

$$\begin{aligned}
\|\psi_{X_1}^{s_1}(p,q)\|_{\text{stab}} &= \left\|\left(e^{\frac{s_1}{2}}p, e^{\frac{s_1}{2}}(q+2c_1) - 2c_1\right)\right\|_{\text{stab}} \\
&< \left\|\left(e^{\frac{s_1}{2}}p, e^{\frac{s_1}{2}}q\right)\right\|_{\text{stab}} \\
&= e^{\frac{s_1}{2}}\left\|(p,q)\right\|_{\text{stab}}
\end{aligned}$$

as desired.

Case 2: $e^{\frac{s_1}{2}}(q+2c_1) - 2c_1 > 0$.

Recall that it suffices to assume $q(x) < -q_+$. Furthermore, by definition of H_1, we necessarily have

$$e^{\frac{s_1}{2}}(q+2c_1) - 2c_1 < q_+.$$

Thus,

$$0 < e^{\frac{s_1}{2}}(q+2c_1) - 2c_1 < q_+ < |q| < e^{\frac{s_1}{2}}|q|.$$

It again follows that

$$\begin{aligned}\left\|\psi_{X_1}^{s_1}(p,q)\right\|_{\text{stab}} &= \left\|\left(e^{\frac{s_1}{2}}p, e^{\frac{s_1}{2}}(q+2c_1)-2c_1\right)\right\|_{\text{stab}} \\ &< \left\|\left(e^{\frac{s_1}{2}}p, e^{\frac{s_1}{2}}|q|\right)\right\|_{\text{stab}} \\ &= e^{\frac{s_1}{2}}\left\|(p,q)\right\|_{\text{stab}}.\end{aligned}$$

With this claim, we then have

$$\left\|h(x)\right\|_{\text{stab}} = \left\|\psi_{X_1}^{s_1}(x)\right\|_{\text{stab}} < e^{\frac{s_1}{2}}\left\|x\right\|_{\text{stab}} < e^{\frac{s_0}{2}}\left\|x\right\|_{\text{stab}}$$

and (i) is proven.

□

Now we describe why the above proof fails in the smooth setting, if implemented as described. As we discussed in 4.2.4, in the smooth setting there will be a membrane of points between H^{τ}_{trap} and H^{τ}_{pass} that may experience holonomy with significant influence from the characteristic foliation of ∂H_1. In particular, points near $\psi_{X_1}^{-s_1}(\partial W_1)$ may exit the fold near ∂H_1 after travelling along the characteristic foliation to some degree. This is a concern in proving (i) of Proposition 5.8, because a flowline could enter the fold near $\{q=-q_+\}$ and exit as far away as $\{q=-q_-\}$. In fact, this will almost certainly happen: since $\delta > 0$ is small, this generally forces the characteristic foliation of ∂H_1 to intensely spiral around $\underline{\partial W_1}$, almost certainly lending to erratic behavior of the flowlines entering near $\psi_{X_1}^{-s_1}(\partial W_1)$. One might hope to deal with this by balancing the parameters of the fold differently, but this phenomenon persists under such perturbations. The point of a chimney fold is to drastically redirect this traffic along the long and thin base $[0,t_-]\times W_0$. Even more uncontrollable is the smooth holonomy of flowlines entering the fold along the t-axis near $t=\delta_1$ and $t=t_0-\delta_1$. Again, there will be such flowlines that are heavily influenced by the characteristic foliation of ∂H_1, exiting the fold far away from the t-axis. This violates both (i) and (ii) of Proposition 5.8, and no amount of parameter tweaking can fix this.

There is another subtle but fundamental reason why this strategy is ultimately futile in the smooth setting, and it has to do with the index of introduced critical points. In many of our applications, we ultimately need to introduce critical points of index n, where the dimension of the stabilized domain is $2n$. For example, when we apply Proposition 1.7 to Mitsumatsue's examples, the low-dimensional blocking apparatus of Proposition 5.8 needs to introduce a critical point of index 2. The positive region of ∂H_1 in the above piecewise-linear strategy only has a critical point of index 0, and so the resulting critical points of the Liouville vector field are of index 0 and index 1. In contrast, a blocking apparatus as defined in the next subsection does introduce a critical point of index 2. Indeed, one of the components of a blocking apparatus is a chimney fold, and the positive region of the boundary of the supporting contact region in a chimney fold necessarily has a critical point of index 1, leading to an overall critical point of index 2.

5.2.3 The low-dimensional blocking apparatus

In this subsection we define a *blocking apparatus* in 4 dimensions, which is is a two-fold apparatus installed in a model Weinstein cobordism. The design is such that it leads to a smooth proof of Proposition 5.8. Briefly, a blocking apparatus will consist of a chimney fold $C\Pi_1$ and an ordinary box hole II_2. The chimney fold will be installed so that the chimney portion traps the t-axis in $[0, t_0] \times r_0\mathbb{D}^2$, and the trapping region of the box hole is lined up to engulf the stove of the chimney fold. The construction of the chimney fold is similar to the piecewise-linear box fold defined in 5.2.2. The details of this construction are explained in this subsection, and the proof of its effectiveness towards Proposition 5.8 is given in the next subsection.

As before, we consider the cobordism

$$\left([0, s_0] \times [0, t_0] \times \mathbb{R}^2,\, e^s \left(dt + \lambda_{\mathrm{stab}}\right)\right).$$

For now we use an infinite stabilization direction. We are also given $0 < \delta \ll t_0$ as in the statement of Proposition 5.8. First, we choose the parameters necessary to define

the chimney fold $C\Pi_1$ and provide some informal explanation for each. Note that our convention in this section is as follows, in contrast to the chimney fold model: parameters with a 0 subscript (like s_0, t_0) correspond to the given model cobordism, parameters with a 1 subscript correspond to the chimney fold $C\Pi_1$, and parameters with a 2 subscript correspond to the box hole Π_2. Furthermore, we will often use the radial coordinate $r = \sqrt{o^2 + q^2}$.

(1) Fix $s_1 < s_0$ and $0 < \delta_1 < \delta$.

The parameter s_1 will be the symplectization length of the chimney fold, and δ_1 is simply a smaller δ-like parameter meant to introduce some wiggle room to account for smoothing.

(2) Fix $c_1 > 0$.

This will be the (negative) p-slope of the Weinstein base $W_1 \subset [0, t_0] \times \mathbb{R}^2_{p,q}$ that will define the chimney fold.

(3) Choose $p_1 > 0$ such that $c_1 p_1 < \delta$.

This will determine the p-thickness of the Weinstein base W_1, ensuring that the support of the chimney fold is a subet of $[0, t_0] \times r_0\mathbb{D}^2$.

(4) Set $t_1 = t_0 - 2\delta$ and $t_{1,-} = \delta$.

These parameters are the lengths of the Reeb chords of the chimney and stove of $C\Pi_1$, respectively.

(5) Choose $0 < \rho_1 < p_1$ sufficiently small to satisfy the requirements described below.

This will be the radius of the chimney. Ultimately, W_1 will be of the form

$$W_1 = \{t = -c_1 p\} \subset [0, t_0] \times \mathbb{R}^2_{p,q} \quad \text{for} \quad (p, q) \in ([-p_1, p_1] \times [-q_1, 0]) \cup (\{r \leq \rho_1\})$$

for some $q_1 > 0$ to be chosen later; see Figure 5.7. We require ρ_1 to be small enough so that:

(5a) $\{r \leq \rho_1\} \subset N^{s_1}(\partial W_1)$.

This ensures that $C_1 := \{r \leq \rho_1\}$ is a viable chimney region.

(5b) $p\left(h_{\partial W_1}(p = -\rho_1, q = 0)\right) > \rho_1$.

Here $h_{\partial W_1}$ is the boundary holonomy map of the stove as in Section 5.1. This ensures that $\gamma_{C_1} \cap h_{\partial W_1}(\gamma_{C_1}) = \emptyset$, part of the main assumption needed to define $C\Pi_1$.

Both (5a) and (5b) are trivially true as $\rho_1 \to 0$.

(6) Define γ_{C_1} as described below.

Let $\gamma_{C_1} \subset \partial W_1$ be an arc containing $\{r = \rho_1\} \cap \{q \geq 0\} \cap \partial W_1$ such that $\gamma_{C_1} \cap h_{\partial W_1}(\gamma_{C_1}) = \emptyset$ and $\{r \leq \rho_1\} \subset N^{s_1}(\gamma_{C_1})$. Again, refer to Figure 5.7.

(7) Choose $q_1 > 2c_1 > 0$ large enough so that the main chimney fold assumption holds.

In other words, we choose the q-length of W_1 large enough to ensure that $\gamma_{C_1} \cap h^j_{\partial W_1}(\gamma_{C_1}) = \emptyset$ for all $1 \leq j \leq n$, where n satisfies $nt_{1,-} > t_1$.

It is possible to give a precise quantitative estimate on q_1, but it isn't necessary. We need $q > 2c_1$ to ensure that W_1 is a domain (the critical point of the Liouville vector field of W_1 will be at $(p = 0, q = -2c_1)$), and we simply need q_1 to be large enough so that $h^n_{\partial W_1}(\gamma_{C_1})$ does not circle all the way around ∂W_1 back to γ_{C_1}. It is clear that such a q_1 exists, provided we have an arbitrarily large stabilization direction.

With these choices, we can formally define the Weinstein base

$$W_1 := \{t = \delta_1 - c_1 p\} \subset [0, t_0] \times \mathbb{R}^2_{p,q} \quad \text{for} \quad (p, q) \in ([-p_1, p_1] \times [-q_1, 0]) \cup \{r \leq \rho_1\}$$

and the set $C_1 := W_1 \cap \{r \leq \rho_1\}$. We then define $\tilde{H}_1^{C_1} \subset [0, t_0] \times \mathbb{R}^2$ by flowing W_1 along ∂_t for time $t_{1,-}$ and C_1 for time t_1 to generate the stove and chimney, respectively. We then define a region $H_1^{C_1}$ as a slight modification of $\tilde{H}_1^{C_1}$, mostly for convenience. In particular, we may assume that the chimney region extends up to $t = t_0 - \delta_1$ and that $H_1^{C_1} \subset \{t \leq t_0 - \delta\}$; see Figure 5.7. Strictly speaking, this contact region $H_1^{C_1}$ is more complicated than the model region that supports a chimney fold as defined in Section 5.1, because the Reeb chords have variable length over C_1. It should be clear from the analysis of Section 5.1 that this does not result in any significant change to the dynamics of the resulting chimney fold. It is also possible to instead use $\tilde{H}_1^{C_1}$ in accordance with the strict model of Section 5.1. The blocking apparatus would require an extra ordinary box fold to account for this. We will not describe

the details here, and we choose to instead use $H_1^{C_1}$ for convenience. The intention of this choice is to ensure that the index 2 critical point of the characteristic foliation of $\partial H_1^{C_1}$ at the top of the chimney coincides with the t-axis.

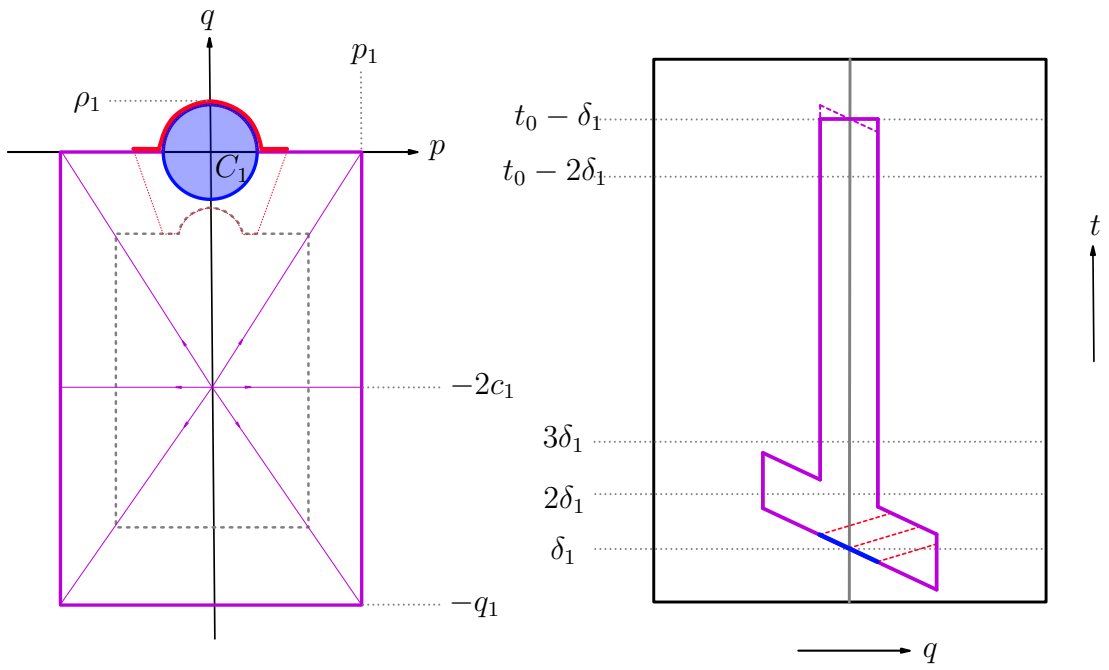

Figure 5.7: Two projections of $H_1^{C_1}$. On the left, γ_{C_1} is the thick red curve, and the region $N^{s_1}(\gamma_{C_1})$ is given by the dashed red region. On the right, the outline of $\tilde{H}_1^{C_1}$ near $t = t_0 - \delta_1$ is given by the dashed purple line to contrast with the outline of $H_1^{C_1}$. The dashed red lines indicate the characteristic foliation of ∂W_1.

Let $C\Pi_1$ be a chimney fold installed over $H_1^{C_1}$ with symplectization length s_1. This fold is the main component of a blocking apparatus. The point is that the chimney region of $H_1^{C_1}$ is lined up to trap a large portion of the t-axis in $[0, t_0] \times r_0\mathbb{D}^2$.

Next, we define the second component of a blocking apparatus: a box hole Π_2 placed behind $C\Pi_1$ (in the s-sense) to trap points exiting $C\Pi_1$ along the stove.

(1) Pick $s_2 > 0$ such that $s_1 + s_2 < s_0$.

This will be the symplectization length of Π_2.

(2) Pick $r_2 > 0$ such that $\sqrt{p_1^2 + q_1^2} < r_2 < r_0$.

This will be the radius of the stabilization support of Π_2, which needs to be large

enough to engulf the stove of $H_1^{C_1}$.

(3) Set $t_2 = \frac{t_0}{2}$ and pick $z_2 < \frac{t_2}{2}$. Assume that $(1 - e^{-s_2})z_2 > 3\delta_1$.

These will be the Reeb length and z-parameter of $\amalg_2$. We choose z_2 to be *smaller* than $\frac{t_2}{2}$ to ensure that there is no interaction between the two components of the trapping region of $\amalg_2$. The assumption is to ensure that the Reeb-thickness of the trapping region of $\amalg_2$ is large enough to engulf the stove of $H_1^{C_1}$. We are free to make δ_1 smaller in our earlier choice, so this is certainly possible to achieve. The cost of decreasing δ_1 is an increase in the stabilization footprint of the stove. In particular, there is an increase in n in the main assumption needed to define $C\Pi_1$, and thus an increase in q_1 and r_0.

With these choices, define $W_2 := \{t = 0\} \cap \{r \leq r_2\} \subset [0, t_0] \times r_0\mathbb{D}^2$ and let $\amalg_2$ be an ordinary box hole installed over $H_2 := [0, t_2] \times W_1$ with z-parameter z_2 and symplectization length s_2.

Definition. Let $\sigma_1, \sigma_2 \subset [0, s_0]$ be intervals such that $|\sigma_j| = s_j$ and $\sup \sigma_2 < \inf \sigma_1$. A **blocking apparatus** consists of the fold $C\Pi_1$ installed over $\sigma_1 \times H_1^{C_1}$ and the fold $\amalg_2$ installed over $\sigma_2 \times H_2$.

Before formally proving Proposition 5.8 in the next subsection, we emphasize the basic idea of the blocking apparatus. The first step is $C\Pi_1$, in the sense that $C\Pi_1$ is installed closest to $\partial_+ U = \{s = s_0\}$. By construction the chimney portion of $C\Pi_1$ traps a neighborhood of a large part of the t-axis, at the cost of introducing a great deal of complicated holonomy, most of which is funneled along the stove of $H_1^{C_1}$. With just $C\Pi_1$, the norm estimate (i) in Proposition 5.8 is aggressively violated. However, the ordinary box hole $\amalg_2$ is conveniently placed behind $C\Pi_1$ to trap any flowlines exiting along the stove. Furthermore, the design of $C\Pi_1$ and $\amalg_2$ will be such that their interaction is compatible with the desired norm estimate of Proposition 5.8. See Figure 5.8.

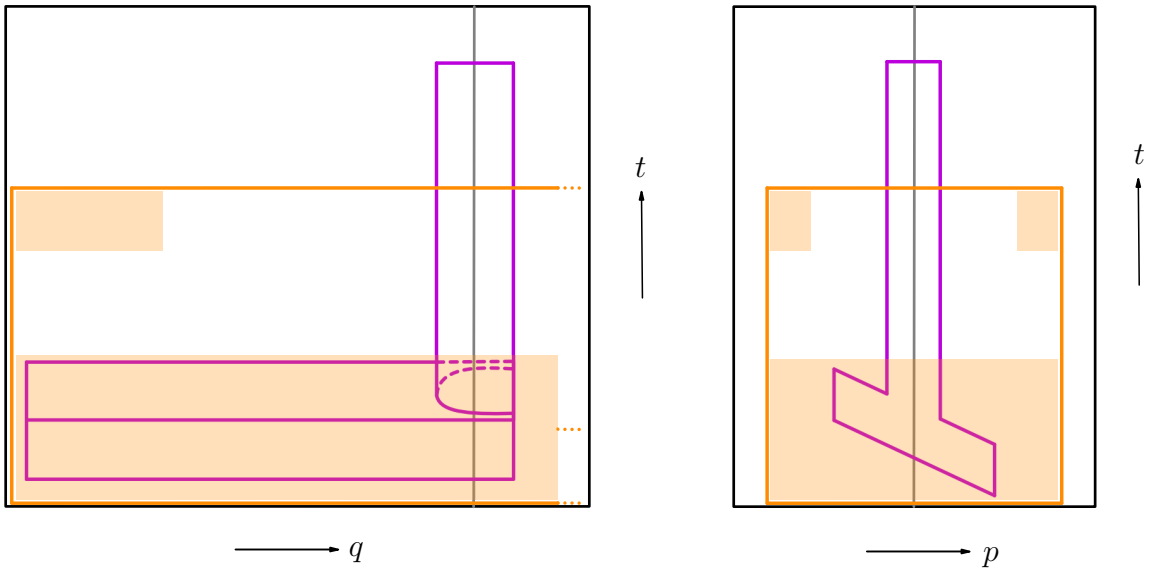

Figure 5.8: A (not to scale) depiction of the supporting contact regions of a blocking apparatus. The region $H_1^{C_1}$ is in purple, and the handlebody H_2 is in orange. The various trapping regions of Π_2 are shaded in light orange. In particular, the stove of $H_1^{C_1}$ is entirely contained in the lower trapping region of Π_2.

5.2.4 The low-dimensional smooth case

In this subsection we prove Proposition 5.8, the low dimensional version of Proposition 1.7. We begin with a lemma which is an immediate corollary of Lemma 4.11, which gives an estimate on the induced movement in the Weinstein direction of an ordinary box fold. The following lemma gives an explicit interpretation of this for an ordinary box fold in the stabilization direction.

Lemma 5.9. *Let Π_0 be a smooth box fold installed over the contact handlebody $(H_0 = [0, t_0] \times r_0\mathbb{D}^2,\ dt + \frac{1}{2}r^2\, d\theta)$ with symplectization length s_0. Let $h : \{s_0\} \times H_0 \dashrightarrow \{0\} \times H_0$ be the partially-defined holonomy map given by backward passage through Π_0. Then*

$$\|h(x)\|_{\text{stab}} \leq e^{\frac{s_0}{2}} \|x\|_{\text{stab}}.$$

Remark. The slogan of this lemma is that an ordinary box fold with flat base can be installed "for free" with respect to the radial holonomy. That is, in the quest to prove an estimate of

the form $\|h(x)\|_{\text{stab}} \leq K\, e^{\frac{s_0}{2}} \|x\|_{\text{stab}}$ as in (i) of Proposition 5.8, one can install such a fold and remain compatible with the radial estimate. In contrast, the installation of the chimney fold $C\Pi_1$ by itself does not come for free, because the holonomy through $C\Pi_1$ aggressively violates any estimate of the form $\|h(x)\|_{\text{stab}} \leq K\, e^{\frac{s_0}{2}} \|x\|_{\text{stab}}$. Also observe that the lemma applies to an ordinary box hole with flat base as well, so that the second fold Π_2 of the blocking apparatus can be installed for free.

Proof. Observe that the Liouville vector field of the base $(r_0\mathbb{D}^2,\ \frac{1}{2}r^2\, d\theta)$ is $X_{\lambda_0} = \frac{1}{2}r\, \partial_r$. An elementary calculation shows that the time-s_0 flow of $\frac{1}{2}\, \partial_r$ induces an expansion by a factor of $e^{\frac{s_0}{2}}$. Thus, by Lemma 4.11,

$$\|h(x)\|_{\text{stab}} \leq e^{\frac{s_0}{2}} \|x\|_{\text{stab}}.$$

□

Proof of Proposition 5.8. Install a blocking apparatus as defined in 5.2.3. To prove the proposition we need to verify three things. First, that there is a neighborhood U_{trap} of $[\delta, t_0 - \delta] \times \{(0,0)\}$ with any flowline passing through $\{s = s_0\} \times U_{\text{trap}} \subseteq \partial_+ U$ converging to a critical point in backward time. This is immediate from the definition of $C\Pi_1$ and Proposition 5.2: by construction, the chimney fold in a blocking apparatus traps a neighborhood of $[\delta, t_0 - \delta] \times \{(0,0)\}$.

Secondly and thirdly, we need to prove that the partially-defined holonomy map $h : \partial_+ U \dashrightarrow \partial_- U$ given by backward passage through the blocking apparatus satisfies the following two properties:

(i) $\|h(x)\|_{\text{stab}} \leq K e^{\frac{s_0}{2}} \|x\|_{\text{stab}}$ for some constant $0 < K < 1$, and

(ii) $h(\{[0,\delta) \cup (t_0 - \delta, t_0]\} \times \{(0,0)\}) \subset \{0\} \times \{[0,\delta) \cup (t_0 - \delta, t_0]\} \times \{(0,0)\}$.

We will prove (i) first. Fix $s_{\text{mid}} \in (\sup \sigma_2, \inf \sigma_1)$. Let $h_1 : \{s = s_0\} \dashrightarrow \{s = s_{\text{mid}}\}$ and $h_2 : \{s = s_{\text{mid}}\} \dashrightarrow \{s = 0\}$ be the individual holonomy maps through the regions of U containing $C\Pi_1$ and Π_2, respectively, so that $h : \partial_+ U \dashrightarrow \partial_- U$ is given by $h = h_2 \circ h_1$. By Lemma 5.9, $\|h_2(x)\|_{\text{stab}} \leq e^{\frac{s_2}{2}} \|x\|_{\text{stab}}$, and so $\|h(x)\|_{\text{stab}} \leq e^{\frac{s_2}{2}} \|h_1(x)\|_{\text{stab}}$ whenever $h_1(x)$ is

in the domain of h_2. Thus it suffices to prove that if $h_1(x)$ is in the domain of h_2, then $\|h_1(x)\|_{\text{stab}} \leq e^{\frac{s_1}{2}}\|x\|_{\text{stab}}$. This is trivial for points that are not influenced by $C\Pi_1$, so it remains to consider such points that are influenced by $C\Pi_1$.

By design of the blocking apparatus, points that are influenced by $C\Pi_1$ and not trapped by II_2 satisfy $t(h_1(x)) > (1 - e^{-s_2})z_2$ (up to an arbitrarily small perturbation, due to smoothing) because the lower trapping region of the ordinary box hole II_2 has t-thickness $(1 - e^{-s_2})z_2$. In particular, any flowline exiting $C\Pi_1$ along the stove of $H_1^{C_1}$ is trapped by II_2, so we only need to consider points that pass through $C\Pi_1$ and exit above the stove. Such points necessarily exit $C\Pi_1$ in the chimney portion of $H_1^{C_1}$.

Recall that $H_1^{C_1}$ was defined in a slightly modified way from that of Section 5.1, so that the top of $H_1^{C_1}$ is parallel to $\{t = t_0\}$. Locally, the holonomy through $C\Pi_1$ for points beginning and exiting near this region comes for free — that is, it satisfies $\|h_1(x)\|_{\text{stab}} \leq e^{\frac{s_1}{2}}\|x\|_{\text{stab}}$ — by Lemma 5.9. Therefore, it suffices to consider points that pass through $C\Pi_1$ and exit in the central portion of the chimney, say, those satisfying

$$t(h_1(x)) \in [3\delta_1, t_0 - 3\delta_1].$$

This is where Lemma 5.5 enters the play. According to that lemma, if $t(h_1(x)) \in [3\delta_1, t_0 - 3\delta_1]$ and $W_1(h_1(x)) \in \text{int}^\tau(C_1)$, then $W_1(x) \in W_1 \setminus \text{int}^\tau(C_1)$. In words, if a flowline exits $C\Pi_1$ in the central portion of the chimney in $\text{int}^\tau(C_1)$, then it necessarily began its journey from *outside* $\text{int}^\tau(C_1)$. Since $\text{int}^\tau(C_1)$ is an arbitrarily close approximation of the disc C_1 centered at the stabilization origin, it follows that the estimate $\|h_1(x)\|_{\text{stab}} \leq e^{\frac{s_1}{2}}\|x\|_{\text{stab}}$ holds trivially for these points.

The remaining points to consider fall into the following worst-case scenario: those that enter $C\Pi_1$ near $\partial\text{int}^\tau(C_1)$ and exit with $t(h_1(x)) \in [3\delta_1, t_0 - 3\delta_1]$ as far away as possible in the stabilization direction, necessarily near ∂C_1. Because $\text{int}^\tau(C_1) \to \text{int}(C_1)$ as $\tau \to 0$, by choosing a sufficiently small smoothing parameter τ for $C\Pi_1$ we can ensure the estimate $\|h_1(x)\|_{\text{stab}} \leq e^{\frac{s_1}{2}}\|x\|_{\text{stab}}$ holds for these points. This proves that if $h_1(x)$ is in the domain of

h_2, then $\|h_1(x)\|_{\text{stab}} \leq e^{\frac{s_1}{2}}\|x\|_{\text{stab}}$. Thus,

$$\|h(x)\|_{\text{stab}} \leq e^{\frac{s_2}{2}}\|h_1(x)\|_{\text{stab}} \leq e^{\frac{s_1+s_2}{2}}\|x\|_{\text{stab}}.$$

Since $s_1 + s_2 < s_0$, $e^{\frac{s_1+s_2}{2}} < e^{\frac{s_0}{2}}$ and so (i) is proven.

Finally, we prove (ii). Note that, abusing notation slightly, $h((t_0-\delta, t_0]) = h_1((t_0-\delta, t_0])$. This is because the supporting handlebody of II_2 is contained below $t = \frac{t_0}{2}$. By Lemma 5.9 and Proposition 4.9, essentially nothing interesting happens near t_0 and in particular $h_1((t_0-\delta, t_0]) \subset (t_0-\delta, t_0]$. The matter is slightly more complicated near $[0, \delta)$ because the holonomy induced by $C\Pi_1$ is nontrivial along the t-axis near $t = \delta$. However, by Lemma 5.5, any nontrivial $C\Pi_1$-holonomy beginning near $t = \delta$ is funneled along the stove of $H_1^{C_1}$, where it is ultimately trapped by II_2. The holonomy near $t = 0$ along the t-axis induced by II_2 is trivial, and so $h([0, \delta)) \subset [0, \delta)$. This proves (ii).

□

We again emphasize the idea of the proof, which can get lost in the details. The chimney fold $C\Pi_1$ traps a neighborhood of the t-axis, at the same time introducing complicated holonomy along the stove of $H_1^{C_1}$. The ordinary box hole II_2 is placed behind $C\Pi_1$ to trap all of this complicated holonomy. Consequently, the only possible way to violate the main radial estimate in Proposition 5.8 is for a flowline to enter $C\Pi_1$ sufficiently close to the t-axis near the bottom of $H_1^{C_1}$ and exit $C\Pi_1$ above the trapping region of II_2, necessarily in the chimney. But the main assumption of a chimney fold — in particular, Lemma 5.5 — rules out this possibility.

5.2.5 The high-dimensional smooth case

In this subsection we extend the definition of a blocking apparatus to arbitrary dimensions and prove that Proposition 5.8 implies Proposition 1.7. Both of these tasks are straightforward.

In general, wish to install a blocking apparatus in a cobordism of the form

$$\left(U = [0, s_0] \times [0, t_0] \times W_0 \times r_0\mathbb{D}^2,\, e^s\left(dt + \lambda_0 + \lambda_{\text{stab}}\right)\right)$$

where (W_0, λ_0) is a Weinstein domain of arbitrary dimension. Let $H_1^{C_1}, H_2 \subset [0, t_0] \times r_0\mathbb{D}^2$ be constructed exactly as in 5.2.3. Let $C\Pi_1$ be a high-dimensional chimney fold as defined in 5.1.3 over $H_1^{C_1} \times W_0$ with symplectization length s_1, and let II_2 be a box hole installed over $H_2 \times W_0$ with symplectization length s_2. The definition of a blocking apparatus is the same as before.

Definition. Let $\sigma_1, \sigma_2 \subset [0, s_0]$ be intervals such that $|\sigma_j| = s_j$ and $\sup \sigma_2 < \inf \sigma_1$. A **blocking apparatus** consists of the fold $C\Pi_1$ installed over $\sigma_1 \times H_1^{C_1}$ and the fold II_2 installed over $\sigma_2 \times H_2$.

In words, we have extended the two folds comprising a low-dimensional blocking apparatus to the additional W_0 direction as simply as possible, using all of W_0 to support each fold.

Proof of Proposition 1.7. First, observe that Proposition 5.7 implies that a the smooth chimney fold $C\Pi_1$ traps a neighborhood of $[\delta, t_0 - \delta] \times I_\epsilon(W_0, \lambda_0) \times \{(0, 0)\}$; this gives the trapping statement of Proposition 1.7.

Next, we prove (iii) of Proposition 1.7. This follows immediately from (ii) of Proposition 5.8 and the discussion at the end of 5.1.3; namely, if the W_0-coordinate of the entry point of the flowline avoids $N^{s_0}(\partial W_0)$ — that is, if $W_0(x) \in I_{1-e^{-s_0}}(W_0, \lambda_0)$ — then there is no unexpected dynamical behavior arising due to the extra W_0 direction, as the flowline stays far enough away from ∂W_0.

It remains to prove the norm estimates in (i) and (ii) of Proposition 1.7.

We begin by proving (ii), the stabilization estimate $\|h(x)\|_{\text{stab}} \leq Ke^{\frac{s_0}{2}} \|x\|_{\text{stab}}$ provided $\|x\|_{W_0} < e^{-s_0}$. The assumption $\|x\|_{W_0} < e^{-s_0}$ is equivalent to $W_0(x) \notin N^{s_0}(\partial W_0)$. By Lemma 4.11, this ensures that, as the flowline through x enters the chimney fold, there is

no interaction with $\underline{\partial W_0}$. In particular, the t-holonomy of any flowline that passes through the chimney fold is entirely dictated by the low-dimensional chimney fold behavior in $H_1^{C_1} \subset [0, t_0] \times r_0 \, \mathbb{D}^2$. We may then apply Proposition 5.8 to conclude that $\|h(x)\|_{\text{stab}} \leq Ke^{\frac{s_0}{2}} \|x\|_{\text{stab}}$. To rephrase this part of the argument, the only way that the stabilization estimate of Proposition 5.8 could *fail* when extended to higher dimensions is if the flowline's trajectory is significantly perturbed in the t-direction by smoothing near $\underline{\partial W_0}$, which does not exist in a low-dimensional blocking apparatus. A flowline entering the chimney fold near the bottom of the chimney, but very close to $\underline{\partial W_0}$, could experience significant t-holonomy after being influenced by the characteristic foliation of $\underline{\partial W_0}$, potentially avoiding the trapping the box hole behind the chimney. The almost-negligible movement away from the stabilization origin followed by avoidance of the trapping region of the box hole results in a flowline that does not technically satisfy the $\|h(x)\|_{\text{stab}} < e^{\frac{s_0}{2}} \|x\|_{\text{stab}}$ estimate. However, for a flowline sufficiently far from $\underline{\partial W_0}$, this does not occur. See also the discussion in 5.1.3.

The argument to show that the W_0 estimate holds in Proposition 1.7 also is immediate from Lemma 4.11. In particular, after installation of a high-dimensional blocking apparatus, points with holonomy satisfy

$$\|h(x)\|_{W_0} \leq e^{s_1+s_2} \|x\|_{W_0}$$

because the total symplectization length of $C\Pi_1$ and Π_2 is $s_1 + s_2$.

This completes the proof of Proposition 1.7.

□

5.3 Some technical properties of the blocking apparatus

In this section, we state a few more technical properties of the blocking apparatus. Their utility will become clear in Section 6, in particular for the purpose of ruling out the existence of broken loops. First, we introduce some terminology to identify certain critical points in a blocking apparatus.

Definition. Let $C\Pi_1$ be the chimney fold of a blocking apparatus. A **stove critical point** of $C\Pi_1$ is a critical point with a t-coordinate satisfying $t^* < 3\delta_1$.

Informally, a stove critical point is — unsurprisingly — a critical point of a chimney fold located sufficiently close to the stove region of the fold. We simply want to consider critical points other than the ones occurring at the very top of the chimney.

Proposition 5.10. *A stove critical point in a blocking apparatus cannot be included in a broken loop.*

Proof. We make the trivial observation that any critical point of index 0 cannot be included in a broken loop. Thus, it suffices to prove the following. If γ is a broken flowline involving a stove critical point, then every broken flowline containing γ is further contained in a broken flowline that involves a critical point of index 0. Indeed, if this is the case, then there are no broken loops containing stove critical points.

First, note that the dynamics of a chimney fold are Morse-Smale, and thus there are no broken loops contained entirely inside $C\Pi_1$. It therefore suffices to consider a broken flowline that contains a stove critical point and exits the stove region in backward time.

In this case, consider a low-dimensional blocking apparatus installed over $[0, s_0] \times [0, t_0] \times r_0\mathbb{D}^2$, with no W_0-component. In this setting, the main trapping region of the box hole $\amalg_2$ is an $\{s = \frac{s_0}{2}\}$ cross section of the unstable manifold of a critical point of index 0. By design of a blocking apparatus, the entire stove region of the chimney fold $C\Pi_1$ is a subset of this $\amalg_2$ trapping region. In particular, any broken flowline emanating from a stove critical point in backward time and exiting the stove, if extended sufficiently far, will intersect this trapping region and ultimately converge to a critical point of index 0.

In the high-dimensional setting — when the blocking apparatus is installed with a W_0 component — the proposition follows almost immediately from the low-dimensional case, because critical points of the blocking apparatus project to critical points of X_{λ_0} in W_0. In particular, any sufficiently extended broken flowline emanating from the stove region via a stove critical point in backward time is ultimately engulfed by the main trapping

region of $\amalg_2$, hence by a critical point with 0 index in the $[0, t_0] \times r_0\mathbb{D}^2$ projection. In the W_0 projection, because W_0 is a Weinstein domain, X_{λ_0} has Morse dynamics, and every broken flowline descends to a critical point with 0 index in W_0. As such, every broken flowline then eventually reaches a critical point of total index 0, as desired. □

Corollary 5.11. *After applying Proposition 1.7 to a Weinstein cobordism*

$$(U = [0, s_0] \times [0, t_0] \times W_0 \times r_0\,\mathbb{D}^2, e^s\,(dt + \lambda_0 + \lambda_{\text{stab}}))$$

there are no broken loops contained in U.

Proof. By the previous proposition, no stove critical point can be involved in any broken loop, let alone one contained in U. Thus, a broken loop contained in U must be contained either entirely in $\amalg_2$, or must involve one of the critical points corresponding to the top of the chimney. By definition of a box fold — which requires Morse-Smale dynamics — there are no broken loops entirely contained in $\amalg_2$. Finally, none of the critical points near the top of the chimney interact with any critical point in $\amalg_2$, so these critical points can not be involved in a broken loop contained in U. Thus, there are no broken loops contained in U. □

The ultimate efficacy of Proposition 5.10 is due to the following observation about the main trapping mechanism of a blocking apparatus.

Proposition 5.12. *After applying Proposition 1.7, any flowline which passes through $\{s = s_0\} \times U_{\text{trap}} \subseteq \partial_+ U$ converges in backward time to a stove critical point.*

Proof. This is immediate from the design and definition of a chimney fold in Section 5.1. In particular, in a low-dimensional piecewise-linear chimney fold, any flowline entering the chimney region is trapped in the stove region. The extension to higher dimensions does not impact this behavior, and U_{trap}, by definition, is a set approximating the interior of the chimney region. □

Remark. We remind the reader that the trapping neighborhood $\{s = s_0\} \times U_{\text{trap}} \subseteq \partial_+ U$ in the statements of Proposition 1.7 and Proposition 5.12 is not the *entire* trapping region of the blockng apparatus. There are a number of other codimension 0 regions that are trapped by other critical points of the apparatus. We are simply identifying one such region — a region approximating the chimney region of $C\Pi_1$ — which is ultimately trapped in the stove.

Finally, we have the following proposition which concerns the behavior of flowlines entering a blocking apparatus in *forward* time. Note that the perspective of this proposition is drastically different than the backward time analysis that permeates the majority of the previous sections.

Proposition 5.13. *After applying Proposition 1.7 to a Weinstein cobordism* $(U = [0, s_0] \times [0, t_0] \times W_0 \times r_0 \, \mathbb{D}^2, e^s \, (dt + \lambda_0 + \lambda_{\text{stab}}))$ *with parameters* δ *and* ϵ*, consider a point* $(0, t^*, x, p, q) \in \partial_- U$*. If the flowline through this point converges to a critical point of the blocking apparatus in forward time, then* $x \in \text{Skel}(W_0)$*,* $(p, q) = (0, 0)$*, and* $t^* \in [0, 2\delta) \cup (t_0 - 2\delta, t_0]$*.*

We begin with a lemma that concerns the forward time trapping behavior of a normal box fold.

Lemma 5.14. *Let* Π^τ *be a smooth box fold installed over* $([0, s_0] \times [0, t_0] \times W_0, \, e^s \, (dt + \lambda_0))$*. Let* X *denote the perturbed Liouville vector field, and suppose that* $(0, t^*, x) \in \{s = 0\} \times [0, t_0] \times W_0$ *is a point such that the flowline of* X *through* $(0, t^*, x)$ *converges to a critical point in forward time. Then* $x \in \text{Skel}(W_0, \lambda_0)$ *and* $t^* > t_0 - \varepsilon(\tau)$*, where* $\varepsilon(\tau)$ *is an arbitrarily small parameter dependent only on the smoothing parameter* τ*.*

Proof. Recall that the Liouville vector field after installing a box fold is, away from ∂W_0,

$$X = \partial_s + e^{-s} \, X_F^{ds \, dt} - e^{-s} \frac{\partial F}{\partial t} \, X_{\lambda_0}.$$

Rewriting this gives

$$X = \left(1 + e^{-s} \frac{\partial F}{\partial t}\right) \partial_s - e^{-s} \frac{\partial F}{\partial s} \, \partial_t - e^{-s} \frac{\partial F}{\partial t} \, X_{\lambda_0}.$$

Similarly, identify the collar neighborhood of ∂W_0 as $([-\varepsilon, 0]_r \times \partial W_0,\ \lambda_0 = e^r\, \eta_0)$ where $\eta_0 := \lambda_0 \mid_{\partial W_0}$. Assuming that $d_{\partial W_0} F = 0$, the Liouville vector field here is

$$X = \left(1 + e^{-s}\frac{\partial F}{\partial t}\right) \partial_s - e^{-s}\frac{\partial F}{\partial s}\, \partial_t - e^{-s}\frac{\partial F}{\partial t}\, X_{\lambda_0} - e^{-s}\frac{\partial F}{\partial r}\, \left(-\partial_t + e^{-r}\, R_{\eta_0}\right).$$

We may also assume without loss of generality that $\mathrm{Skel}(W_0, \lambda_0) \cap ([-\varepsilon, 0]_r \times \partial W_0) = \emptyset$. This assumption implies that

$$((\pi_{W_0})_* X) \mid_{\mathrm{Skel}(W_0, \lambda_0)} = -e^{-s}\frac{\partial F}{\partial t}\, X_{\lambda_0}.$$

In words, the W_0-projection of X to (a neighborhood of) the skeleton of (W_0, λ_0) is parallel to X_{λ_0} throughout the entire box fold. This implies that if $x \notin \mathrm{Skel}(W_0, \lambda_0)$, then the flowline of X through $(0, t^*, x)$ never traverses $\mathrm{Skel}(W_0, \lambda_0)$.

Next, observe that if p is a critical point of X, then $\frac{\partial F}{\partial t}(p) < 0$. Thus, in a neighborhood of p, $(\pi_{W_0})_* X$ is a positive multiple of X_{λ_0}. In particular, $\pi_{W_0}(p)$ is a critical point of X_{λ_0}. Moreover, this implies that if the flowline of X through $(0, t^*, x)$ converges to a critical point in forward time, then flowline must eventually reach $\mathrm{Skel}(W_0, \lambda_0)$. By the above remark, it follows that $x \in \mathrm{Skel}(W_0, \lambda_0)$. Finally, the fact that $t^* > t_0 - \varepsilon(\tau)$ is immediate from the observation that in a piecewise-linear box fold, every flowline passing through $\{s = 0\} \times (0, t_0) \times W_0$ travels through the fold and reaches $\{s = s_0\}$ in forward time. This behavior is C^0-approximated by a smooth box fold, and hence $t^* > t_0 - \varepsilon(\tau)$. This proves the lemma. □

Proof of Proposition 5.13. We claim that such a flowline $(0, t^*, x, p, q)$ is not trapped by a stove critical point. That is, the critical point must either be in II_2, the box hole, or the critical point at the top of the chimney of $C\Pi_1$. Assuming this, Proposition 5.13 follows immediately from the previous lemma: indeed, II_2 is an ordinary fold, and near the top of the chimney of $C\Pi_1$ the chimney fold is locally an ordinary fold. In particular, the skeleton of the stabilization direction component of each of these folds is the origin and the t-coordinates are arbitrarily close to $t = 0$ and $t = t_0 - \delta_1$, respectively.

Thus, it suffices to show that the flowline through $(0, t^*, x, p, q)$ cannot converge to a stove critical point in forward time. But this is immediate from the design of a blocking apparatus: in *backward* time, every flowline emanating from a stove critical point enters the trapping region of II_2; see the proof of Proposition 5.10. This implies that all flowlines through $\{s = 0\}$ avoid stove critical points of $C\Pi_1$ in forward time.

□

5.4 Partial folds

Earlier, we developed the theory of box folds based over symplectizations of genuine contact handlebodies, i.e., Reeb-thickened Weinstein domains. We then generalized the construction to define a chimney fold in low dimensions, based over the symplectization of a region which is not literally a contact handlebody. However, the generalization of a chimney fold to higher dimensions involved an extra direction W_0 which is a Weinstein domain, so that a high-dimensional chimney fold is based over the symplectization of a product of a certain contact manifold with a Weinstein domain. We are now interested in defining the notion of a *partial* chimney fold, where the extra W_0 direction is allowed to be a Weinstein *cobordism* with nonempty negative boundary. This has the effect of changing the dynamical behavior of a chimney fold in significant fashion, depending on the topology of W_0. In particular, if W_0 has no skeleton, then the resulting partial chimney fold will not trap any flowlines in backward time. Still, a partial fold can be useful for directing holonomy in specific ways.

5.4.1 Partial box folds

One of the principles from the previous sections is that the behavior of a high-dimensional chimney fold in the W_0 direction is similar to that of a normal box fold, and the "interesting" behavior of a chimney fold is focused in the $[0, t_0] \times r_0\mathbb{D}^2$ direction. As such, we begin by studying *partial box folds*. This is similar to the notion of a *partial C-fold* in [HH19].

Definition. A **generalized contact handlebody** is a contact manifold of the form

$$(H_0 := [0, t_0] \times W_0,\ dt + \lambda_0)$$

where (W_0, λ_0) is a Weinstein cobordism, possibly with nonempty negative boundary.

Let $(H_0 = [0, t_0] \times W_0^{2n-2},\ dt + \lambda_0)$ be a generalized contact handlebody and let

$$([0, s_0] \times H_0,\ e^s(dt + \lambda_0))$$

be its symplectization. This represents a region in our given $2n$-dimensional Liouville domain that we wish to perturb. As before, we realize this region as the hypersurface $\{z = 0\}$ inside its contactization:

$$(\mathbb{R}_z \times [0, s_0] \times H_0,\ dz + e^s(dt + \lambda_0))\,.$$

A partial box fold is defined identically to a normal box fold. The important difference is the presence of a new side, $\underline{\partial_- W_0}$.

Definition. Fix $z_0 > 0$. A **(piecewise-linear, high-dimensional) partial box fold with parameters** z_0, s_0, t_0, denoted Λ^{PL}, is the hypersurface

$$\Lambda^{PL} := \overline{\partial\left([0, z_0] \times [0, s_0] \times H_0\right) \setminus \{z = 0\}}.$$

The following lemma is immediate from the techniques of previous sections.

Lemma 5.15. *Let X_{λ_0} denote the Liouville vector field of (W_0^{2n-2}, λ_0), let $\eta_0^{\pm} := \lambda_0 \mid_{\partial_\pm W_0}$ be the induced contact forms on the positive and negative boundary of W_0, and let $R_{\eta_0^{\pm}}$ denote the respective Reeb vector fields on $\partial_\pm W_0$ of $\eta_0^{\pm}$. The backward oriented characteristic foliation of Λ^{PL} is given by Table 5.2.*

Before we state the main proposition describing the dynamical impact of a partial box

Side	Characteristic foliation
$\underline{z = z_0}$	$-\partial_s$
$\underline{s = 0}$	$\partial_t - \partial_z$
$\underline{s = s_0}$	$-\partial_t + e^{s_0}\partial_z$
$\underline{t = 0}$	$-\partial_s + X_{\lambda_0}$
$\underline{t = t_0}$	$\partial_s - X_{\lambda_0}$
$\underline{\partial_+ W_0}$	$\partial_t - R_{\eta_0^+}$
$\underline{\partial_- W_0}$	$-\partial_t + R_{\eta_0^-}$

Table 5.2: The oriented characteristic foliation of a partial box fold.

fold, we introduce some more notation to deal with the cobordism W_0. First, define

$$\|W_0\| := \inf_{x \in \partial_- W_0} -\ln \|x\|_{W_0}.$$

In words, $\|W_0\|$ is simply the time-length of the shortest flowline of X_{λ_0} from $\partial_- W_0$ to $\partial_+ W_0$. For reasons that will eventually become clear, we will typically require $\|W_0\| > 2s_0$. We also remind the reader of the following notation:

$$N^{s_0}(\partial_+ W_0) := \bigcup_{s \in (-s_0, 0]} \psi^s(\partial_+ W_0)$$
$$N^{s_0}(\partial_- W_0) := \bigcup_{s \in [0, s_0)} \psi^s(\partial_- W_0).$$

Here, ψ^s is the time-s flow of X_{λ_0}, and $N^{s_0}(\partial_\pm W_0)$ is a distinguished collar neighborhood of $\partial_\pm W_0$ determined by the time-s_0 flow. Observe that the assumption $\|W_0\| > 2s_0$ implies that $N^{s_0}(\partial_+ W_0) \cap N^{s_0}(\partial_- W_0) = \emptyset$.

Proposition 5.16. *Let Λ^{PL} be a high-dimensional partial box fold with $z_0 \geq e^{s_0} t_0$ and $\|W_0\| > 2s_0$, and let $h^{PL} : \{z = 0\} \times \{s = s_0\} \times H_0 \dashrightarrow \{z = 0\} \times \{s = 0\} \times H_0$ be the partially-defined holonomy map given by the oriented characteristic foliation of Λ^{PL}. Let $x \in H_0$ be the entry point of a flowline in H_0, and let $t(x)$ and $W_0(x)$ be the t-coordinate and W_0-coordinate of x, respectively.*

(*i*) *If either $t(x) \in (e^{-s_0} t_0, t_0)$ or $W_0(x) \in N^{s_0}(\partial_+ W_0)$, then the flowline through x is either*

trapped in backward time or

$$W_0(h^{PL}(x)) \in N^{s_0}(\partial_- W_0).$$

(*ii*) *For all* $(t, w) \in (0, e^{-s_0}t_0) \times (W_0 \setminus N^{s_0}(\partial_+ W_0))$,

$$h^{PL}(t, w) = (e^{s_0}t, \psi^{s_0}(w)).$$

Proof. First, we remark that the statement and proof of (ii) is identical to the holonomy of a piecewise-linear box fold. Indeed, for such a flowline, because $t(x) < e^{-s_0}t_0$ and $W_0(x) \notin N^{s_0}(\partial_+ W_0)$, the flowline never reaches $\underline{t = t_0}$ and so there is no interaction with $\underline{\partial_- W_0}$.

Next, we consider (i). If W_0 has a skeleton, then some flowlines exhibit identical behavior to a normal box fold and are trapped in backward time. Thus, it is sufficient to prove (i) in the case that W_0 is a trivial Weinstein cobordism with no skeleton. Suppose first that $t(x) \in (e_{-s_0}t_0, t_0)$. In backward time, the flowline first travels along $\underline{s = s_0}$ via $-\partial_t + e^{s_0}\,\partial_z$ and reaches $\underline{t = 0}$. The flowline then travels along $\underline{t = 0}$ via $-\partial_s + X_{\lambda_0}$, and there are two possibilities: either the flowline reaches $\underline{\partial_+ W_0}$, or $\underline{s = 0}$. Both of these possibilities result in the flowline reaching $\underline{t = t_0}$ by the assumption $t(x) \in (e_{-s_0}t_0, t_0)$, just as with a box fold.

Thus, from this point we consider a flowline on $\underline{t = t_0}$. It travels via $\partial_s - X_{\lambda_0}$ to either $\underline{s = s_0}$ or $\underline{\partial_- W_0}$. If the flowline reaches $\underline{s = s_0}$ first, the typical cycling process from $\underline{t = t_0}$ to $\underline{t = 0}$ and back while spiraling up in the z-direction will repeat — as in a normal box fold — until the flowline eventually reaches $\underline{z = z_0}$. When this happens, the cycling process will no longer involve $\underline{t = 0}$, and so the only movement in the W_0 direction will occur on $\underline{t = t_0}$ via $\partial_s - X_{\lambda_0}$. Thus, such a flowline will eventually reach $\underline{\partial_- W_0}$ with some s-coordinate $s^* \in (0, s_0)$. In particular, the flowline reaches $\underline{\partial_- W_0}$ at point K.

In a normal box fold (where there is no negative boundary of W_0), the cycling process would continue forever and the flowline would be trapped. But a partial box fold has a second phase of movement which is not present in a normal box fold, beginning with

movement along $\underline{\partial_- W_0}$ via $-\partial_t + R_{\eta_0^-}$. The flowline reaches $\underline{t = t_0}$, without having traveled along $\underline{s = s_0}$. This latter point is crucial, as the z-coordinate of the flowline does not increase. Along $\underline{t = t_0}$ the flowline travels via $-\partial_s + X_{\lambda_0}$ and reaches $\underline{s = 0}$. Note that this induces precisely a time-s^* flow along X_{λ_0}. The flowline then traverses $\underline{s = 0}$ via $\partial_t - \partial_z$ either to $\underline{s = s_0}$ — where the just described downward cycling process repeats — or to $\underline{z = 0} \cap \underline{s = 0}$, where the flowline exits the fold with $W_0(h^{PL}(x)) \in N^{s_0}(\partial_- W_0)$, as desired.

It is clear that if instead we assume $W_0(x) \in N^{s_0}(\partial_+ W_0)$ in (i) then the conclusion is the same, as such a flowline will eventually reach $\underline{t = t_0}$ via $\underline{\partial_+ W_0}$.

□

In words, the above proposition says that a partial box fold functionally behaves like a normal box fold, with the trapping region being replaced by a region whose holonomy (when defined) exits in the collar neighborhood $N^{s_0}(\partial_- W_0)$.

The smoothing of a partial fold carries the same type of complications as with normal box folds, but with more subtle behavior. We hope to carefully investigate the holonomy of smooth partial folds in a future work. For now, we point out that the statement of Lemma 4.11 still holds, namely, the estimate $\|h(x)\|_{W_0} \leq e^{s_0} \|x\|_{W_0}$ for all x in the generalized contact handlebody.

Finally, we remark that one can define a partial box hole, which we will denote $\mathbb{V}^{PL}$, in the same way. The analysis of partial box holes is the exact analogue of partial box folds given above, reinterpreted correctly. We omit the details.

5.4.2 Partial chimney folds

Next, we extend the notion of a partial box fold to that of a chimney fold. While one could define a partial chimney fold in full generality, we will define such a fold with a stabilization direction in mind, as in Section 5.1. The extension is identical, in the sense that we consider the low-dimensional chimney-stove region

$$[0, s_0] \times H_0^C \subset [0, s_0] \times [0, t_0] \times \tilde{W}_0^2$$

where $(\tilde{W}_0^2, \tilde{\lambda}_0)$ is a Weinstein domain of dimension 2, and in higher dimensions we replace the additional Weinstein domain W_0 with a Weinstein *cobordism*. In particular, we make the following definition.

Definition. Let $(\tilde{W}_0^2, \tilde{\lambda}_0)$ be a Weinstein domain, and let (W_0, λ_0) be a Weinstein cobordism. Fix $z_0, s_0, t_0, t_- > 0$ with $z_0 = e^{s_0} t_0$, and define $H_0^C \subset [0, t_0] \times \tilde{W_0}^2$ as in Section 5.1. A **piecewise-linear partial chimney fold with parameters** z_0, s_0, t_0, t_-, denoted $C\Lambda^{PL}$, is the hypersurface

$$C\Lambda^{PL} := \overline{\partial([0, z_0] \times [0, s_0] \times H_0^C \times W_0) \setminus \{z = 0\}}.$$

As before, the only difference between this and a normal chimney fold is the presence of the side $\underline{\partial_- W_0}$. The main feature of a piecewise-linear partial chimney fold is given by the following proposition.

Proposition 5.17. *Let $C\Lambda^{PL}$ be a partial chimney fold with $\|W_0\| > 2s_0$, and let $h^{PL} : \{s = s_0\} \dashrightarrow \{s = 0\}$ be the partially-defined holonomy map given by the oriented characteristic foliation of $C\Lambda^{PL}$. Suppose that $x \in \{s = s_0\} \times (0, t_0) \times \mathit{int}(C) \times W_0$. Then either the flowline through x is trapped in backward time, or*

$$W_0(h^{PL}(x)) \in N^{s_0}(\partial_- W_0) \quad \textit{and} \quad t(h^{PL}(x)) \in (0, t_-).$$

Before we prove this proposition, we record the notation for each side of $C\Lambda^{PL}$, as well as the corresponding oriented characteristic foliation on each side.

$$
\begin{aligned}
\underline{z = z_0} &:= \{z = z_0\} \times [0, s_0] \times H_0^C \times W_0 \\
\underline{s = 0} &:= [0, z_0] \times \{s = 0\} \times H_0^C \times W_0 \\
\underline{s = s_0} &:= [0, z_0] \times \{s = s_0\} \times H_0^C \times W_0 \\
\underline{t = 0} &:= [0, z_0] \times [0, s_0] \times \{t = 0\} \times \tilde{W}_0 \times W_0 \\
\underline{t = t_-} &:= [0, z_0] \times [0, s_0] \times \{t = t_-\} \times (\tilde{W}_0 \setminus C) \times W_0 \\
\underline{t = t_0} &:= [0, z_0] \times [0, s_0] \times \{t = t_0\} \times C \times W_0 \\
\underline{\partial \tilde{W}_0} &:= [0, z_0] \times [0, s_0] \times [0, t_-] \times \partial \tilde{W}_0 \times W_0 \\
\underline{\partial C} &:= [0, z_0] \times [0, s_0] \times [t_-, t_0] \times \partial C \times W_0 \\
\underline{\partial_+ W_0} &:= [0, z_0] \times [0, s_0] \times H_0^C \times \partial_+ W_0 \\
\underline{\partial_- W_0} &:= [0, z_0] \times [0, s_0] \times H_0^C \times \partial_- W_0.
\end{aligned}
$$

Table 5.3 gives the oriented characteristic foliation on each of the above sides.

Side	Characteristic foliation
$\underline{z = z_0}$	$-\partial_s$
$\underline{s = 0}$	$\partial_t - \partial_z$
$\underline{s = s_0}$	$-\partial_t + e^{s_0}\partial_z$
$\underline{t = 0}$	$-\partial_s + X_{\tilde{\lambda}_0} + X_{\lambda_0}$
$\underline{t = t_-}$	$\partial_s - X_{\tilde{\lambda}_0} - X_{\lambda_0}$
$\underline{t = t_0}$	$\partial_s - X_{\tilde{\lambda}_0} - X_{\lambda_0}$
$\underline{\partial \tilde{W}_0}$	$\partial_t - R_{\tilde{\eta}_0}$
$\underline{\partial C}$	$X_{\partial C}$
$\underline{\partial_+ W_0}$	$\partial_t - R_{\eta_0^+}$
$\underline{\partial_- W_0}$	$-\partial_t + R_{\eta_0^-}$

Table 5.3: The oriented characteristic foliation of a partial chimney fold.

Here, $X_{\partial C}$ is simply a placeholder for the backward oriented characteristic foliation of $\underline{\partial C}$ (which does not matter for the purpose of our discussion), and $\tilde{\eta}_0 = \tilde{\lambda}_0 \mid_{\partial \tilde{W}_0}$.

Proof of Proposition 5.17. The holonomy analysis is very similar to that of Proposition 5.16 and also the analysis of a normal chimney fold, but we give explicit details here for the

sake of clarity on how the design of a (partial) chimney fold influences the dynamics.

Suppose that $x \in \{s = s_0\} \times (0, t_0) \times \text{int}(C) \times W_0$. In other words, suppose we begin with a point that enters in the chimney region. The flowline initial travels along $\underline{s = s_0}$ via $-\partial_t + e^{s_0}\,\partial_z$ to $\underline{t = 0}$. From here it travels via $-\partial_s + X_{\tilde{\lambda}_0} + X_{\lambda_0}$. There are two possibilities. Either the flowline reaches $\underline{\partial \tilde{W}_0}$ first or $\underline{\partial_+ W_0}$. In particular, if $\|x\|_{\tilde{W}_0} > \|x\|_{W_0}$, then the former will occur, and vice versa if $\|x\|_{\tilde{W}_0} < \|x\|_{W_0}$.

Assume first that $\|x\|_{\tilde{W}_0} > \|x\|_{W_0}$, so that the flowline reaches $\underline{\partial \tilde{W}_0}$. Later, we will reduce the case $\|x\|_{\tilde{W}_0} < \|x\|_{W_0}$ to the present one. Along $\underline{\partial \tilde{W}_0}$. the flowline travels via $\partial_t - R_{\tilde{\eta}_0}$ to $\underline{t = t_-}$. From here, the flowline cycles around the stove (the cycling happens in the $[0, t_-] \times \tilde{W}_0$ direction) with an increasing z-coordinate, just as in a normal chimney fold, until reaching $\underline{z = z_0}$. One slight difference here is that there is movement back and forth in the W_0 direction, concurrent with the back and forth movement in the $\tilde{W}_0$ direction. But by the assumption $\|x\|_{\tilde{W}_0} > \|x\|_{W_0}$, there is no interaction with ∂W_0 in this stage.

When the flowline reaches $\underline{z = z_0}$, the it ceases cycling around the stove via $\underline{\partial \tilde{W}_0}$ and begins primarily flowing via $\partial_s - X_{\tilde{\lambda}_0} - X_{\lambda_0}$ on $\underline{t = t_-}$. We refer the reader to the proof of the trapping behavior of a normal chimney fold, as this stage of the dynamics is exactly the same. The difference in this situation is the presence of $\underline{\partial_- W_0}$. Again we assume for simplicity that W_0 is a trivial cobordism with no skeleton. Under this assumption, the flowline will eventually reach $\underline{\partial_- W_0}$. From this point the behavior is identical to that of Proposition 5.16 with a t-thickness of t_- and we have $W_0(h^{PL}(x)) \in N^{s_0}(\partial_- W_0)$ and $t(h^{PL}(x)) \in (0, t_-)$ as desired.

Next we prove that if $\|x\|_{W_0} > \|x\|_{\tilde{W}_0}$, then the flowline eventually enters the case described above. For such a flowline, it will reach $\underline{\partial_+ W_0}$ (with a $\tilde{W}_0$-coordinate still in C) and will travel via $\partial_t - R_{\eta_0^+}$ up to $\underline{t = t_0}$, in contrast to the previous situation where it reaches $\underline{t = t_-}$. Upon reaching $\underline{t = t_0}$, the dynamics are identical to that of a pre-chimney fold as in 4.1.4. In particular, it will cycle around the edge of the chimney region with a net negative movement in the W_0 direction. Eventually the flowline will reach $\underline{\partial_- W_0}$. Here it will follow $-\partial_t + R_{\tilde{\eta}_0}$ down to $\underline{t = 0}$, and now we are in the case where $\tilde{W}_0(x) \in C$ and

$\|x\|_{\tilde{W}_0} > \|x\|_{W_0}$. By the earlier case work, we are done.

□

Like with the complications of smooth partial folds, we hope to thoroughly understand the complications of smooth chimney folds in a future work.

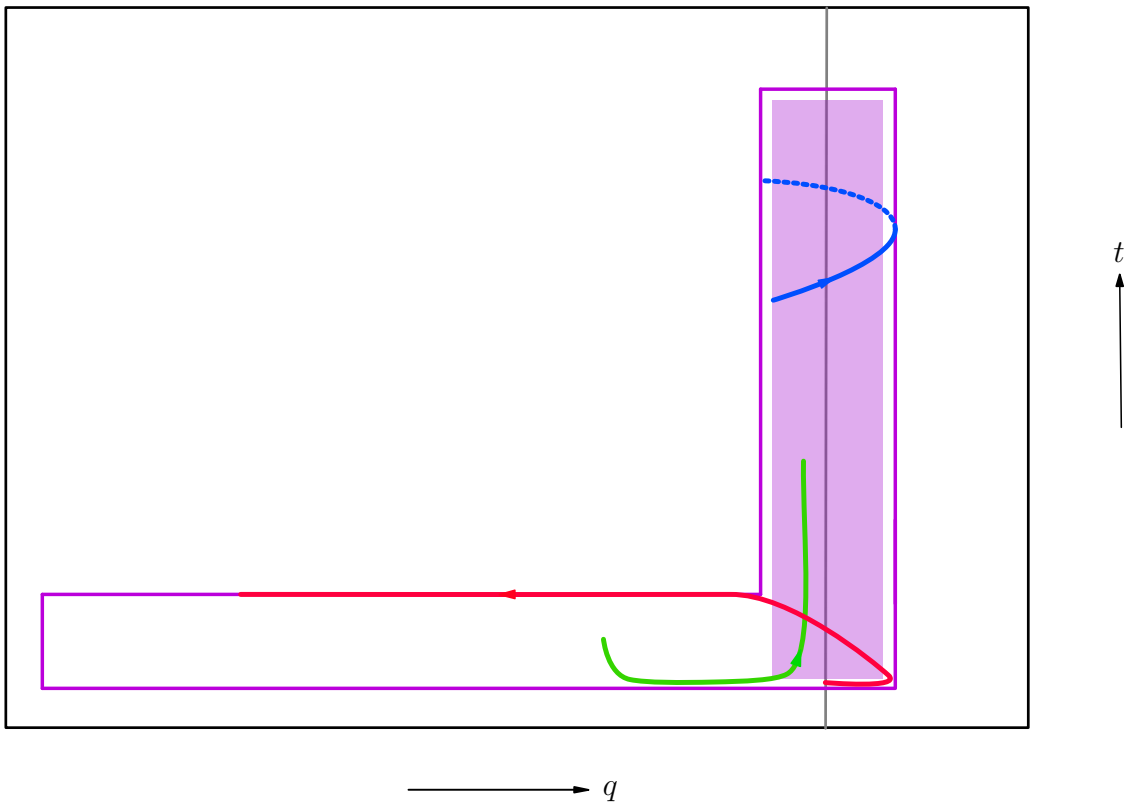

Figure 5.9: A visualization of the proof of Proposition 5.8. Pictured is $H_1^{C_1}$ with a few sample trajectories of points with holonomy. The shaded region indicates the trapping region of the chimney. The green point enters the fold in the stove and exits somewhere in the chimney; this is clearly compatible with the statement of the proposition. The red point enters along the t-axis near $t = \delta_1$, is heavily influenced by the characteristic foliation of $\partial H_1^{C_1}$, and exits far away in the stove. By itself, this violates the desired properties of Proposition 5.8, but $\amalg_2$ will trap such a point. The blue point enters near $\partial \text{int}^\tau(C_1)$, is influenced by the characteristic foliation of $\partial H_1^{C_1}$, and exits near ∂C_1. This is compatible with the statement of the proposition, provided τ is small enough.

CHAPTER 6

Mitsumatsu's Liouville domains

In this chapter we use Proposition 1.7 to show that the Liouville-but-not-Weinstein domains constructed by Mitsumatsu in [Mit95] are in fact stably Weinstein. This gives an affirmative answer to Question 0.8 of [Hua19].

We begin by giving a criterion for determining when a Liouville domain is Weinstein in Section 6.1. We then restate Proposition 1.7 for *standard stabilized regions* in Section 6.2. These are regions $U \subset (W, \lambda)$ in a Liouville domain that have the form

$$(U, \lambda|_U) \cong ([0, s_0] \times [0, t_0] \times W_0 \times r_0 \mathbb{D}^2,\, e^s (dt + \lambda_0) + \lambda_{\text{stab}}),$$

for some Weinstein domain (W_0, λ_0). That is, $(U, \lambda|_U)$ is a region that is a stabilization of a symplectization of a contact handlebody. These regions appear naturally in the stabilization of a Liouville domain, and thus a version of Proposition 1.7 stated for such regions will be useful to us in this section.

After restating Proposition 1.7 in this manner, we will recall the definition of Mitsumatsu's domains, identify the standard stabilized regions on which we want to perturb the Liouville form, and finally verify that this perturbed domain is in fact Weinstein.

6.1 A Weinstein criterion

Our end goal in this chapter is to conclude that a certain Liouville domain admits a Weinstein structure. Though the definition of a Weinstein domain is simple from an abstract point of view, when handed an arbitrary Liouville domain it may not be clear how

to verify that it admits a Weinstein structure. Thus, we begin with a Weinstein criterion based on the dynamics of the Liouville vector field.

Proposition 6.1. *A Liouville domain (W, λ), with Liouville vector field X_λ, is Weinstein if and only if the following conditions are satisfied:*

(1) *for any zero $p \in W$ of X_λ, there is a neighborhood of p on which X_λ admits a Morse Lyapunov function;*

(2) *for any $p \in W$, the unique flowline of X_λ passing through p converges to a zero of X_λ in backward time;*

(3) *the vector field X_λ does not admit any* broken loops, *where a broken loop is a map $c\colon \mathbb{R}/\mathbb{Z} \to W$ with $0 = a_0 < a_1 < \cdots < a_N = 1$ such that $c(a_i)$ is a zero of X_λ and $c(a_i, a_{i+1})$ is an oriented flowline of X_λ from $c(a_i)$ to $c(a_{i+1})$.*

Remark. Proposition 6.1 and its proof are adapted from [HH19, Proposition 2.1.3], which gives criteria for a vector field on a closed manifold to be Morse.

Proof of Proposition 6.1. If (W, λ) is Weinstein, then certainly conditions (1)-(3) are satisfied, since in this case X_λ admits a globally-defined Morse Lyapunov function. Let us assume that these conditions hold and show that (W, λ) is Weinstein. For this, it suffices to construct a handle decomposition of W which is compatible with X_λ.

Let $C(X_\lambda) = \{p_1, \ldots, p_k\}$ be the zeros of X_λ, a finite set by the compactness of W and (1). Criterion (3) allows us to put a partial order on $C(X_\lambda)$, with $p_i \prec p_j$ whenever X_λ admits a (possibly broken) flowline from p_i to p_j. Criterion (2) then implies that any minimal element of $C(X_\lambda)$ is a critical point of index 0. We let C_0 denote the set of minimal elements of $C(X_\lambda)$, and for $j \geq 0$ we let C_{j+1} be the union of C_j and the minimal elements of $C(X_\lambda) \setminus C_j$. Our handle decomposition of W can then be constructed inductively: we begin with a standard neighborhood of C_0, then attach the handles corresponding to C_1, then those of C_2, and so on. □

Because we are considering Liouville domains up to Liouville homotopy, we will always assume that criterion (1) is satisfied. Indeed, standard transversality arguments show that

a generic vector field has only nondegenerate critical points. Thus, with X_λ as above, we may choose an arbitrarily small vector field $\tilde{X}$ on W so that $X_\lambda + \tilde{X}$ has only nondegenerate critical points. We choose $\tilde{X}$ small enough to ensure that $X_t := X_\lambda + t\tilde{X}$ is outwardly transverse to ∂W, for $t \in [0,1]$. Then

$$\lambda_t := \iota_{X_t}\omega$$

defines a Liouville homotopy from (W,λ) to (W,λ_1), the latter of which has Liouville vector field $X_\lambda + \tilde{X}$.

Verifying that a given Liouville domain is Weinstein will thus consist of verifying two criteria: first, that all flowlines converge to critical points in backward time; second, that the domain contains no broken loops. Our local operations are developed with these criteria in mind — the operations aim to trap large sets of flowlines in backward time, and to do so with a holonomy which prevents broken loops from developing. In the rest of this chapter we will verify these criteria in the specific case of Mitsumatsu's examples.

6.2 The local operation for standard stabilized regions

Proposition 1.7 perturbs the Liouville form on the symplectization of a stabilized contact handlebody. When modifying the Liouville dynamics of a stabilized Liouville domain, we will often find it more convenient for the stabilization and symplectization to be decoupled. Precisely, we are interested in regions which appear to be stabilizations of symplectizations (rather than symplectizations of stabilizations).

Definition. Given a Liouville domain (W,λ), a *standard stabilized region* is a subset $U \subset (W,\lambda)$ such that there exists a diffeomorphism

$$\varphi\colon [0,s_0]_s \times [0,t_0]_t \times W_0 \times r_0\,\mathbb{D}^2 \to U,$$

with $\varphi^*(\lambda|_U) = e^s\,(dt + \lambda_0) + \lambda_{\mathrm{stab}}$, for some Weinstein domain (W_0,λ_0) and some choice of

constants $s_0, t_0, r_0 > 0$. If $U \subset (W, \lambda)$ is a standard stabilized region, we will typically write

$$(U, \lambda|_U) \cong ([0, s_0]_s \times [0, t_0]_t \times W_0 \times r_0\, \mathbb{D}^2,\ e^s\,(dt + \lambda_0) + \lambda_{\mathrm{stab}}),$$

making no mention of the diffeomorphism φ.

Note that the Liouville vector field in a standard stabilized region is given by $\partial_s + \frac{1}{2}(p\,\partial_p + q\,\partial_q)$; with a careful choice of coordinates, we may identify a subregion of a standard stabilized region to which Proposition 1.7 applies. The upshot is that some version of Proposition 1.7 holds for standard stabilized regions, with minor modifications to the holonomy statements.

Corollary 6.2. *Let $(U = [0, s_0] \times [0, t_0] \times W_0 \times r_0\, \mathbb{D}^2,\ e^s\,(dt + \lambda_0) + \lambda_{\mathrm{stab}})$ be a standard stabilized region in a Liouville domain (W, λ). Fix $0 < \delta \ll t_0$ and $0 < \epsilon \ll 1$ arbitrarily small. If $e^{-s_0/2}\, r_0 > 0$ is sufficiently large, a blocking apparatus can be installed in U such that there is a neighborhood U_{trap} of*

$$[\delta, t_0 - \delta] \times I_\epsilon(W_0, \lambda_0) \times \{(0, 0)\},$$

with any flowline passing through $\{s = s_0\} \times U_{\mathrm{trap}} \subseteq \partial_+ U$ converging to a critical point in backward time. Moreover, the partially-defined holonomy map $h\colon \partial_+ U \dashrightarrow \partial_- U$ satisfies

- (*i*) *for some constant $0 < K < 1$, we have $\|h(x)\|_{W_0} \leq K\, e^{s_0}\, \|x\|_{W_0}$;*
- (*ii*) *for the same constant K, we have that $\|h(x)\|_{\mathrm{stab}} \leq K\, \|x\|_{\mathrm{stab}}$, whenever $\|x\|_{W_0} < e^{-s_0}$;*
- (*iii*) *any element of $([0, \delta) \cup (t_0 - \delta, t_0]) \times (W_0 \setminus N^{s_0}(\partial W_0)) \times \{(0, 0)\}$ in $\partial_+ U$ which is not trapped is mapped by h to an element of $([0, 2\delta) \cup (t_0 - 2\delta, t_0]) \times W_0 \times \{(0, 0)\}$.*

Proof of Corollary 6.2. The corollary follows quickly from Proposition 1.7 once we identify a *standard subregion* in $(U, \lambda|_U)$. In particular, consider the subset

$$\overline{U} := \{(s, t, w, p, q) \in U \mid e^{(s_0 - s)/2}\, \|(p, q)\| \leq r_0\} \subset U.$$

We can give $\overline{U}$ coordinates via a map

$$\psi\colon [0,s_0]_{\overline{s}} \times [0,t_0]_{\overline{t}} \times W_0 \times e^{-s_0/2}\, r_0\, \mathbb{D}^2 \to \overline{U} \subset U$$

defined by

$$\psi(\overline{s},\overline{t},\overline{w},\overline{p},\overline{q}) := (\overline{s},\overline{t},\overline{w},e^{\overline{s}/2}\,\overline{p},e^{\overline{s}/2}\,\overline{q}).$$

Note that $\psi^*(\lambda|_{\overline{U}}) = e^{\overline{s}}\,(d\overline{t} + \lambda_0 + \lambda_{\text{stab}})$, and thus that $(\overline{U},\lambda_{\overline{U}})$ is a Weinstein cobordism of the type hypothesized in Proposition 1.7. If the stabilization radius $e^{-s_0/2}\,r_0$ is sufficiently large, then Proposition 1.7 gives us the conclusions of Corollary 6.2.

In particular, part (ii) of Proposition 1.7 tells us that if $\|\overline{x}\|_{W_0} < e^{-s_0}$, then $\|h(\overline{x})\|_{\text{stab}} \leq \overline{K}\,\|\overline{x}\|_{\text{stab}}$, for a constant $0 < \overline{K} < e^{s_0/2}$. This inequality holds in the coordinates on $\overline{U}$ given by ψ. Because $\overline{x}$ is an element of $\partial_+ U$ and $h(\overline{x})$ is an element of $\partial_- U$, we have

$$\|h(\overline{x})\|_{\text{stab}} = \|\psi(h(\overline{x}))\|_{\text{stab}} \quad \text{and} \quad \|\overline{x}\|_{\text{stab}} = e^{-s_0/2}\,\|\psi(\overline{x})\|_{\text{stab}},$$

so

$$\|\psi(h(\overline{x}))\|_{\text{stab}} = \|h(\overline{x})\|_{\text{stab}} \leq \overline{K}\,\|\overline{x}\|_{\text{stab}} = \overline{K}\,e^{-s_0/2}\,\|\psi(\overline{x})\|_{\text{stab}},$$

giving us part (ii) of Corollary 6.2. □

6.3 The domains

In [McD91], McDuff gave the first examples of symplectic structures with contact-type boundaries on compact 4-manifolds with disconnected boundaries. Such examples distinguish symplectic geometry from complex geometry, as a complex manifold with convex boundary cannot have a disconnected boundary. Mitsumatsu presented a variation on this theme in [Mit95], where he constructed a 4-dimensional Liouville domain W_A with disconnected boundary for any Anosov map $A\colon T^2 \to T^2$. We recall this construction here, borrowing heavily from the exposition in [Hua19, Example 0.7].

Let $T^2 = \mathbb{R}^2/\mathbb{Z}^2$ denote the torus, and consider a linear Anosov map $A\colon T^2 \to T^2$.

That is, we may take A to be an element of $\mathrm{SL}(2,\mathbb{Z})$ with eigenvalues λ_{u} and λ_{s}, with $0 < \lambda_{\mathrm{u}} < 1 < \lambda_{\mathrm{s}}$. We may then choose linearly independent linear 1-forms β_{u} and β_{s} on T^2 satisfying

$$A^*\beta_{\mathrm{u}} = \lambda_{\mathrm{u}}\,\beta_{\mathrm{u}} \quad \text{and} \quad A^*\beta_{\mathrm{s}} = \lambda_{\mathrm{s}}\,\beta_{\mathrm{s}}.$$

Now consider the 3-manifold-with-boundary $M := [-1,1]_\tau \times T^2$. We define a contact form on M by

$$\alpha := \beta_{\mathrm{u}} + \tau\,\beta_{\mathrm{s}},$$

and define a map $\phi_A \colon M \to M$ by

$$\phi_A(\tau, x) := (\lambda_{\mathrm{u}}^2\,\tau, Ax).$$

Observe that ϕ_A is a diffeomorphism onto its image $[-\lambda_{\mathrm{u}}^2, \lambda_{\mathrm{u}}^2] \times T^2 \subset M$, and that $\phi_A^*\alpha = \lambda_{\mathrm{u}}\,\alpha$. In the language of [Hua19], this makes ϕ_A a *contraction* of (M,α), and thus we may use ϕ_A to define a Liouville domain W_A as a partial mapping torus. We begin with the symplectization $(\mathbb{R}_s \times M, d(e^s\,\alpha))$ of M and consider the map $\Phi_A \colon \mathbb{R} \times M \to \mathbb{R} \times M$ defined by

$$\Phi_A(s,\tau,x) := (s + \ln(\lambda_{\mathrm{s}}), \lambda_{\mathrm{u}}^2\,\tau, Ax).$$

Then

$$\Phi_A^*(e^s\,\alpha) = e^{s+\ln(\lambda_{\mathrm{s}})}\,\phi_A^*\alpha = \lambda_{\mathrm{s}}\,\lambda_{\mathrm{u}}\,e^s\,\alpha = e^s\,\alpha,$$

so the Liouville 1-form $e^s\,\alpha$ descends to the partial mapping torus

$$W_A := ([0, \ln(\lambda_{\mathrm{s}})]_s \times M)/(0,\tau,x) \sim \Phi_A(0,\tau,x).$$

Of course, the vector field dual to $\lambda := e^s\,\alpha$ via $d(e^s\,\alpha)$ is ∂_s, which does not point out of the *vertical boundary* $[0, \ln(\lambda_{\mathrm{s}})] \times \partial M$ of W_A. This is easily fixed with a small perturbation of the vertical boundary, and the precise choice of perturbation does not affect the Liouville homotopy class of the resulting Liouville domain (W_A, λ).

It is clear from this construction that the skeleton of (W_A, λ) is given by

$$\mathrm{Skel}(W_A, \lambda) = ([0, \ln(\lambda_s)]_s \times \{0\}_\tau \times T^2)/(0, 0, x) \sim (\ln(\lambda_s), 0, Ax),$$

which, topologically, is simply the mapping torus of $A\colon T^2 \to T^2$. Our 4-dimensional Liouville domain (W_A, λ) thus has the homotopy type of a 3-manifold, and therefore fails to admit a Weinstein structure. Our goal is to show that (W_A, λ) is *stably* Weinstein — i.e., that $(W_A \times r_0\,\mathbb{D}^2, \lambda + \frac{1}{2}(p\,dq - q\,dp))$ is Weinstein, up to homotopy, for some $r_0 > 0$.

6.4 Identifying standard stabilized regions

Stabilization does not fundamentally alter the skeleton of our Liouville domain; we have

$$\mathrm{Skel}(W_A \times r_0\,\mathbb{D}^2, \lambda + \tfrac{1}{2}(p\,dq - q\,dp)) = \mathrm{Skel}(W_A, \lambda) \times \{(0, 0)\}.$$

As outlined in Section 1.2, our strategy for simplifying Liouville dynamics focuses on using local perturbations to interrupt the Liouville flow along the skeleton of our domain. When identifying the standard stabilized regions that will support our perturbations (i.e., where Corollary 6.2 will be applied), it is thus important to consider how these regions intersect our skeleton.

Because our skeleton has no interesting behavior in the stabilization direction, our search for standard stabilized regions will be guided only by the nature of the initial domain (W_A, λ) and its skeleton. This search is eased considerably by the fact that (W_A, λ) agrees locally with the symplectization of (M, α). This allows us to construct a standard stabilized region by identifying a contact handlebody $([0, t_0] \times W_0, dt + \lambda_0)$ in (M, α) and then considering the standard stabilized region

$$(\sigma_0 \times [0, t_0] \times W_0 \times r_0\mathbb{D}^2, e^s(dt + \lambda_0) + \tfrac{1}{2}(p\,dq - q\,dp)) \subset W_A,$$

for some closed interval $\sigma_0 \subset (0, \ln(\lambda_s))$ and some $r_0 > 0$. The contact handlebody arises as a

standard neighborhood of a closed Legendrian in (M, α), chosen so that this neighborhood meets $\mathrm{Skel}(W_A, \lambda)$ in a desirable manner.

6.4.1 Identifying contact handlebodies

Note that the intersection of $\mathrm{Skel}(W_A, \lambda)$ with a contact slice

$$M_s := \{s\} \times [-1, 1]_\tau \times T^2 \subset (W_A, \lambda), \quad 0 \leq s < \ln(\lambda_{\mathrm{s}})$$

is given by $\{s\} \times \{0\}_\tau \times T^2$. As a hypersurface in the contact manifold $(M_s, \alpha_s := e^s\,(\beta_{\mathrm{u}} + \tau\,\beta_{\mathrm{s}}))$, this intersection has a linear characteristic foliation, directed by the eigenvector $-V_{\mathrm{s}}$ of A. However, because A is Anosov, V_{s} has irrational slope, and thus the leaves of this foliation will not be closed. This means that the closed Legendrians whose standard neighborhoods will be our contact handlebodies cannot lie on the intersection of $\mathrm{Skel}(W_A, \lambda)$ with M_s. Nonetheless, we can identify closed Legendrians in (M_s, α_s) that are arbitrarily close to this intersection. We may choose $\tau_0 \neq 0$ arbitrarily close to 0 such that $\tau_0\,V_{\mathrm{u}} - V_{\mathrm{s}}$ has rational slope and consider the foliation of T^2 directed by $\tau_0\,V_{\mathrm{u}} - V_{\mathrm{s}}$. By construction, the leaves of this foliation are closed, and for any leaf L, the knot

$$\{s\} \times \{\tau_0\} \times L \subset (M_s, \alpha_s)$$

is Legendrian. With some choice of $\tau_0 \neq 0$ fixed[1], we now construct a standard neighborhood of a Legendrian such as this.

Let us denote by L_0 the leaf which passes through $(0, 0)$ in T^2 and consider a strip $S_0 \subset T^2$ centered on L_0. That is, S_0 has coordinates (t, θ), with $\partial_t = V_{\mathrm{u}}$ and $\partial_\theta = \tau_0\,V_{\mathrm{u}} - V_{\mathrm{s}}$, and we write $S_0 = [0, t_0] \times L_0$, with the original leaf L_0 given by $\{t_0/2\} \times L_0$. The strip S_0 is chosen so that its area is at least 2/3 in the flat metric on $T^2 = \mathbb{R}^2/\mathbb{Z}^2$. Now $N_0 := \{s\} \times [-1, 1]_\tau \times S_0 \subset (M, \alpha)$ is a contact handlebody; in the natural coordinates (τ, t, θ) on

[1] In practice, this choice doesn't matter, provided it's between -1 and 1.

this neighborhood, we have

$$\alpha|_{N_0} = dt + (\tau_0 - \tau)\, d\theta.$$

At last we may choose a closed interval $\sigma_0 \subset (0, \ln(\lambda_{\mathrm{s}}))$ and define

$$V_0 := \sigma_0 \times [0, t_0]_t \times L_0 \times [-1, 1]_\tau \subset W_A,$$

so that $\lambda|_{V_0} = e^s\,(dt + (\tau_0 - \tau)\, d\theta)$. We emphasize that $(V_0, \lambda|_{V_0})$ is a region in the *unstabilized* domain (W_A, λ). It remains to choose a radius $r_0 > 0$ and define a standard stabilized region $U_0 := V_0 \times r_0\,\mathbb{D}^2$. Before doing so, we point out that a second region, $(V_1, \lambda|_{V_1})$, may be constructed by letting $L_1 \subset T^2$ be the unique leaf directed by $\tau_0\, V_{\mathrm{u}} - V_{\mathrm{s}}$ with the property that the two components of $T^2 \setminus (L_0 \cup L_1)$ are annuli of equal area. We then construct a strip $S_1 = [0, t_0] \times L_1 \subset T^2$ of the same Reeb thickness t_0 as S_0, with coordinates (t, θ). At last we define

$$V_1 := \sigma_1 \times [0, t_0]_t \times L_1 \times [-1, 1]_\tau \subset W_A,$$

where σ_1 is an as-yet-undetermined closed subinterval of $(0, \min(\sigma_0))$.

6.4.2 Choosing parameters for Corollary 6.2

At this stage, we are treating the quantities $t_0 > 0$ and $\tau_0 \neq 0$ as fixed; it remains to choose the intervals σ_0 and σ_1, as well as the radius $r_0 > 0$ that will be used for our standard stabilized regions. Moreover, applying Corollary 6.2 to $U_i := V_i \times r_0\,\mathbb{D}^2$, $i = 0, 1$, will require the choice of some parameters $\delta > 0$ and $\epsilon > 0$. Our plan is to carefully choose ϵ and δ, then the intervals σ_0 and σ_1, and finally r_0.

For any $0 < \delta \ll t_0$, let us denote by S_i^δ the strip

$$S_i^\delta := [\delta, t_0 - \delta] \times L_i \subset S_i \subset T^2,$$

for $i = 0, 1$. We then choose $\delta > 0$ sufficiently small to ensure that $S_0^{2\delta} \cup S_1^{2\delta} = T^2$. This accounts for the "Reeb stretching" that is induced by Corollary 6.2. Next, we consider the

codimension 2 domains underlying V_0 and V_1. That is, we have

$$(W_i, \lambda_i) = (L_i \times [-1,1]_\tau, (\tau_0 - \tau)\, d\theta),$$

the skeleton of which is given by $L_i \times \{\tau_0\}$. We choose $\epsilon > 0$ sufficiently small to ensure that the band $L_i \times [0, \tau_0]$ is contained in the interior of $I_\epsilon(W_i, \lambda_i)$. This is because the intersection of $\mathrm{Skel}(W_A, \lambda)$ with V_i is given by $\sigma_i \times [0, t_0] \times L_i \times \{0\}$; by choosing $\epsilon > 0$ sufficiently small, we ensure that this intersection is trapped when Corollary 6.2 is applied.

With $\delta > 0$ and $\epsilon > 0$ chosen, we now set about defining the intervals σ_0 and σ_1. We have already insisted that σ_1 come "before" σ_0, in the sense that $\max(\sigma_1) < \min(\sigma_0)$. We now place some restrictions on the lengths of these intervals; beyond the order and lengths, the precise choice for these intervals is unimportant. Our first restriction on the lengths is simple: we require that $|\sigma_i| < -\ln(1-\epsilon)$, for $i = 0, 1$. This restriction allows us to conclude that $N^{|\sigma_i|}(\partial W_i)$ is a strict subset of $W_i \setminus I_\epsilon(W_i, \lambda_i)$. So $I_\epsilon(W_i, \lambda_i)$ is contained in $W_i \setminus N^{|\sigma_i|}(\partial W_i)$, and thus part (iii) of Corollary 6.2 (regarding the Reeb holonomy) applies to any point whose W_i-component is contained in $I_\epsilon(W_i, \lambda_i)$.

The second restriction on the lengths of σ_0 and σ_1 is quite a bit more complicated to state. We begin with the observation that the Liouville flow $\psi^s \colon W_i \to W_i$ is given by

$$\psi^s(\theta, \tau) = (\theta, \tau_0 + e^s\,(\tau - \tau_0)),$$

for $i = 0, 1$. We could use this to explicitly compute the norm $\|\cdot\|_{W_i}$, but the important point is that this norm depends only on τ. Now Corollary 6.2 considers the partially-defined holonomy map $h \colon \partial_+ U \dashrightarrow \partial_- U$ as consisting more-or-less of three distinct components: a component in the stabilization direction, another in the Weinstein direction, and a third in the Reeb direction. Consider the following three maps $h_\bullet \colon W_i \to W_i$:

$$h_i(\theta, \tau) := (\theta, \tau_0 + e^{|\sigma_i|}\,(\tau - \tau_0)), \;\; i = 0, 1, \quad h_g(\theta, \tau) := (\theta, \lambda_{\mathrm{u}}^2\, \tau).$$

According to Corollary 6.2, h_0 and h_1 represent a sort of worst-case Weinstein τ-holonomy

for points which are not trapped (ignoring any changes which might happen in the θ-component). The final map, h_g, comes from the global holonomy of (W_A, λ). We observe that h_0 and h_1 have an unstable fixed point at (θ, τ_0), while h_g brings the τ-component closer to 0, since $|\lambda_{\mathrm{u}}| < 1$. By our choice of $\epsilon > 0$, the band in W_i bounded by $\tau = 0$ and $\tau = \tau_0$ is contained in the interior of $I_\epsilon(W_i, \lambda_i)$, and thus we can choose $|\sigma_0|$ and $|\sigma_1|$ sufficiently small to ensure that the image of $(h_g \circ h_1 \circ h_0)^k$ is contained in $I_\epsilon(W_i, \lambda_i)$, for some $k \geq 1$. This constitutes our second requirement on $|\sigma_0|$ and $|\sigma_1|$.

Our third and final requirement on $|\sigma_0|$ and $|\sigma_1|$ is that these quantities be chosen sufficiently small to ensure that $(h_0 \circ h_g \circ h_1)(\theta, \tau)$ is contained in the interior of $I_\epsilon(W_i, \lambda_i)$, for any $0 \leq \tau \leq \tau_0$. This condition will be used when verifying that our perturbed Liouville domain contains no broken loops.

Finally, we choose $r_0 > 0$ sufficiently large, given our choices of ϵ and δ, so that the conclusions of Corollary 6.2 hold for both $(U_0, (\lambda + \frac{1}{2}(p\,dq - q\,dp))|_{U_0})$ and $(U_1, (\lambda + \frac{1}{2}(p\,dq - q\,dp))|_{U_1})$.

Remark. It is worth pointing out one small wrinkle with our standard stabilized regions: the domains (W_i, λ_i) are not technically Weinstein domains. However, these particular domains can be made Weinstein via arbitrarily small perturbations supported in arbitrarily small neighborhoods of their skeleta. The argument given below does not concern itself with the precise dynamics of (W_i, λ_i) near the skeleton, and thus we may treat (W_i, λ_i) has having been made Weinstein.

6.5 Verifying the Weinstein criteria

Let $(W_A \times r_0\,\mathbb{D}^2, \tilde{\lambda})$ denote the Liouville domain which results from applying Corollary 6.2 to each of the regions U_0 and U_1 identified above. We now verify that every flowline of this domain limits to a critical point in backward time, and that this domain has no broken loops. According to Proposition 6.1, this will allow us to conclude that $(W_A \times r_0\,\mathbb{D}^2, \tilde{\lambda})$ is a Weinstein domain.

6.5.1 The critical points criterion

Notice that if a flowline of the perturbed Liouville domain fails to limit to a critical point in backward time, then this flowline must pass through the slice $M_{\ln(\lambda_s)} \times r_0\,\mathbb{D}^2$ of $(W_A \times r_0\,\mathbb{D}^2, \tilde{\lambda})$. The same is true before perturbation (in which case our domain has no critical points), and thus we consider a point $(\ln(\lambda_s), \tau, x, y, p, q)$ in $W_A \times r_0\,\mathbb{D}^2$. We let ℓ denote the flowline through this point before perturbation, while $\tilde{\ell}$ is the flowline through the point after perturbation. Our goal is to show that $\tilde{\ell}$ must converge to a critical point of our modified Liouville domain in backward time.

We first observe that, since the strips S_0 and S_1 in T^2 on which U_0 and U_1 are modeled cover T^2, the flowline ℓ must intersect at least one of $\partial_+ U_0$ and $\partial_+ U_1$ in backward time. Our hope, of course, is that the perturbations installed on U_0 and U_1 will cause the new flowline $\tilde{\ell}$ to limit to a critical point in one of these regions without returning to the slice $M_{\ln(\lambda_s)}$, but there are several ways in which this might fail to occur.

The τ holonomy

First, if τ is near one of the extreme values of -1 or 1, then our perturbations cannot be expected to trap $\tilde{\ell}$. However, the global holonomy of W_A ensures that τ cannot stay near -1 or 1. In particular, we have chosen the lengths of the intervals σ_0 and σ_1 so that the global holonomy, which tends to shrink the absolute value of τ, dominates the holonomy due to our perturbations on U_0 and U_1. Eventually, if $\tilde{\ell}$ does not first limit to a critical point, we will have τ sufficiently near τ_0 so that $\tilde{\ell}$ intersects either $\partial_+ U_0$ or $\partial_+ U_1$ in $\{\max(\sigma_i)\} \times [0, t_i] \times I_\epsilon(W_i, \lambda_i)$. For this reason we may assume that $\|x\|_{W_0} \leq e^{-|\sigma_0|}(1-\epsilon) < 1 - \epsilon$.

The stabilization holonomy

According to the first condition placed on σ_0 and σ_1, we have $1 - \epsilon < e^{-|\sigma_i|}$ for $i = 0, 1$. Thus we know that $\|x\|_{W_0} < e^{-|\sigma_i|}$, allowing us to use part (ii) of Corollary 6.2 to analyze the behavior of $\tilde{\ell}$ in the stabilization direction. Specifically, Corollary 6.2 associates a constant

$0 < K_i < 1$ to U_i and ensures that if $\tilde{\ell}$ is not trapped as it passes through U_i, then the stabilization norm of the point through which it passes will be scaled by a factor of K_i. That is, the holonomy associated to U_i brings untrapped flowlines closer to $W_A \times \{(0,0)\}$. We may therefore restrict our attention to the case where $(p,q) = (0,0)$; if all flowlines through such points limit to critical points in backward time, then in fact all flowlines of our perturbed Liouville domain limit to critical points in backward time.

The Reeb holonomy

We are now considering a flowline $\tilde{\ell}$ which passes through a point $(\ln(\lambda_s), \tau, x, y, 0, 0)$, with τ sufficiently close to τ_0 to ensure that $\|x\|_{W_0} \leq e^{-|\sigma_0|}(1-\epsilon)$. Because $S_0^{2\delta}$ and $S_1^{2\delta}$ cover T^2, we know that the original flowline ℓ encounters the trapping region of either U_0 or U_1 in backward time. If ℓ meets the trapping region of U_0, then the new flowline $\tilde{\ell}$ will be trapped in U_0 in backward time, and we are finished. If ℓ does not intersect U_0, then this flowline must intersect U_1 in its trapping region, and thus $\tilde{\ell}$ will be trapped by U_1 in backward time. The only potentially troubling possibility is the case where the unperturbed flowline ℓ intersects U_0 somewhere outside its trapping region and then meets the trapping region of U_1. We need to verify that the holonomy induced by our perturbations on U_0 does not cause $\tilde{\ell}$ to miss the trapping region of U_1. But this is ensured by our choice of δ and the holonomy statement in part (iii) of Corollary 6.2. Because ℓ meets $\partial_+ U_0$ somewhere outside its trapping region, we know that the T^2-component of this intersection is in $S_0 \setminus S_0^{\delta}$, and thus the relevant holonomy statements are in parts (i) and (iii) of Corollary 6.2. Namely, part (i) ensures that the W_0-norm of $\tilde{\ell}$ maintains an upper bound of $1-\epsilon$, while part (iii) ensures that the holonomy induced by our perturbations on U_0 keeps the T^2-component of $\tilde{\ell}$ outside of $S_0^{2\delta}$. But T^2 is covered by $S_0^{2\delta}$ and $S_1^{2\delta}$, and thus the T^2-component of the intersection between $\tilde{\ell}$ and $\partial_- U_0$ will be contained in $S_1^{2\delta}$, and $\tilde{\ell}$ will meet $\partial_+ U_1$ in its trapping region.

We conclude that every flowline of $(W \times r_0 \mathbb{D}^2, \tilde{\lambda})$ limits to a critical point in backward time.

6.5.2 The broken loops criterion

With the above preparations, it is very easy to verify that $(W \times r_0\,\mathbb{D}^2, \tilde{\lambda})$ contains no broken loops. Suppose that a broken loop c did exist in this Liouville domain. Because we know that all flowlines limit in backward time to critical points, c must be genuinely broken — that is, at least one critical point is party to the broken loop. This means that c must intersect at least one of U_0 and U_1; recall, however, that Corollary 5.11 ensures that c is not contained entirely in either U_0 or U_1.

Recall that our Liouville domain is a quotient of the product $[0, \ln(\lambda_s)]_s \times [-1,1]_\tau \times T^2_{x,y} \times r_0\,\mathbb{D}^2_{p,q}$ and consider a flowline γ of c which is not entirely contained in either U_0 or U_1. In forward time, γ converges to a critical point of the blocking apparatus installed on U_i for $i = 0$ or $i = 1$, and thus intersects $\partial_- U_i$ in a point $(s^*, \tau^*, x, y, p, q)$ satisfying $\tau^* = \tau_0$ and $(p, q) = (0, 0)$. This conclusion follows from Proposition 5.13, as well as the fact that $\mathrm{Skel}(W_i) = L_i \times \{\tau_0\}$.

Now consider flowing backwards from $(s^*, \tau_0, x, y, 0, 0)$ along γ until either limiting to a critical point or reaching the slice $M_{\ln(\lambda_s)} \times r_0\,\mathbb{D}^2$. Notice that flowing backwards will not change the stabilization coordinates $(p, q) = (0, 0)$ of γ whenever γ is outside of U_0 and U_1. Within U_0 and U_1, part (iii) of Corollary 6.2 ensures that if γ is not trapped in backward time, it will exit the region with $(p, q) = (0, 0)$. For these reasons, we won't concern ourselves with the stabilization coordinates.

We now know that γ converges in forward time to a critical point of the blocking apparatus installed on U_i, for $i = 0$ or $i = 1$. If $i = 1$, then γ reaches $M_{\ln(\lambda_s)} \times r_0\,\mathbb{D}^2$. As we move backwards along γ, the τ-coordinate may be drawn towards 0, but cannot leave the interval $[0, \tau_0]$. If $i = 0$ we must consider the possibility that γ limits to a critical point in U_1. The previous observations about the (p, q)- and τ-coordinates apply in this case as well, and we see that γ intersects $\partial_+ U_1$ in the set

$$\{s = s_1\} \times [0, t_0] \times I_\epsilon(W_1, \lambda_1) \times \{(0, 0)\}.$$

We can be sure that the W_1-coordinate of this intersection point will be contained in $I_\epsilon(W_1, \lambda_1)$ because the τ-coordinate is contained in $[0, \tau_0]$. According to Corollary 6.2 and Proposition 5.12, there are then three possibilities as we flow backwards into U_1 along γ:

- γ limits in backward time to a stove critical point of U_1;
- γ limits in backward time to a non-stove critical point of U_1;
- γ exits $\partial_- U_1$ with τ-coordinate in the interval $[(1 - e^{|\sigma_1|})\tau_0, \tau_0]$, and with $(p, q) = (0, 0)$.

Proposition 5.10 excludes the first case, as stove critical points cannot be party to a broken loop. In the second case, we may simply recast γ as the flowline of c which limits in forward time to a non-stove critical point of U_1 and resume the above analysis. In particular, a flowline which limits in forward time to a non-stove critical point cannot be entirely contained in a blocking apparatus region. In the final case, we see that γ will reach $M_{\ln(\lambda_s)} \times r_0 \, \mathbb{D}^2$ with τ-coordinate in $[(1 - e^{|\sigma_1|})\tau_0, \tau_0]$ and with $(p, q) = (0, 0)$.

We now continue our analysis at a point $(\ln(\lambda_s), \tau, x, y, 0, 0)$ where γ meets $M_{\ln(\lambda_s)} \times r_0 \, \mathbb{D}^2$, with the knowledge that, following the global holonomy, τ is contained in the interval $[\lambda_u^2(1 - e^{|\sigma_1|})\tau_0, \lambda_u^2 \tau_0]$. Recall that the quantities $|\sigma_0|$ and $|\sigma_1|$ were chosen to ensure that any point in W_i with τ-coordinate in this interval is contained in $I_\epsilon(W_i, \lambda_i)$, for $i = 0, 1$. It follows that if (x, y) is contained in S_0^δ, then γ will meet $\partial_+ U_0$ in its trapping region and, according to Proposition 5.12, limit in backward time to a stove critical point. If (x, y) is not contained in S_0^δ, then, by construction, (x, y) is contained in $S_1^{2\delta}$.

We have now reduced our analysis to flowing backwards from a point $(\ln(\lambda_s), \tau, x, y, 0, 0)$, with (x, y) contained in $T^2 - S_0^\delta$ and τ contained in $[\lambda_u^2(1 - e^{|\sigma_1|})\tau_0, \lambda_u^2 \tau_0]$. There are three possibilities for the behavior of our flowline γ as we flow backwards from this point:

- γ misses U_0 entirely;
- γ passes through U_0 without encountering a critical point;
- γ converges in backward time to a non-stove critical point of U_0.

The first case is the simplest: because (x, y) is contained in S_1^δ, γ will meet $\partial_+ U_1$ in its trapping region and, according to Proposition 5.12, converge to a stove critical point of U_1.

In the second case, we note that (x, y) is in fact contained in $S_1^{2\delta}$, and thus Corollary 6.2(iii) ensures that, following the holonomy induced by U_1, our the T^2-coordinates of γ will be contained in S_1^δ. Moreover, part (i) allows us to bound the τ-coordinate of γ following this holonomy. In particular, γ will exit U_0 through $\partial_- U_0$ with τ-coordinate contained in the interval $[\tau_0 + e^{|\sigma_0|}(\lambda_u^2(1 - e^{|\sigma_1|})\tau_0 - \tau_0), \lambda_u^2 \tau_0]$. Despite being wholly unattractive, this interval is useful for us: the quantities $|\sigma_0|$ and $|\sigma_1|$ were chosen sufficiently small as to ensure that $(h_0 \circ h_g \circ h_1)(\theta, \tau)$ is contained in the interior of $I_\epsilon(W_i, \lambda_i)$, for any $0 \leq \tau \leq \theta$. The τ-interval we now have precisely matches this description. The upshot is that as we continue flowing backwards along γ from $\partial_- U_0$, γ will eventually encounter $\partial_+ U_1$ in its trapping region, and thus converge in backward time to a stove critical point.

At last we consider the case where γ converges in backward time to a non-stove critical point of U_0. In this case, we change our focus once again, thinking instead about the flowline of c which limits in forward time to the non-stove critical point which serves as the backwards limit of γ. Proposition 5.13 tells us that this flowline meets $\partial_- U_0$ with τ-coordinate τ_0, and with T^2-coordinate contained in $T^2 - S_0^{2\delta}$. As a result, this flowline will meet $\partial_+ U_1$ in its trapping region, and thus will converge in backward time to a stove critical point.

The conclusion of this analysis is that any broken loop c in our Liouville domain must contain a flowline which limits in backward time to a stove critical point. Because Proposition 5.10 tells us that stove points cannot appear in broken loops, we conclude that our Liouville domain is free of broken loops.

Per Proposition 6.1, we conclude that $(W_A \times r_0 \mathbb{D}^2, \tilde{\lambda})$ is a Weinstein domain.

BIBLIOGRAPHY

[BC21] Joseph Breen and Austin Christian. "Mitsumatsu's Liouville domains are stably Weinstein." *arXiv preprint arXiv:2109.07615*, 2021.

[Bre21] Joseph Breen. "Morse-Smale characteristic foliations and convexity in contact manifolds." *Proc. Amer. Math. Soc. 149 (2021), 3977-3989*, **149**:3977–3989, 2021.

[CE12] K. Cieliebak and Y. Eliashberg. *From Stein to Weinstein and Back: Symplectic Geometry of Affine Complex Manifolds*. American Mathematical Society colloquium publications. American Mathematical Society, 2012.

[CM18] Sylvain Courte and Patrick Massot. "Contactomorphism groups and Legendrian flexibility." *arXiv preprint arXiv:1803.07997*, 2018.

[EG91] Yakov Eliashberg and Mikhael Gromov. "Convex symplectic manifolds." *Proc. Sympos. Pure Math*, **52.2**:135–162, 1991.

[EOY21] Yakov Eliashberg, Noboru Ogawa, and Toru Yoshiyasu. "Stabilized convex symplectic manifolds are Weinstein." *Kyoto J. Math.*, **1**(1):1–15, 2021.

[Gei94] Hansjörg Geiges. "Symplectic manifolds with disconnected boundary of contact type." *Int. Math. Res. Not. IMRN*, **1994**(1):23–30, 1994.

[Gei95] Hansjörg Geiges. "Examples of symplectic 4-manifolds with disconnected boundary of contact type." *Bull. Lond. Math. Soc.*, **27**(3):278–280, 1995.

[Gei08] H. Geiges. *An Introduction to Contact Topology*. Cambridge Studies in Advanced Mathematics. Cambridge University Press, 2008.

[Gir91] Emmanuel Giroux. "Convexité en topologie de contact." *Comment. Math. Helv.*, **66**(1):637–677, 1991.

[HH18] Ko Honda and Yang Huang. "Bypass attachments in higher-dimensional contact topology." *arXiv preprint arXiv:1803.09142*, 2018.

[HH19] Ko Honda and Yang Huang. "Convex hypersurface theory in contact topology." *arXiv preprint arXiv:1907.06025*, 2019.

[Hon00a] Ko Honda. "On the classification of tight contact structures I." *Geom. Topol.*, **4**(1):309–368, 2000.

[Hon00b] Ko Honda. "On the classification of tight contact structures II." *J. Differential Geom.*, **55**(1):83–143, 2000.

[Hua19] Yang Huang. "A dynamical construction of Liouville domains." *arXiv preprint arXiv:1910.14132*, 2019.

[McD91] Dusa McDuff. "Symplectic manifolds with contact type boundaries." *Invent. Math.*, **103**(1):651–671, 1991.

[Mit95] Yoshihiko Mitsumatsu. "Anosov flows and non-Stein symplectic manifolds." In *Annales de l'institut Fourier*, volume 45, pp. 1407–1421, 1995.

[MNW13] Patrick Massot, Klaus Niederkrüger, and Chris Wendl. "Weak and strong fillability of higher dimensional contact manifolds." *Invent. Math.*, **192**(2):287–373, 2013.

[Mor09] Atsuhide Mori. "Reeb foliations on S^5 and contact 5-manifolds violating the Thurston-Bennequin inequality." *arXiv preprint arXiv:0906.3237*, 2009.

[Mor11] Atsuhide Mori. "On the violation of Thurston-Bennequin inequality for a certain non-convex hypersurface." *arXiv preprint arXiv:1111.0383*, 2011.

[MS98] D. McDuff and D. Salamon. *Introduction to Symplectic Topology*. Oxford mathematical monographs. Clarendon Press, 1998.

[PPM98] J. Palis, J. Palis, and W. de Melo. *Geometric Theory of Dynamical Systems: An Introduction*. Selected monographies. Collaege Press, University of Beijing, 1998.

[Sac] Kevin Sackel. "Getting a handle on contact manifolds." preprint 2019, arXiv:1905.11965.

[Wei91] Alan Weinstein. "Contact surgery and symplectic handlebodies." *Hokkaido Math. J.*, **20**(2):241–251, 1991.